DESIGN AND SYNTHESIS OF TRIAZINE DERIVATIVES AS NON-NUCLEOSIDE REVERSE TRANSCRIPTASE INHIBITORS

Wendy Munatsi 1724273

A dissertation submitted to the Faculty of Science

University of the Witwatersrand

Johannesburg

In fulfillment of the requirements of the Degree of Master of Science

March 2024

Declaration

I declare that the work presented in this dissertation was carried out extensively by myself under the super-vision of Professor Moira Bode and Dr Kennedy Ngwira. It is submitted for the degree of Master of Science at University of the Witwatersrand, Johannesburg. It has not been submitted before for any degree or examination at any other university.

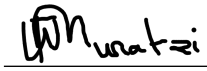

Wendy Munatsi

08 JUNE 2024

Abstract

This research work was carried out to investigate the properties of different groups that can be used to modify the triazine core with the aim of designing a new library of possible HIV non-nucleoside reverse transcriptase inhibitors (NNRTIs). Triazine derivatives have been used extensively in the synthesis of numerous classes of drugs due to their significant biological activity. In this project, the specific focus was to synthesize 1,3,5-triazine derivatives by successive nucleophilic substitution reactions of the Cl atoms from cyanuric chloride.

In the first step of the substitution reactions, 2,4,6-trichloro-1,3,5-triazine was reacted with various anilines, phenols and thiophenols which acted as nucleophiles to displace one of the Cl atoms upon reaction completion. The yields varied from 28% -90% with the best yields being observed when the anilines were used as a nucleophile and most of the substituents in this first step were anilines. The substituents used at each step of the substitution were vital in terms of determining the order of the reaction to enable a successful reaction. The introduction of different linkers to the triazine core such as -NH, -S, -O yielded compounds with different properties expected to provide significant interactions in the NNRTI binding pocket. We expected better binding properties from the -NH bearing compounds due to hydrogen bond formations with amino acid residues inside the allosteric binding pocket of the HIV-1 RT.

The success of the second step of the substitution reactions was identified to be dependent on the substituent attached to the triazine ring from the first step. Some reactions were not successful when a stronger nucleophile was used in the first step and a weaker nucleophile was being used as the incoming nucleophile substituting the second Cl atom. Therefore, these

reactions were repeated and the order of the reaction rearranged. Temperatures were increased and reaction times were increased at this stage as the reactivity of the triazine ring was reduced and therefore higher kinetic energy was required for successful reactions. In general, the synthesized triazine derivatives bearing two aromatic substituents exhibited the most significant presence of tautomers. The final stage in the synthesis of the trisubstituted triazine derivatives was relatively complex and required much higher temperatures and longer reaction times. The reactions were also performed at smaller scales and difficulties with the purification processes also contributed to the loss of product thereby resulting in lower yields, with one of the compounds giving a yield of 11%.

The results obtained from the anti-HIV assay studies from the selected compounds tested, showed that antiviral activity was observed in triazine derivatives with electron withdrawing groups attached to the aromatic substituent as well as -NH and -O linkers at the right and left wing of the triazine core, respectively.

Acknowledgement

I would like to show my greatest appreciation to the Almighty God for granting me life and taking me through this journey that has been truly a challenging and at times heartbreaking. At all the points where I felt the weakest, he carried me on his shoulders and at those points he did what I couldn't do.

My sincere gratitude goes out to my supervisors Prof Moira Bode and Dr Kennedy Ngwira. My journey has been tough but at every point you have guided me and taught me so much.

Thank you Andrew my love, your support has been unwavering it has been a tough journey, but you always stood by me. To my family, I love you all so much and I appreciate your support and encouragement, in your eyes I could always achieve anything.

To my beloved mother Elitha, the rock, the commander in chief of our family no words can ever express how thankful I am for being the woman you are. My angel in the skies and all around me, my dad George, I have your perseverance and resilience that has carried me thus far, I will always love you.

A special thank you for all my colleagues from Wits university who helped me through and through to name a few, Dr Charles, Bianca, Nompumelelo, Adelaide, Mudzuli, Robin, Thabo, Idah, Edward, Fatema, Songesizwe, Dr Memory.

Thank you to the mass spec team (Eric, Refilwe, Thapelo and Naledi) for all your assistance. It's been very humbling to work with you. I would like to thank the Glass blower (Tapuwa) and the storekeepers (Ntate Moloto and Baloi).

Thank you very much Dr Adriaan Basson from the Faculty of Health Sciences, School of Pathology (Wits) for your assistance with the antiviral activity studies.

A special thank you to all my specialist doctors and medical care team who saved my life for me to be able to complete this work. God Bless you all.

List of Abbreviations

AIDS- Acquired immunodeficiency syndrome.

HIV- Human immunodeficiency virus

CDC-Centre for Disease Control

SIV- Simian immunodeficiency virus

TB-Tuberculosis

RNA- Ribonucleic acid

DNA- Deoxyribonucleic acid

HLA- Human leukocyte antigen

STD-Sexually Transmitted Disease

RBC-Red Blood Cells

WBC-White Blood Cells

NKC-Natural Killer Cells

ART-Antiretroviral therapy

RT-Reverse transcriptase

HAART-Highly active antiretroviral therapy

NRTI-Nucleoside reverse transcriptase inhibitor

NNRTI-Non-nucleoside reverse transcriptase inhibitor

NNRTI-BP- Non-nucleoside reverse transcriptase inhibitor- binding pocket

PPT-Polypurine tracts

EWG-Electron withdrawing group.

EDG-Electron donating group.

HEK- Human embryonic kidney

Table of Contents

Chapter 1

1. Introduction

1.1 HIV

1.1.1 History of HIV/AIDS

The Acquired Immuno-Deficiency Syndrome (AIDS) is a worldwide pandemic that has claimed the lives of approximately 32.0 million people since it was confirmed in 1981 while 37.7 million people were documented to be living with HIV in 2020, including 10.2 million who were not on HIV treatment. In 1981 numerous outbreaks of *Pneumocystis carinii* pneumonia and Kaposi's sarcoma in the male population that did not previously exhibit any health complications were reported to the Centre for Disease Control (CDC) in Atlanta, Georgia in the United States of America.[1,2] As reports of cases of individuals with suppressed immune systems acquiring a vast range of diseases increased, this led to a collective classification of the clinical symptoms. Studies ensued to determine from a cellular level the direct cause of these opportunistic infections and cancers that were plaguing humans as it was not known at the time that a lengthy window period existed between exposure and disease manifestation.[3]

The Human Immunodeficiency Virus (HIV) was established to be the main activator for the syndrome. A distinct chimpanzee of Central African origin was linked as the original source of HIV infection to human beings as scientists carried out research to gain better understanding of this rare virus. The type of the immunodeficiency virus that existed in the above mentioned species is called Simian Immunodeficiency virus, or SIV, and it exhibited properties very

closely related to the human version HIV-1 and HIV-2. The interactions between humans and chimpanzees initiated infections between different species to be transferred from one species to another. This led to the transmission of SIV from chimpanzees to humans and due to the nature of this virus it was able to mutate and generate a different version that can replicate in human cells. This was ultimately the beginning of the HIV-1 and HIV-2 species which was later identified to be a retrovirus.[4] This virus leads to HIV infection in the human body and its inexorable replication accelerates the HIV infection to an advanced stage whereby it becomes AIDS. At this stage, the body's immune system has deteriorated to such an extent that opportunistic infections can easily target the body with an immune system that has been highly compromised. HIV-1 associated opportunistic infections envelop an extensive number of life-threatening infections and these infections typically affect patients with low CD4+ counts which seldom occurs in an immunocompetent host. Opportunistic infections such as tuberculosis (TB), pneumonia and meningitis eventually result in the death of infected individuals.[5] Therefore, researchers have a mammoth task of finding ways to halt the progression of HIV infections.

To date, a cure for AIDS has not been discovered despite numerous clinical trials, but various ways of curbing the rate of HIV infection are being implemented successfully. More solutions are being explored due to the resistance of the HI virus as a result of mutations that reduce the efficacy of drugs utilized in the treatment process.[6] In order to combat the HI virus, it is important to study all the factors that surround its spread, survival and replication, as this information is vital in making informed decisions as to how a cure and treatments can be designed and implemented.

1.1.2 Characteristics of HIV

The HI virus is unique in comparison to other viruses in the sense that once it enters the human body, it cannot be removed or treated in such a way that it no longer exists in the body. Retroviruses form part of the family of RNA viruses that have the ability to engineer double-stranded DNA copies of their genome which are then merged into the chromosome of cell in which it is resident.[7] HIV belongs to the Lentivirus genus which forms part of Retroviridaes. These types of viruses are termed retroviruses due to their ability to transcribe the RNA genome into DNA which is a reverse of the pathway of genetic information transfer. The HI Virus has been distinguished into two types namely the HIV-1 and HIV-2 type and this is derived from the genetic makeup and variations in the viral antigens.[8] As mentioned earlier HIV-1 was identified to be majorly responsible for the progression of AIDS between the two HIV strains. It is vital to understand its structure to equip researchers with insight as to how modifications or designs could be implemented to curb its replication and ultimately design a treatment regimen.

The HI virus possesses important target areas for growth and replication. These are the internal structural proteins, viral enzymes, external structural proteins and the transmembrane glycoproteins. The viral enzymes comprise of reverse transcriptase (RT, p66/p51), integrase (IN, p32) and protease (PR, p11).[9-10] HIV-1 is a unique virus as it is able to convert single stranded RNA to double stranded DNA and the viral enzymes play a significant part in the HI-virus replication processes. The translation of the viral enzymes is not conducted as single unique entities but as parts of a larger macromolecule named Pr160gag-pol and the

encapsulated viruses are congregated using these polyprotein parent units. The formation of each active enzyme arises from proteolytic cleavage of the polyprotein at particular sites at the

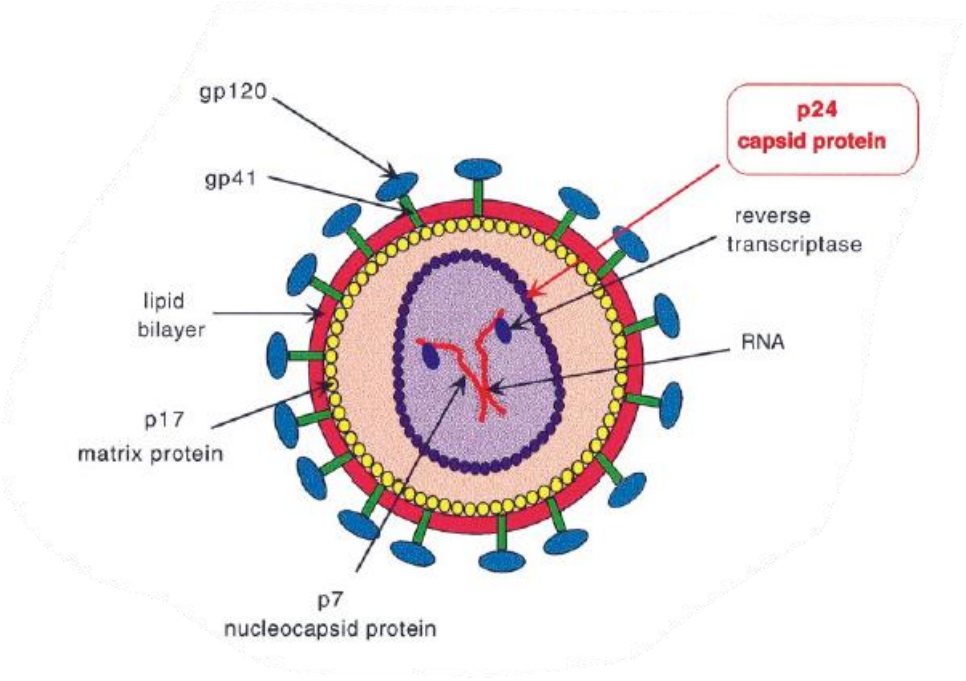

Figure 1: Schematic representation the HI-Virus displaying its internal and external components. (Figure reproduced from Berthet-Colominas *et al*)[9]

point of virion assembly and budding stages, the protease enzyme is responsible for this process. The virus is made up of components such as the p17 nucleic acid binding protein and p9 gag protein in its innermost shell. The p17 myristylated gag matrix protein is responsible for the inner and outermost components of the virus and it also plays a vital role in sustaining the structure of the virus. The gag matrix protein (p17) is bound to a lipid bilayer membrane (**Figure 1**) which contains pockets comprising of gp120 and gp41 proteins. The main role of the gp120 protein is that it bears the receptor binding region which is vital in the initiation of the infection process, and it initiates the formation of syncytia. One of the important stages in the viral life cycle is the fusion stage which is initiated by the gp41 protein. A number of essential cell proteins are derived from the host during the virus budding stage, and these include the HLA class I and II.[10-12]

1.1.3 HIV transmission

The virus enters the human body via several ways such as the exchange of body fluids between infected and uninfected individuals and these fluids include blood, semen, vaginal fluid, rectal fluids and breastmilk. In order for HIV transmission to occur, the virus within these fluids must enter the bloodstream of a human body via a mucous membrane which is found in the rectum, penis tip, mouth and vagina or via an opening in the epidermal layer such as a cut or sore. The extent of the infection in the infected partner which is graded by the viral load contributes greatly in the risk for HIV-1 transmission from the infected individual to the person they have been exposed to during sexual or other high-risk engagements. Studies have shown that the ratio of increase in transmission to increase in viral load is 1:4 and this indicates that the higher the viral load the greater the chances of HIV transmission.[13] The highest HIV infection rates are due to unprotected sex between an HIV-infected individual and an uninfected HIV individual. Anal sex has exhibited the greatest risk in HIV transmission of all the classes of sex, however vaginal sex has recorded the largest number of reports of HIV infection and this may be due to the large female- male population ratio. The risk is increased as compared to other forms of sex because the lining of the rectum is thin and this allows a simple pathway for the virus to be transmitted between individuals. Other forms of sex such as oral are deemed to be low risk factors in the transmission of HIV, however a combination of other factors can increase the chances of transmission via this form of sex. These factors may be any cuts or bruises exposing the skin at any points of contact during the engagements, any form of blood exchange between individuals as well as diseases that compromise the immune system largely sexually transmitted infections/diseases (STI/STDs).[13-14]

HIV transmission can also occur from mother to child which is also termed vertical transmission in three common ways: i) during pregnancy, ii) at birth and iii) via breastfeeding.[15] Mother to child HIV transmission occurs when the blood from the mother goes through the placenta to the fetus. The main role of the placenta is to provide a route for transportation of essential components required by the fetus and discard any wastes released by the fetus. This passageway provides a bridge for the movement of the HI-Virus in the blood that moves from the infected mother to the fetus while supplying the required necessities for growth of the fetus.[16] The blood transfer increases the chances of the mother infecting the unborn baby while in the womb. Another way of vertical transmission is during delivery, whereby the foetus can be infected with HIV through the mother's cervical secretions or blood exchange.[17] In some instances, mother-child HIV transmission has been noted during breastfeeding. The risk has been noted to be low during breastfeeding however the mother's viral load can be a high-risk factor, should the mother of the infant have an elevated viral load the chances of HIV infection are high.[18]

Investigations have also shown that having direct contact with a needle or sharp object between an HIV-infected individual and an uninfected individual can lead to HIV transmission should the blood of the infected individual, regardless of the amount, enter the bloodstream of the uninfected individual. This is often seen in instances where narcotics abusers share needles between drug injections, the negligent way these needles are shared increases the rate of HIV transmission.

1.1.4 Stages of HIV infection

1.1.4.1 Acute Infection

Acute HIV infection is the primary phase in HIV infection which occurs in the first 14-28 days after HIV transmission. In the time frame between infection and seroconversion, which is called the window period, markers of infection such as p24 antigen and antibodies are too minute to be detected. Some clinical symptoms experienced during acute HIV infection include flu-like symptoms, such as fever, headache, and rash. At this phase of HIV infection, which is also termed the window period, the virus replicates near the site of infection in the host cell, however it is still undetectable during any tests. Following this window period which lasts for several weeks, HIV begins to multiply rapidly and distributed widely in the host. At this stage the virus can compromise the immune system in the human body and this leads to an increased viral load in the bloodstream. This leads to the weaking of the cells the body uses to fight infection namely the white blood cells (WBC).[19]

1.1.4.2 Chronic Infection

The subsequent phase in HIV infection is the chronic infection stage (**Figure 2**), which is also termed asymptomatic HIV infection. During this stage of infection, HIV continues to multiply in the body but the rate of multiplication is moderate. Individuals at the chronic HIV infection stage do not necessarily have any HIV-related symptoms and may even look as healthy as uninfected individuals. Depending on the lifestyle an infected individual leads, the length in which chronic HIV infection leads to AIDS may vary from a few years to over 20 years. People who are on antiretroviral therapy (ART) may be in this stage for an extended period well over 30 years. The possibility of HIV transmission at this stage still exists albeit individuals on anti-retroviral treatment pose very low transmission risk. ART maintains an undetectable viral load

and infected individuals effectively have very little or no chances of transmitting the virus to an uninfected individual. [20]

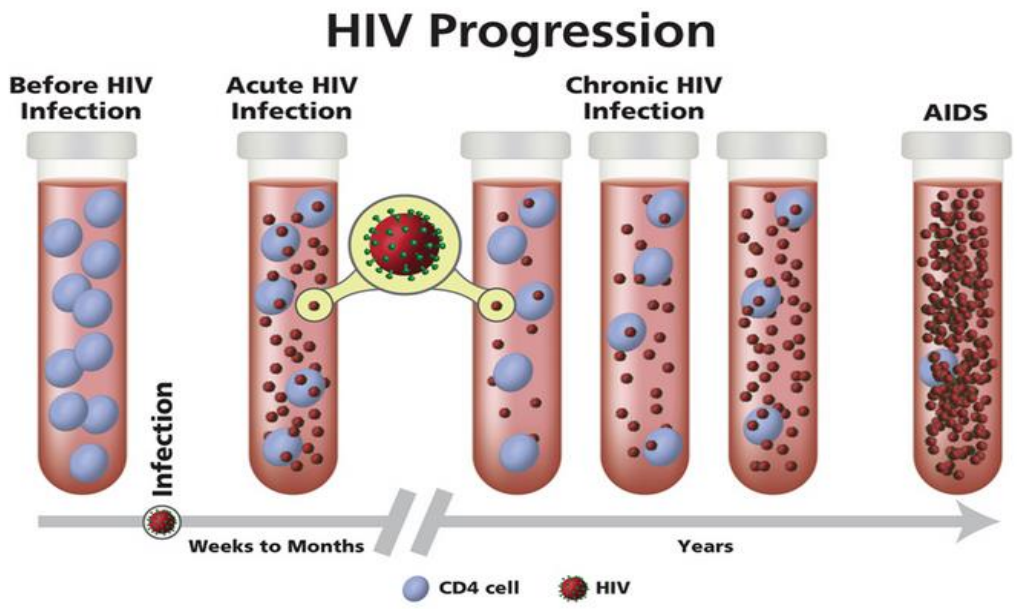

Figure 2: An illustration of the progression of HIV infection in the human bloodstream.[20]

1.1.4.3 Acquired immunodeficiency syndrome.

Acquired immunodeficiency syndrome (AIDS) is the final and most severe phase of HIV infection, at this stage the human body is in a dire state and unable to fight off most of the opportunistic infections. AIDS is diagnosed when the CD4 count levels in the blood falls to below 200 cells/mm^3 and a combination of diagnosis of other related infections such as STIs, STDs and some forms of cancer. An individual's ability to have the body defend itself is diminished as the CD4 cells have been outnumbered by the HI virus and this eventually leads to loss of life.[19,20] A significant amount of weight loss, infections with repeat occurrences, frequent dry and wet coughs, extreme physical weakness of the body, swollen lymph nodes and constant feverish conditions are but a few of the symptoms that are experienced during this final stage of HIV infection.

1.1.5 Invasion of human cells by HI Virus

1.1.5.1 Immunosuppression

In the human body, the cellular composition of blood is divided into groups which comprise of red blood cells (RBCs), white blood cells (WBCs), and platelets. The functions of RBCs is to facilitate gas exchange as well as maintain the blood pH levels while the WBCs are responsible for maintaining the body's immune system. WBCs are expressed in two different forms namely granular and agranular leukocytes. Neutrophils, eosinophils and basophils are responsible for maintaining the body's immune system with neutrophils making up the largest population of leukocytes.

Agranular leukocytes lack granules in their cytoplasm and the two main types are monocytes and lymphocytes. Monocytes are large leukocytes whose primary function is phagocytosis, and their size enables them to conduct this function. Monocytes have the ability to carry out phagocytosis of pathogens, old blood cells, cellular debris and dead cells.[21] Lymphocytes consist of T-lymphocytes and their main role is to directly kill many foreign invaders and B-lymphocytes whose function is to synthesize antibodies and Natural Killer Cells (NKC).[22] T-lymphocytes comprise mainly of CD4 T cells and CD8 T cells and when CD4 cells are activated and differentiated into distinct effector subtypes, they subsequently facilitate the immune system into a course of action by secreting specific cytokines.[23] The major function of CD4 cells is to activate cells that participate in response to the immune system being compromised such as lymphocytes, cytotoxic T cells and non-immune cells.[24] CD4 cells are of immense importance in humans as they are the pillar of the human immune system that is imperative in the regulation of an effective response to pathogens. Due their vital role in the body their

functionality cannot be compromised. When the HI virus enters the human body, it targets the CD4 cells of the host by using its envelope gp120 protein to bind to CD4.

1.1.5.2 Viral Life Cycle

The virus uses the machinery of the CD4 cells to multiply in a stepwise manner namely binding, fusion, reverse transcription, integration, replication assembly and budding.

Binding-The first phase of the viral replication cycle is when the viral envelope protein gp120 binds to the CD4 receptor. This results in the binding of the gp41 subunit to the CCR5 or CXCR4 co-receptor on the host cell's membrane. This increases rate of probability of infection, which has been discussed earlier.

Fusion- When the CCR5 or CXCR4 is bound to the gp41 protein it initiates structural changes in the orientation of the of gp120 protein. This in turn allows the opening of the gp41 protein that is able to embed itself into the membrane of the host cell. The changes in the orientation of the gp41 unit allows it to form a six-helix bundle and the fusion occurs when the viral cell membrane as well as the host cell membrane are in close proximity following the conformational changes.[25,26]

Reverse transcription- This is the stage where the viral RNA converts the single stranded RNA into double stranded DNA initiated by the reverse transcriptase (RT) enzyme. This DNA genome is transported to the host cell's nucleus.

Integration- Once in the host cell's nucleus the integration of the viral DNA into the hosts DNA occurs when the integrase enzyme initiates the action. This gives the virus the ability to generate viral proteins using the host cell's systems.

Replication assembly and budding- The newly formed HIV glycoproteins/envelope proteins are synthesised as polyproteins. These polyproteins undergo cleavage by the protease to form protein subunits that are transported to the cell surface. The HIV protein subunits gp120 and gp41 assemble at the plasma membrane where the newly formed virions bud (**Figure 3**).[27]

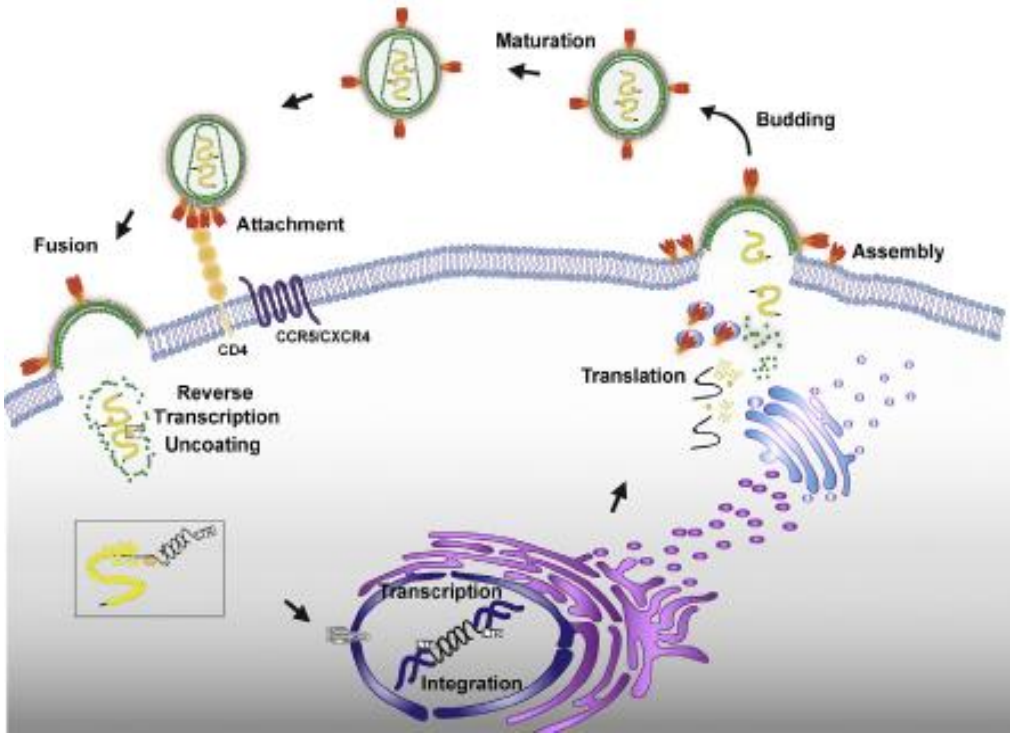

Figure 3: Stages in the replication of the HI virus. (Figure reproduced from Kriesel *et al*) [27]

1.1.6 Highly Active Anti-Retroviral Therapy

To suppress HIV replication, the administration of highly active antiretroviral therapy (HAART) is actioned, which includes a combination of inhibitors targeting essential viral enzymes.[28] The main goals of initiating HAART are to achieve the following:

i) Extensively suppress the amount of virus in the plasma to undetectable levels.

ii) Improve the ability of the immune system to function at optimal levels thereby increasing the CD4 T cell count.

iii) Extend survival and quality of life of individuals infected by the virus.

iv) Reduce HIV-associated morbidity and minimize the rate HIV transmission to uninfected individuals.[29]

There are five classes of inhibitors that constitute the HAART, and they all play distinct roles in inhibiting HIV replication at each phase of the viral replication. Fusion inhibitors (FIs) such as enfuvirtide *(Ac-Tyr-Thr-Ser-Leu-Ile-His-SerLeu-Ile-Glu-Glu-Ser-Gln-Asn-Gln-Gln-Glu-Lys-Asn-Glu-Gln-Glu-Leu-LeuGlu-Leu-Asp-Lys-Trp-Ala-Ser-Leu-Trp-Asn-Trp-Phe-NH2)* are potent inhibitors of HIV. The method of action of this class of inhibitors is by halting the HIV fusion and entry process into the host cell's membrane.[30] The major function of the fusion inhibitors is to prevent the structural changes that are required to ensure the proximity of the host cell's membrane and virus membrane for fusion to occur. Integrase inhibitors (INIs) such as raltegravir **1** (**Figure 4**) inhibit HIV integrase by binding to the active site and this action prevents the viral DNA from bonding to the host cell's DNA. This stage is very vital in the viral life cycle and any interferences can largely alter its replication.[31]

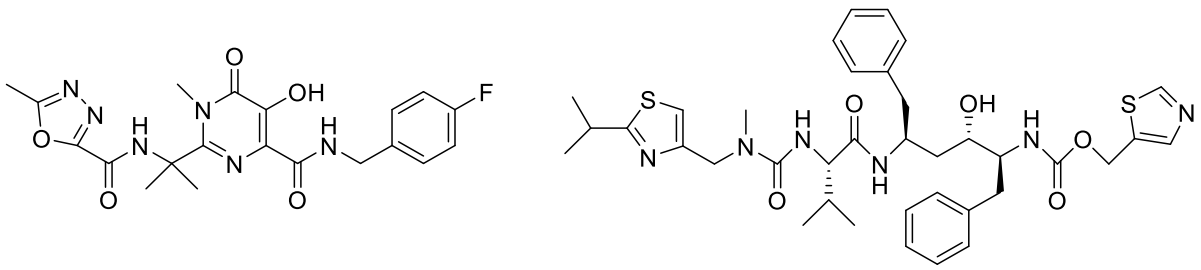

Figure 4: Structures of raltegravir **1** (INI) and ritonavir **2** (PI)

Protease inhibitors (PIs) such as ritonavir **2** (**Figure 4**) exhibit their pharmacological action when they bind to the viral enzyme protease. This enzyme is essential in the production of the viral proteins using the host cell's machinery, the PIs stop the protease in this process as they inhibit its proteolytic actions.

In terms of reverse transcriptase (RT) inhibitors, they are subdivided into two different types namely nucleoside/nucleotide reverse transcriptase inhibitors (NRTIs) such as zidovudine/tenofovir and non-nucleoside reverse transcriptase inhibitors (NNRTIs), for example rilpivirine.

1.1.6.1 Reverse Transcriptase Inhibitors

1.1.6.1.1 Nucleoside/Nucleotide reverse transcriptase

Nucleoside/nucleotide reverse transcriptase inhibitors (**Figure 5**) have similar molecular structures to endogenous nucleosides and nucleotides and are chemically inactive in their original forms.[31] NRTIs are phosphorylated intracellularly to their active diphosphate or triphosphate forms that have the ability to block the enzymatic action of the HIV RT by being embedded as nucleotides as the DNA chain increases, causing DNA chain termination. The mode of operation for the NRTIs differs from the one utilized by the NNRTIs as the NRTIs are not capable of inhibiting the RT enzyme directly while the NNRTIs can form hydrophobic bonds in the NNRTI-Binding Pocket (NNRTI-BP).[32]

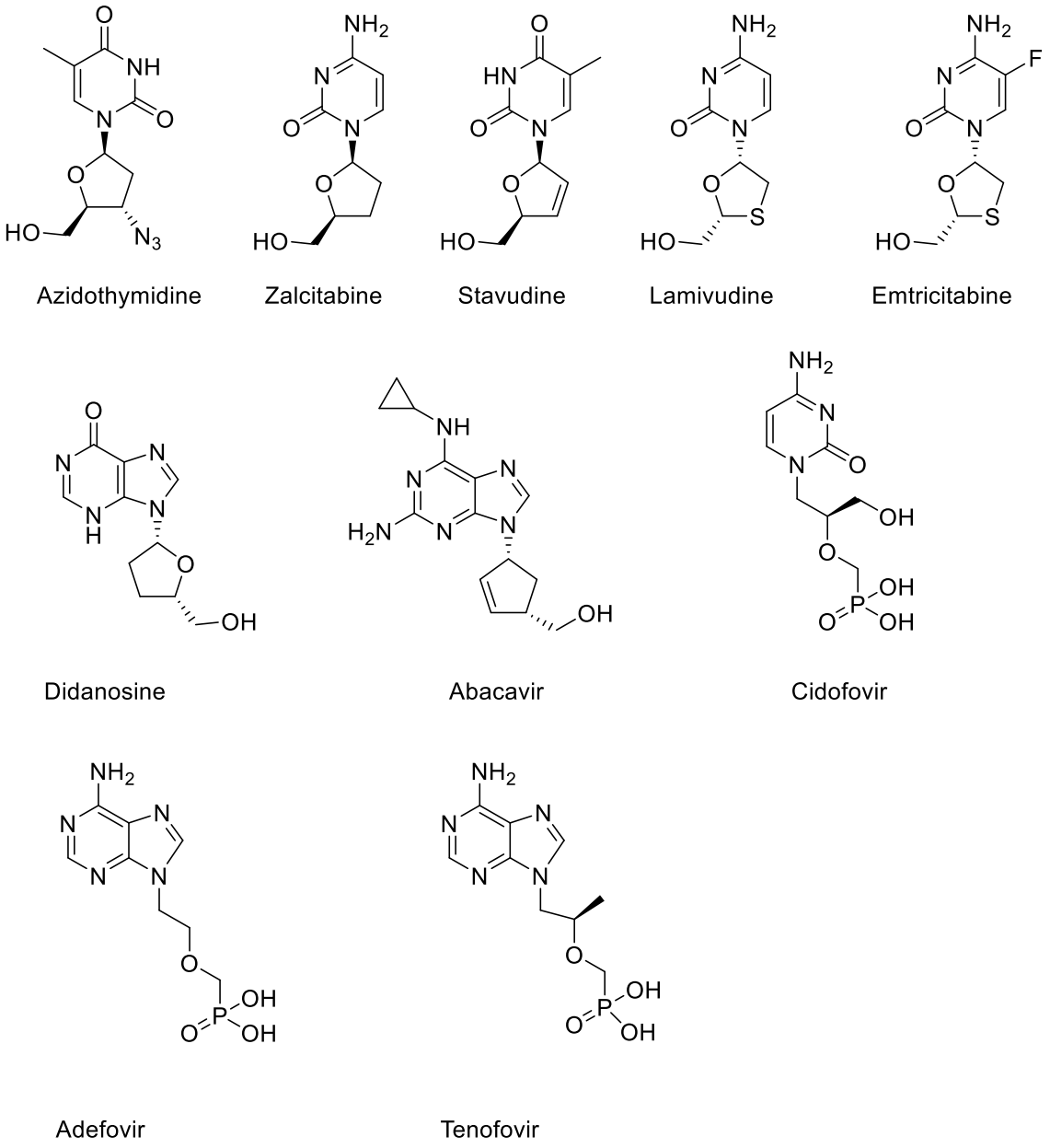

Figure 5: Nucleoside reverse transcriptase inhibitors

1.1.6.1.2 Non-nucleoside reverse transcriptase inhibitors

The NNRTIs are micro molecules that are notably different in their chemical structures from the former NRTIs discussed above. Unlike the NRTIs they do not require activation as they exist in their active form and are not dependent on the host cell's metabolism. These are among the important groups of drugs used in antiretroviral treatment, with each targeting the RT

enzyme at a different site. The NNRTIs halt the activity of the enzyme by binding to the allosteric site thereby blocking the replication process at this stage.[33]

The binding of NNRTIs to RT is highly specific, involving a combination of hydrophobic and hydrogen bonding interactions. The hydrophobic interactions involve the nonpolar regions of the NNRTI molecule and hydrophobic residues lining the binding pocket of the RT enzyme. A well-exhibited illustration is that of nevirapine, which is a widely used NNRTI, that has a flexible lipophilic tail that extends deep into the binding pocket, while the aromatic rings of efavirenz and etravirine make extensive hydrophobic contacts with the enzyme. Hydrogen bonding is also an important interaction between the NNRTIs and the RT enzyme, resulting in conformational changes occurring within the structure of the enzyme.

HIV-1 RT constitutes of two subunits the p66 and the p51.The enzyme has a polymerase domain which comprises of fingers, palm, thumb and connection residues. These form the nucleic binding cleft and the floor of binding cleft from the p66 and the p51 subunits respectively.[34] The action of the NNRTIs is to bind to the allosteric site of the RT to prevent domain motions and these motions are essential in the catalysis for the formation of some essential amino acids. Effectively NNRTIs target the reverse transcription stage by binding non-competitively to a site on the p66 subunit called the NNRTI Binding Pocket (NNRTI-BP) which is an allosteric site and can be seen in the representative diagram in **Figure 6**. The NNRTIs bind to this allosteric site which is lipophilic, and the distance between the NNRTI-BP and the substrate binding site has been determined to be 10Å.[35,36]

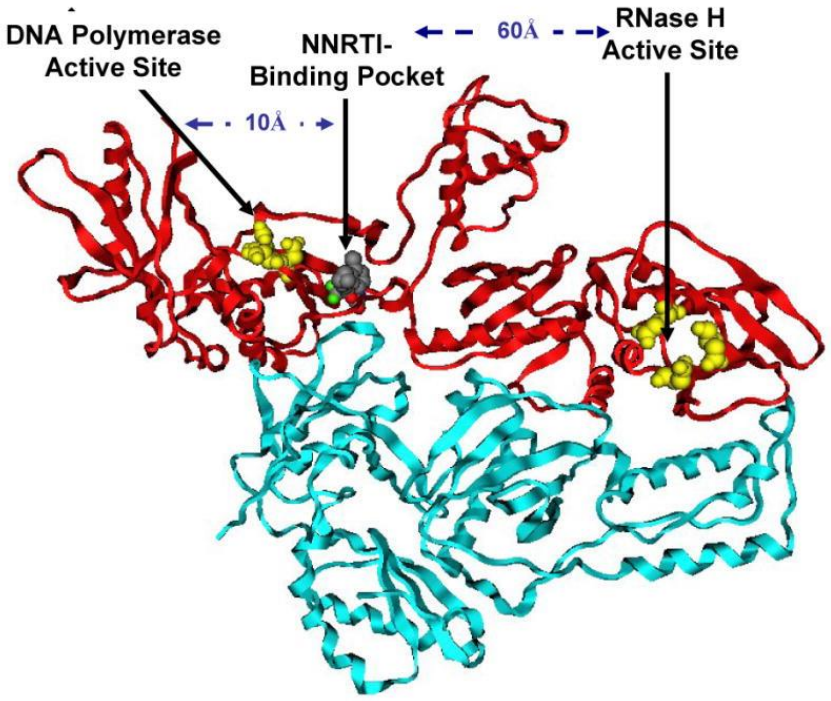

Figure 6: Illustration of the HIV-1 RT (red and blue) bound to efavirenz (NNRTI). The distances of the RNase H active site and the DNA Polymerase active site from NNRTI-BP are indicated. (Figure reproduced from Sluis-Cremer *et al.*)[36]

To initiate the transcription of the viral RNA to DNA, the DNA polymerase and RNase H activities must be aligned. The location of the NNRTI-BP in the RT has been proven to not be a limiting factor in the ability of the effectiveness of the NNRTIs as they can still inhibit the activity at the RNase H active site.[36] Specific inhibition of plus-strand initiation is a vital mechanism by which NNRTIs hinder the replication of HIV-1 and the efficacy of the NNRTIs is noted to have a greater probability in inhibiting polymerization of longer chain products as seen in different types of assays. The synthesis of the plus-strand from polypurine -rich primers (PPTs) is initiated after the minus strand synthesis, however NNRTIs can inhibit the initiation of the plus strand synthesis without having to block the minus strand synthesis.[37]

1.1.6.1.3 FDA-approved NNRTIs and their chemical structures.

Presently there are six NNRTIs that have been approved by the Food and Drug Administration agency (FDA): nevirapine (NVP, 1996), delavirdine (DLV, 1997), efavirenz (EFV, 1998), etravirine (ETR, 2008), rilpivirine (RPV, 2011) and doravirine (DOR, 2018). NNRTIs have the ability to fit within the NNRTI BP as a result of the way that they bind in a "butterfly", "horse-shoe" or "U" mode with a central scaffold and 2 wings as seen in **Figure 7**.[38] They all have very similar chemical structures that permit these molecules to form bonds within the NNRTI-BP of the HIV-1 RT, when this occurs there are changes in conformational orientations and the activity of the DNA polymerase enzyme is halted. The challenge with the HIV-1 is its ability to mutate when it replicates, and the resultant mutant forms have different chemical structures reducing the efficacy of NNRTI that previously could inhibit the wild-type version of the HIV-1. The efficacy of the NNRTI treatment is now dependent on the modification of compounds that will be active to inhibit the mutant forms of the virus as described by Viira *et al.*[39]

The effectiveness of NNRTIs is dependent on their ability to overcome the results of common drug-resistance mutations. Attributes considered when designing new potential drugs, such as torsional flexibility of the chemical bonds are important as the rotation about the axis of the bonds gives rise to different conformations of the compounds. These different conformations or shapes of the molecules in turn have different physical and chemical properties and these qualities can combat single/multi-point drug resistance mutations. The first-generation NNRTIs such as nevirapine's chemical structure had limitations with regard to rotatable bonds and this led to the loss of potency around a single drug resistance mutation.[40]

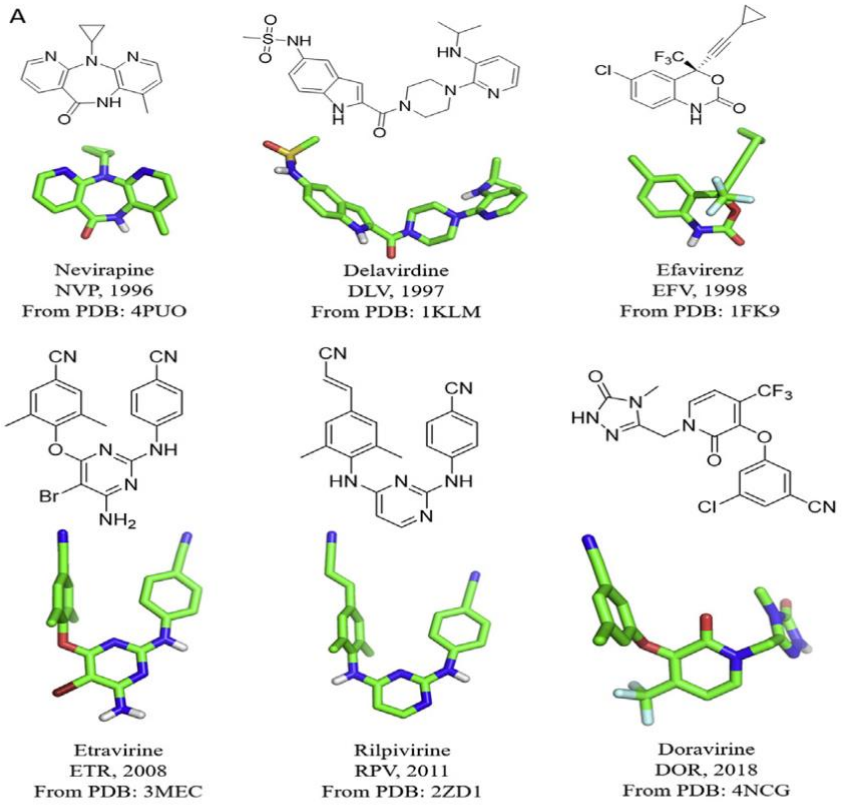

Figure 7*:* Chemical and 3D structures of the 6 currently FDA-approved NNRTIs which have been retrieved while bound to HIV-RT illustrating the "butterfly", "horseshoe", or "U" binding modes with a central scaffold and two "wings" shown in representation **A**. (Figure reproduced from Zhuang *et al*.) [38]

The most vital NNRTI-RT interactions with respect to successful binding are hydrophobic interactions, hydrogen bonds with the K101 main-chain carbonyl oxygen and water-mediated hydrogen bonds. Increased hydrogen bonds present in between these interactions amplify the torsional flexibility, thereby improving the strength against resistance mutations. Therefore, the design of drugs with the ability to remain effective even after several virus mutations is of utmost importance with the consideration of all the important factors such as low toxicity, substantial antiviral activity, and beneficial pharmacokinetic properties.

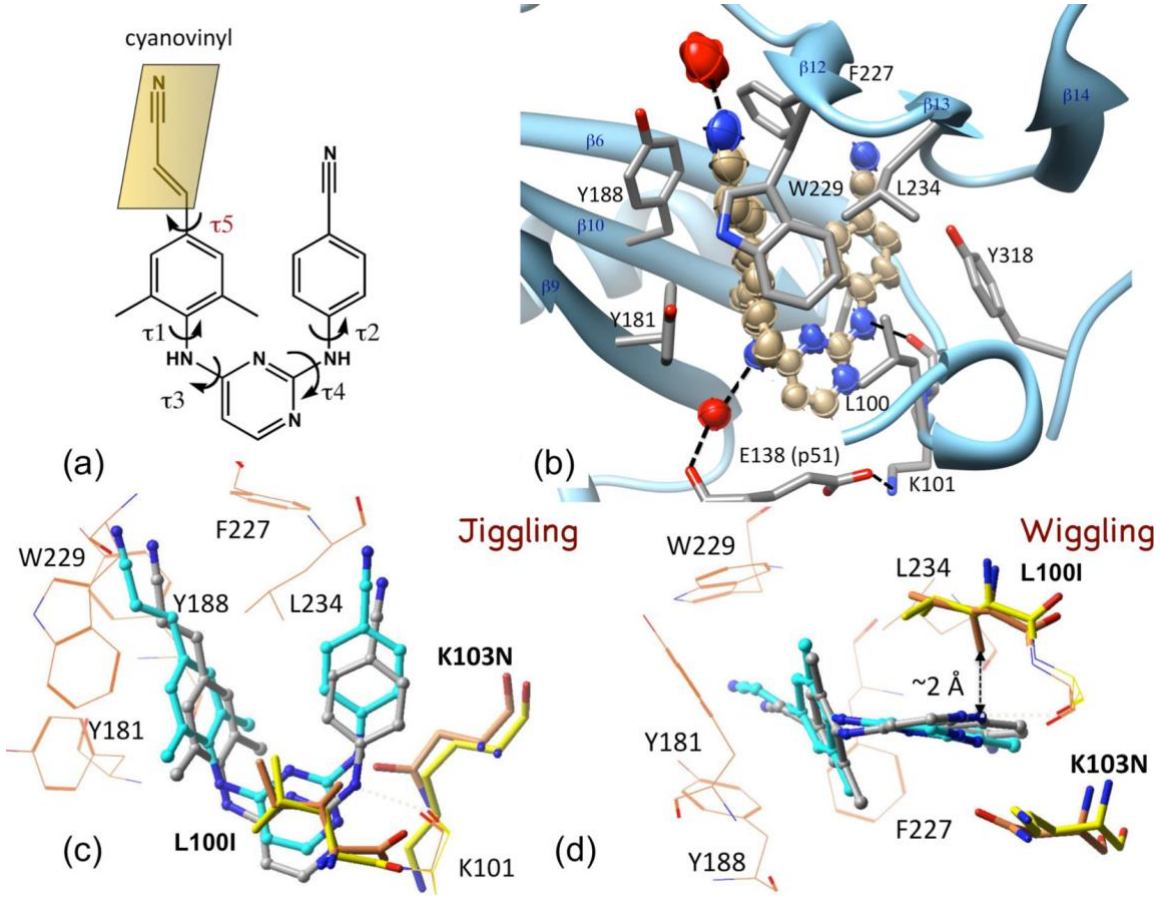

Figure 8*:* Various motions and structural orientations of rilpivirine to maintain efficacy against mutant forms of HIV-1. (**a**) Structure of rilpivirine exhibiting a number of conformational forms. (**b**) Magnitude and directions of thermal vibrations of a RT-rilpivirine complex. (**c & d**) Illustration binding modes exhibited by rilpivirine when bound to

wild-type RT (gray) vs. L100I + K103N mutant RT (cyan). (Figure reproduced from Das *et al*., Chong *et al*.) [41,42]

Figure 8 is a visual representation of rilpivirine's chemical structure and how its design has rendered the drug an effective NNRTI against the resistance mutants K1001+K103(RT) due to its flexible bonds that lead to conformational changes and give rise to the *wiggle* and *jiggle* actions altering the binding in the NNRTI binding pocket. The cyanovinyl group has the capability of maintaining its hydrophobic interactions with the RT even with the mutant formations and this increases the potency of rilpivirine.[41,42]

The chemical structure of rilpivirine which possesses a pyrimidine moiety (**Figure 9**) allows for rotation about the bonds thereby exhibiting various conformations which provide a vital role in the interactions with the RT enzyme. As drug resistance mutations progress, rilpivirine can alter its structural orientation due to the torsionally flexible bonds allowing for effective interactions with the mutant binding site. This led us to explore the properties of the triazine core which is very similar to the pyrimidine core apart from an additional nitrogen atom within the ring (**Figure 9**).[43] The biological activity of the triazine core has been reported in literature for various treatment regimens such as altretamine which is used in treating various cancers (Figure 8). However, limited research has been carried out to test the activity of triazine derivatives, with three nitrogen atoms, as NNRTIs as compared to the pyrimidine core, with two. The biological properties will be discussed in detail in the next section.

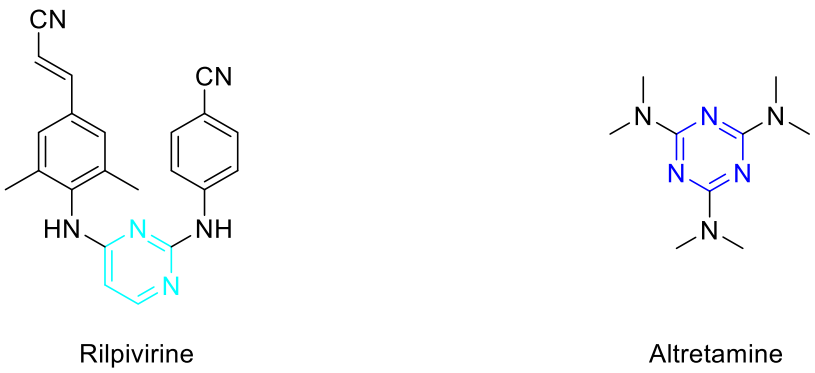

Rilpivirine Altretamine

Figure 9: Structure of rilpivirine (pyrimidine core) in comparison to altretamine (triazine core).

1.2 Chemistry of Triazines

Triazine is a six-membered heterocyclic aromatic ring which consists of three nitrogen atoms and three carbon atoms with alternating single and double bonds. Its structure is similar to that

of benzene with the exception of the three nitrogen atoms replacing three carbon atoms at different positions thereby exhibiting isomeric forms as seen in **Figure 10**.[44]

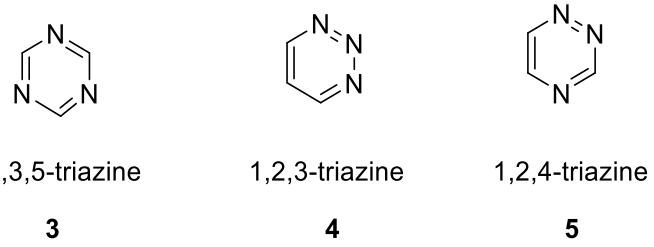

Figure 10*:* Illustration of the 3 isomeric forms of triazine

1.2.1 Triazine isomers

1.2.1.1 1,2,3-Triazines

This isomeric form of the triazine ring is asymmetrical and has the nitrogen atoms at positions 1, 2 and 3 of the ring structure. The 1,2,3-triazine (**4**) moiety is the least stable of the three isomeric forms and synthetic procedures to access this core are limited.[45] The electronic configuration of 1,2,3-triazines is such that one of the p orbitals on each nitrogen atom overlaps with the p orbitals of the adjacent nitrogen atoms to form delocalized π bonds. There are a limited number of electrons available for delocalization thereby rendering the triazine ring electron deficient.[46] This property has led to this isomeric form of triazines being investigated as azadienes in the inverse-electron-demand Diels−Alder reactions.[47] These reactions have proven to be an interesting area of study to develop new synthetic routes that can be explored in the preparation of heteroaromatic systems with multiple substitutions that are not easily accessible via conventional methods. Synthesis of 1,2,3-triazine derivatives (**8)** has been previously carried out via *N*-amination of pyrazoles (**6)** to form *N*-aminopyrazoles (**7**) followed by an oxidative ring expansion as seen in **Scheme 1.**[46 - 48] However, due to the limitations of

the structural or symmetrical forms of the resultant products, other synthetic methods have been explored.

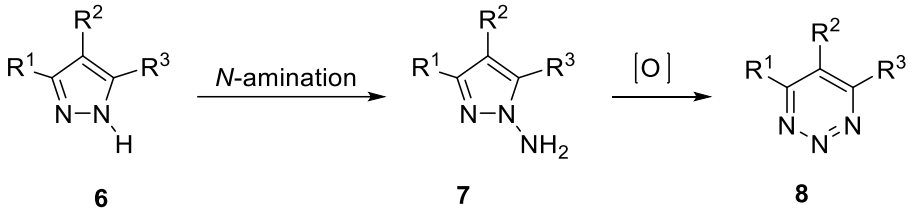

6 **7** **8**

Scheme 1: General schematic route to synthesise 1,2,3-triazines via amination and oxidative ring expansion.

Studies carried out by Boger and his colleagues revealed work on the cycloaddition reactions of 1,2,3-triazine derivatives that enhanced their reactivity thereby substantially expanding the options available to explore with regards to these types of reactions. The mode of the cycloaddition reactions was influenced by the reactants being utilised with the ynamines directing the C5/N2 cycloaddition as compared to the C4/N1 when amidines and enamines are reacted with the 1,2,3-triazines. In some of their findings, they reported excellent yields of reactions between 1,2,3-triazine derivatives **9** and **10** and ynamines **11** as a result of cycloaddition across C5/N2 with the nucleophilic carbon of the ynamine attaching to C5 to result in pyridazine compounds **13** or **14** (**Scheme 2**). They also noted that ynamine-derived C5/N2 cycloadduct **12** exclusively undergoes a retro-Diels−Alder loss of HCN (vs EtO_2CCN) providing a single pyridazine **13**.[49,50]

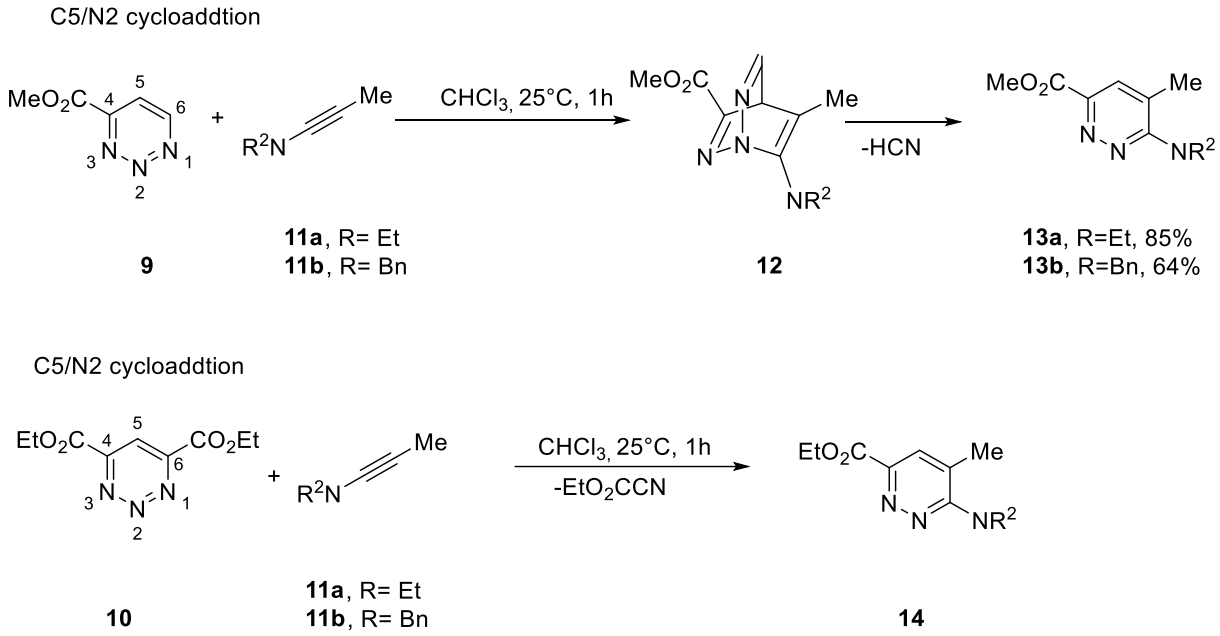

Scheme 2: [4 +2] cycloaddition reactions of 1,2,3-triazines with ynamines to yield pyridazine products carried out by Boger and colleagues.[49]

1.2.1.2 1,2,4-Triazines

The 1,2,4-triazines (**5**) have been investigated in more detail as compared to the 1,2,3-triazines and their reactions are also very similar with respect to Diels-Alder reactions. 1,2,4-Triazine **5**, 1,3-oxazin-6-one **15**, 1,4-oxazin-2-one **16**, pyrazinone **17** and pyrimidines **18** were successfully utilized as 2-azadienes in inter- and intramolecular hetero-Diels Alder (DA) reactions with alkynes, substituted alkenes and heterocycles to prepare functionalized pyridines **20** via bicyclo [2.2.2] intermediates **19**, as shown in **Scheme 3**.[49,53]

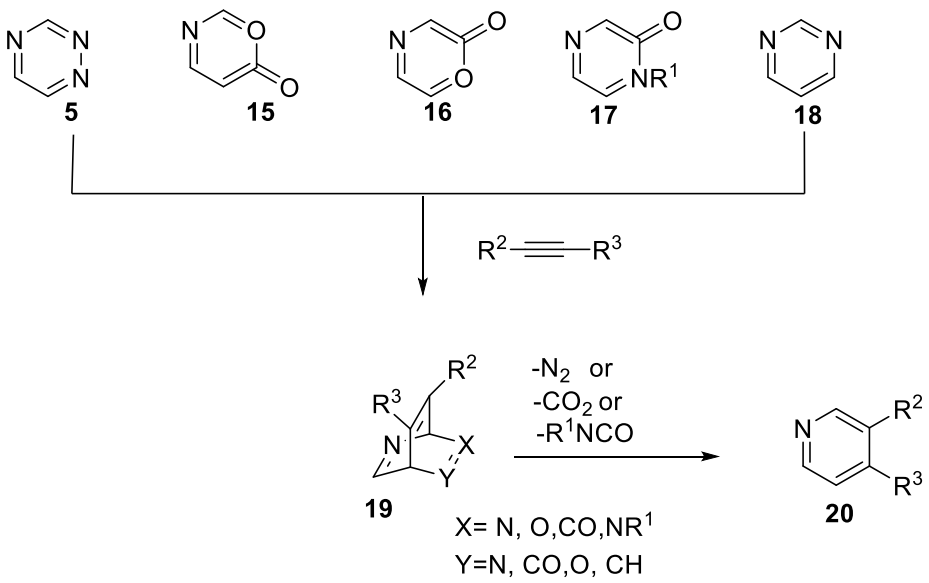

Scheme 3: Compounds acting as 2-azadienes in Diels-Alder reactions to produce pyridines.

Studies carried out and documented by Boger have revealed that the effects of the addition of electron withdrawing groups to the l,2,4-triazine nucleus which include a more reactive triazine ring, modified types of cycloaddition reactions and the favoured regiochemistry of the reactions.[50] 1,2,4-Triazines have been identified as important and diverse biorthogonal reagents and from computational studies of activation free energies, they exhibited themselves as more reactive than the 1,2,3-triazines.[51] Bioorthogonal reagents are chemical compounds or molecules that can react selectively with particular biomolecules or biomolecular processes in living systems without interfering with the natural intracellular biochemical processes.[52] Multi-substituted pyridines have been synthesized via cycloaddition reactions between 1,2,4-triazines and dienophiles such as enamines, enols, alkynes, and specific alkenes.[42,53] Dawane and co-workers synthesised 1,2,4-triazine derivatives by the condensation of substituted 4-(2-chloro-quinoline-3yl methylene)-2-[phenyl-4*H*-oxazol-5-one] and phenyl hydrazine in glacial acetic acid as a solvent. The mechanism of these reactions has been illustrated in **Scheme 4** with the reaction being initiated by the phenyl hydrazine attacking the carbonyl carbon.[54]

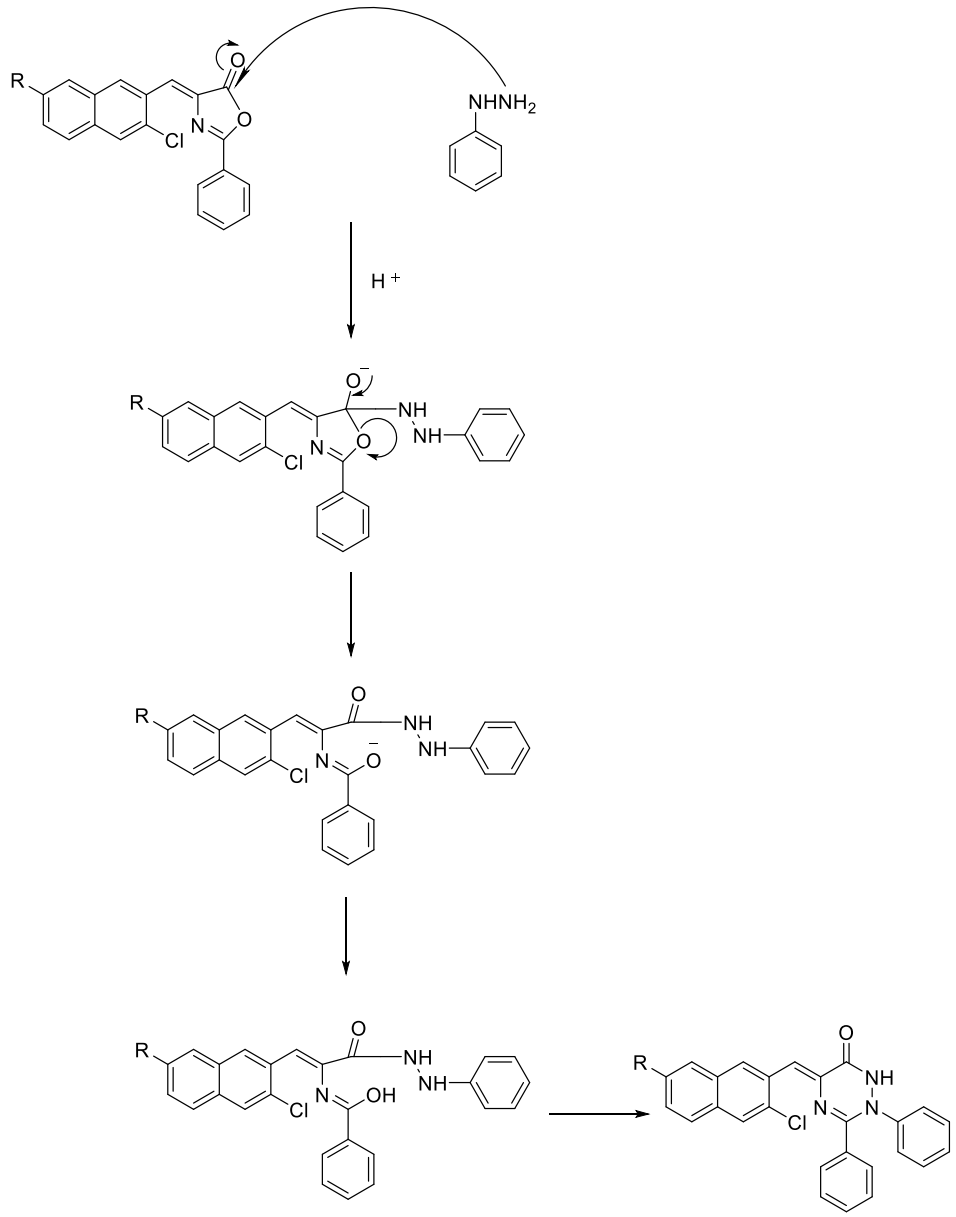

R= CH_3, Br, OCH_3, Cl, NO_2, H, I, F

Scheme 4: Mechanism of reaction to synthesize substituted 1,2,4-triazine derivatives.

1.2.1.3 1,3,5 or s-Triazines

This isomeric form of the triazine has been termed the s-triazine (**3**) due to its symmetry of the nitrogen atoms which are positioned at equal distances to each other in the ring.[55] Numerous forms of the 1,3,5-triazines have been reported (**Figure 11)** which include cyanuric acid (2,4,6-trihydroxy-1,3,5-triazine), cyanurates (2,4,6-trialkoxy-1,3,5-triazine), cyanuric chloride (2,4,6-

trichloro-1,3,5-triazine), isocyanurates (1,3,5-trialkyl-1,3,5-triazine-2,4,6-triones) and melamine (2,4,6-triamino-1,3,5- triazine).[55]

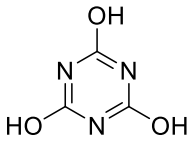

2,4,6-trihydroxy-1,3,5-triazine

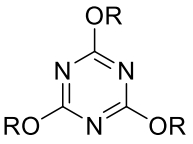

2,4,6-trialkoxy-1,3,5-triazine

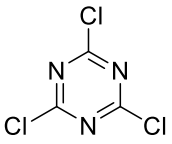

2,4,6-trichloro-1,3,5-triazine

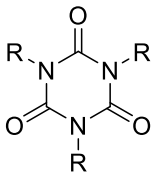

1,3,5-trialkyl-1,3,5-triazine-2,4,6-triones

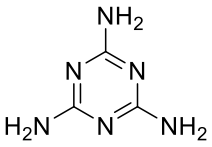

2,4,6-triamino-1,3,5-triazine

Figure 11: Selected forms of s-triazines

The 1,3,5-triazine has a lower resonance energy as compared to benzene and this property gives it the ability to be more reactive, leading to the addition of more functional groups to the molecule in substitution chemical reactions.[54,59] Nitrogen, oxygen, sulfur and halogens are classified as some heteroatoms and their presence in different molecules can alter the chemical properties of that molecule in terms of reactivity and polarity. The s-triazine ring has been highlighted in a number of synthetic methodologies in the past as it can participate in molecular recognition and has synthetic versatility. Formation of interactions with other molecules via hydrogen bonds, metal chelation and π-π interactions gives it desirable attributes in drug synthesis and design models.[57-58] A number of routes have been investigated to successfully synthesise 1,3,5-triazine derivatives and these include cycloaddition and cyclotrimerization

reactions. One example is the cycloaddition reaction of nitriles **21** and cyanoguanidine **22** to form diaminotriazine derivatives **23** as exhibited in **Scheme 5**.[54,59]

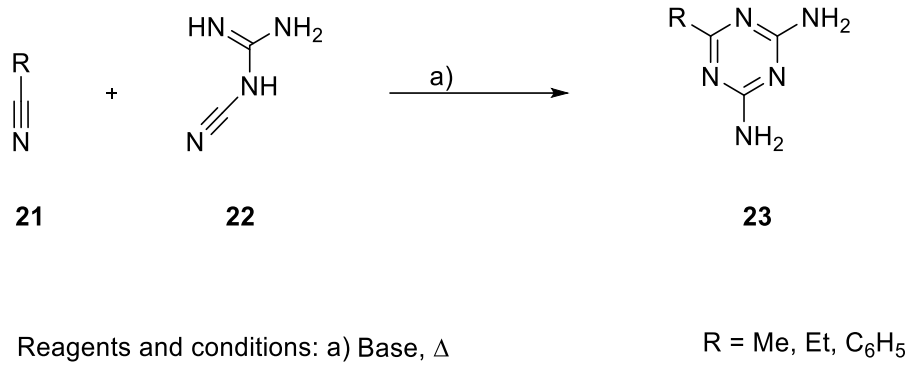

Scheme 5: Cycloaddition reaction to form a diaminotriazine derivative.

Substantial research has also demonstrated that 1,3,5-triazine derivatives can be synthesised from reactions of trichloroazacycles such as trichlorotriazine (TCT) and copper-catalyzed cross-coupling of Grignard reagents.[59] Challenges have been experienced in the past with respect to direct synthesis of symmetrical 1,3,5-triazine derivatives. To curb these challenges, methods such as cyclotrimerization of nitriles whilst monitoring conditions such as pressure and use of catalysts were employed to successfully yield expected outcomes. In **Scheme 6** a one pot reaction of a nitrile R^1CN (**24**) with Tf_2O as the catalyst and two molar equivalents of another nitrile R^2CN (**25**) were reacted to afford a 1,3,5-triazine (**26**).[60]

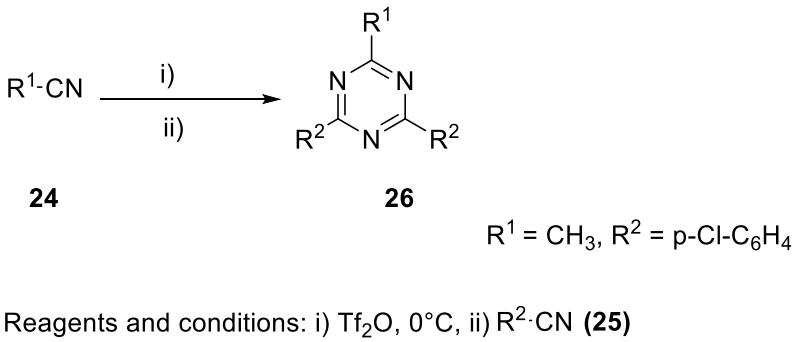

Scheme 6: Cyclotrimezation of nitriles to afford 1,3,5-triazine derivatives.

The s-triazine has also been investigated in the synthesis of triazine dendrimers for medical applications. Triazine dendrimers have been utilized in the delivery of genes during drug dispersal via covalent or noncovalent bonds. The multivalent sites on the surface of the dendrimers offer the platform for the use of covalent and noncovalent bonding interactions drug dispersal, to be implemented in drug delivery.[61] Historically, convergent routes were utilized in the large-scale synthesis of triazine dendrimers, however, recent studies by Lim *et al* have opted for the divergent route for large scale synthesis. (**Scheme 7**).[61-63]

This approach is carried out via a 3-step iterative sequence to successively afford each generation of dendrimers and it was demonstrated that up to 5 generations could be synthesized. Preparation of these dendrimers involved the addition of the dichlorotriazine monomer **27** to the triazine core **28**, followed by capping with piperidine and deprotection with good yields of up to 80 % for generation 1 dendrimer **29**.The success of the preparation of these dendrimers was also counteracted by some challenges such as low solubility of these compounds which was explored in later studies to improve the solubility.[63-64]

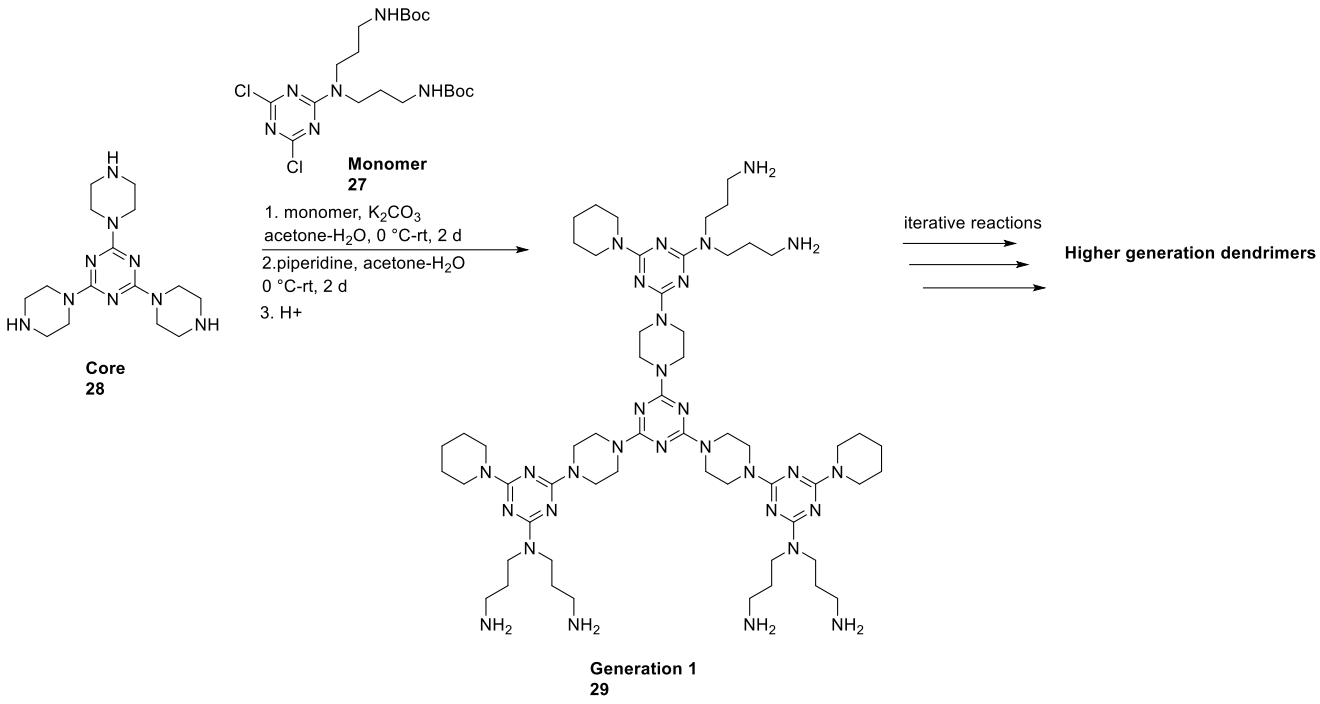

Scheme 7: Synthesis of triazine dendrimers using the divergent route.

Although cycloaddition and cyclotrimerizations reactions have been commonly utilized, 1,3,5-triazine derivatives have also been accessed via the modification of a triazine moiety. As discussed earlier the triazine ring is similar to benzene but differs as it possesses nitrogen atoms within the ring. The C=N bonds are highly polar resulting in a much lower delocalization energy. **Figure 12** shows the results of the polarization to the molecular resonance structure of the s-triazine leading to electron deficient carbon atoms within the ring. This property makes the s-triazine a good moiety in nucleophilic substitution reactions as specific nucleophiles are able to attack the electrophilic carbon atoms.[65]

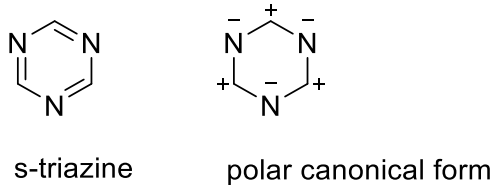

Figure 12: Molecular structure of s-triazine and its polar canonical form

Nucleophilic aromatic substitution of cyanuric chloride **30**, also known as 2,4,6-trichloro-1,3,5-triazine as stated earlier has also proven to be a progressive method in the synthesis of 1,3,5-triazine derivatives and will be the core method utilized for our work (**Scheme 8**). The reactive sites in the s-triazine due to the presence of nitrogen atoms are a favourable property in drug synthesis and modification studies. The substitution of a chlorine atom in cyanuric chloride by a nucleophile is favoured by the ring nitrogen atoms of the s-triazine nucleus, these nitrogen atoms are evenly distributed within the ring. [66]

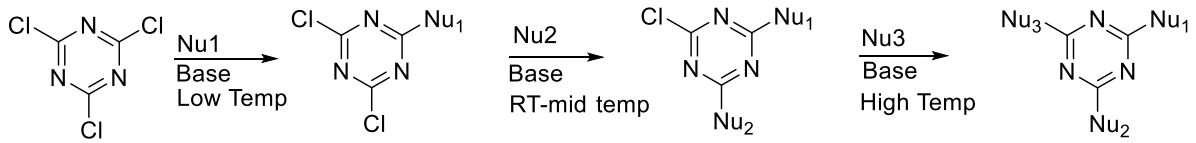

30

Scheme 8*:* Nucleophilic aromatic substitutions of cyanuric chloride.

Synthetic reactions involve a multi-step approach by substituting each chlorine atom attached to the triazine core with different incoming nucleophiles that possess distinct chemical properties which are beneficial to the final desired products. The triazine ring is moderately resistant to electrophilic substitutions.[67] In studies where the triazine core was utilised in the synthesis of high-performance polymers, it was noted that an amino group in the s-triazine ring has characteristics like that of a nitrogen atom in an amide group, because of the electron withdrawing effect of the s-triazine ring. [68]

1.2.2 Biological activity of 1,3,5-triazine derivatives

Our interest in 1,3,5-triazine derivatives lies in using them as the core for the design and synthesis of a new class of potential NNRTIs. This compound class possesses significant biological activity and has found application in various areas. For example, activities include anti-protozoal,[69] anticancer,[70] anti-HIV,[71] oestrogen receptor modulation,[72] anti-inflammatory,[73] antibacterial,[74] antimicrobial[75] and anti-cancer activity.[76] The 1,3,5-triazine core has been used as a building block for numerous classes of medicines with valuable uses as displayed in **Figure 13** owing to its previously mentioned reactivity.[75]

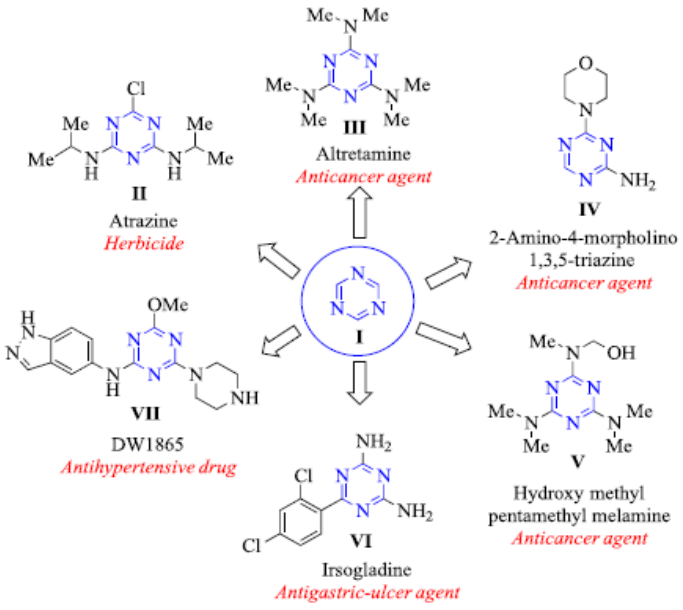

Figure 13: A range of pharmacologically active 1,3,5- triazine core compounds.[75]

1.2.3 Functionalization of the triazine ring

The aim of our work is to design compounds which will exhibit significant interactions with the RT enzyme at its allosteric binding site. Previous studies have investigated structural similarities between NNRTIs with activity against the wild type and mutants and incorporated

information obtained from molecular docking studies and used this information to design new compounds. A number of crystal structures of RT/NNRTIs complexes have been reported.[77-78] We will explore a similar approach wherein modifications will be made by incorporating substituents on to the triazine ring with the ability to form hydrogen bonds with the backbone NH of the Lysine 103. The selection of vital functional groups with optimised target interactions can be guided by the specific properties of each functional group. Alcohols and phenols contain oxygen and hydrogen atoms that are capable of interacting with the targeted viral enzyme binding site via hydrogen bonding. The oxygen atom acts as a hydrogen bond acceptor due to the presence of its lone pairs of electrons and the hydrogen consequently acts as a hydrogen bond donor.

One of the most vital functional groups in drug synthesis which is present in numerous modern drugs is the amine functional group. Amines can act as both hydrogen bond donors and hydrogen bond acceptors, due to the nitrogen atom that contains a lone pair of electrons, and the hydrogen atom that can act as a hydrogen bond donor. This is the case with primary and secondary amines. Aromatic and heteroaromatic amines can only act as hydrogen bond donors due to the fact that the lone pair of electrons is involved within the ring interactions. Notably, when an amine undergoes protonation as it interacts with the binding site of the enzyme it ceases to act as a hydrogen bond acceptor, albeit can act as a hydrogen bond donor with the formation of an even stronger hydrogen bond. [79]

As a result of the interesting biological activities of triazines, they have previously been explored as potential NNRTIs. Diaryltriazine (DATA) analogues with different substituents have been synthesized and evaluated for their *in vitro* anti-HIV activity with positive promising results reported.[38, 79-81] This information has provided insight on modifications that we will explore to optimize the triazine ring to design potential NNRTIs that can exhibit good activity against the HIV-1 wild type and mutant forms. For example, Zhuang and colleagues proved that the 4-cyanophenyl moiety is very useful as it can form hydrophobic interactions with the F227/P236 residues of the RT enzyme.[38]

Aromatic heterocyclic rings are hydrophobic and nonpolar in nature and are able to form hydrophobic and van der Waals bonds in the binding site of the RT enzyme. The use of aromatic substituents coupled to the 1,3,5-triazine will be employed in our work to favour the π-π stacking interactions between the compound and the hydrophobic region (W229) of the RT enzyme.[82-83]

1.3 Project aims and objectives.

NNRTIs are important in the treatment regimens of HIV/AIDS due to their ability to restrict the replication of the HI virus. Development of new NNRTIs is desirable due to the ability of viral mutants to develop resistance to NNRTIs, particularly the earlier generation of compounds. In order to mitigate against the successive progression of the viral mutants, the aim of this project is to prepare triazine centered compounds with the potential of possessing activity against viral mutants. We aim to synthesize structurally diverse triazine derivatives using commercially available cyanuric chloride as a starting material in a multi-step process.

The synthetic strategy will involve nucleophilic substitution reactions to successively replace all of the chlorine atoms from the cyanuric chloride, as illustrated in **Scheme 10**. The use of thiol-, phenol- and amine-bearing nucleophiles is planned. Optimal conditions will be determined to avoid the formation of bis- and tris- substituted triazines at each stage. These substitution reactions will be carried out based on the strength and structure of incoming nucleophile as well as the reactivity profile of cyanuric chloride.

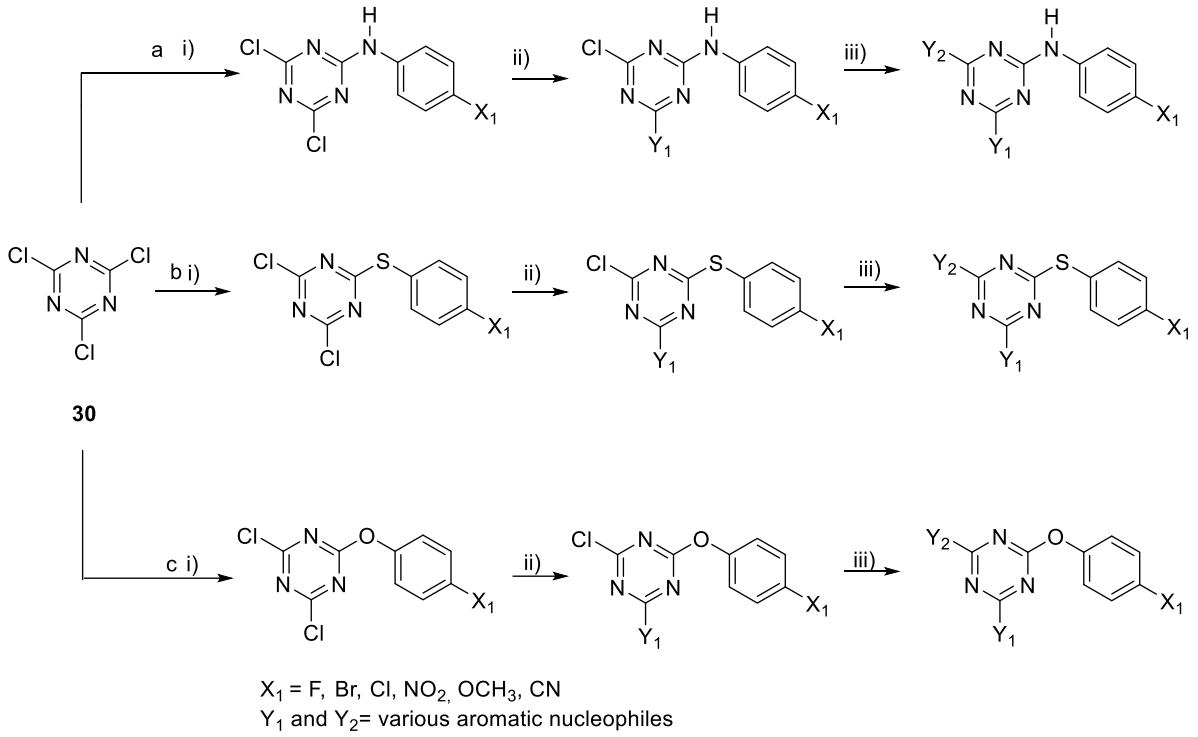

Reagents and conditions: i) Substituted aniline/thiol/phenol, base ii) Y_1, base iii) Y_2, base

Scheme 10: Proposed synthetic plan for the stepwise synthesis of triazine derivatives

Synthesized compounds will be isolated and standard spectroscopic techniques will be used to identify and fully characterize the products. Selected products will be subjected to anti-HIV activity evaluation studies to determine the anti-HIV potency and record EC_{50} values obtained. After all tests are completed, conclusions will be drawn as to which compounds exhibited favorable antiviral activity and low toxicity levels.

Chapter 2

2. Results and Discussion

The main objective of the work carried out was to synthesize diverse substituted triazine derivatives in order to develop an array of possible NNRTIs with low toxicity and high efficacy against viral mutants by the systematic functionalization of cyanuric chloride **30**. As stated in the previous chapter the triazine core has exhibited important pharmacological properties that make it a vital scaffold as a backbone of drug synthesis.

It was deemed viable to utilize the cost effect cyanuric chloride as the substrate for the reactions that would favour the nucleophilic substitution mechanism. To successfully substitute one of the Cl atoms from the triazine moiety in a sequential manner, a number of conditions had to be maintained to avoid accidental synthesis of the bis- and tris- aromatic substituted triazines. Previous studies of the reactivity profile of cyanuric chloride have shown that as more substituents, specifically bulky nucleophiles, replaced the Cl atoms these compounds became less reactive to subsequent nucleophiles and more vigorous conditions were required to achieve trisubstituted triazine derivatives.[83] We began by investigating the chemical structures of the FDA-approved NNRTIs and their limitations and possible areas of improvement, and we also evaluated other possible NNRTIs that have been synthesized using the 1,3,5-triazine nucleus and their structural modifications to satisfy the key objectives of the scientific studies. This information assisted us in determining the types of nucleophiles to be utilized to create the new bonds after the C-Cl bond was broken. S-, N- and O- bearing aromatic rings were selected for all the coupling reactions conducted, which resulted in these different heteroatom linkers being present in the final compounds.

One aspect of the synthesis of these compounds that we had not anticipated was that the NMR characterization of the compounds would be extremely complex. This is due to the splitting of peaks and broad indistinct ^{1}H- and ^{13}C-NMR signals as a result of multiple conformations that can be adopted by these compounds in solution. These phenomena will be demonstrated in detail further on in our findings and is in line with what has been reported previously.

For the purposes of simplicity and convenience we have not adopted the standard IUPAC numbering system for the structures in the discussion, but the naming of the compounds is in accordance with the IUPAC convention.

2.1 First nucleophilic substitution reaction

Nucleophilic substitution reactions were carried out by reacting cyanuric chloride **30** with substituted anilines, thiols and phenols with NaOH solution as a base in acetone. The temperature during these reactions at this stage was kept between 0-5°C to slow down the rate of the reaction and control the selectivity as only 1 substitution of the Cl atoms was desired**.**

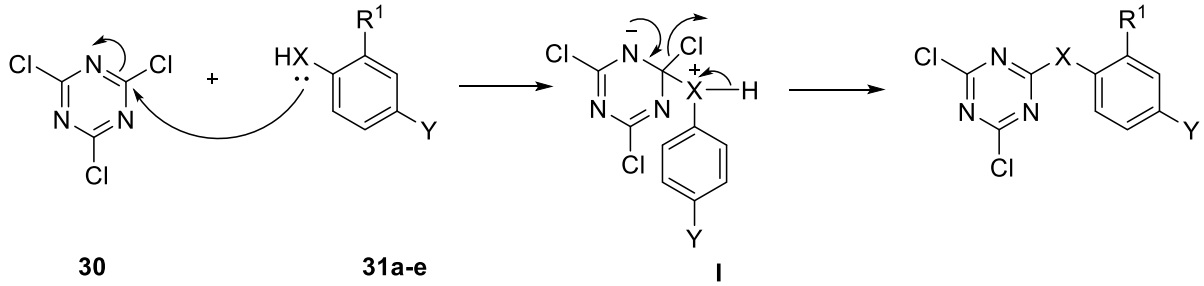

Scheme 11: Mechanism of the S_NAr reaction

The nucleophilic substitution reaction is initiated when an incoming nucleophile which is electron donating attacks the electron deficient carbon that is bonded to one of the chlorine

atoms. The C-Cl bond is polarized with the C bearing a partial positive charge and the Cl bearing a partial negative charge, and this energetically favors the nucleophilic attack (**Scheme 11)**. The strength of the nucleophile is influenced by the substituents attached to the aromatic ring, electron withdrawing groups (EWG) tend to decrease the electron density in the ring system which has an overall effect of reduced nucleophilicity of the incoming nucleophile. The charge and size of the incoming nucleophile also play a significant role in the rate and success of the reaction. The lone pair of electrons donated by the nucleophile **31** activates the formation of a new bond C-Nuc and subsequently the N in the triazine ring is now negatively charged leading to the generation of an intermediate **I**. This intermediate is unstable and elimination of Cl^- allows aromaticity to be restored.

2.1.1 Synthesis of amine-bearing 4,6-dichloro-1,3,5-triazine derivatives

Various substituted anilines with different substituents were reacted with compound **30** to synthesize an array of mono-substituted amine-bearing 4,6-dichloro-1,3,5-triazine derivatives as the first step of the sequential nucleophilic substitution reactions (**Scheme 12**).

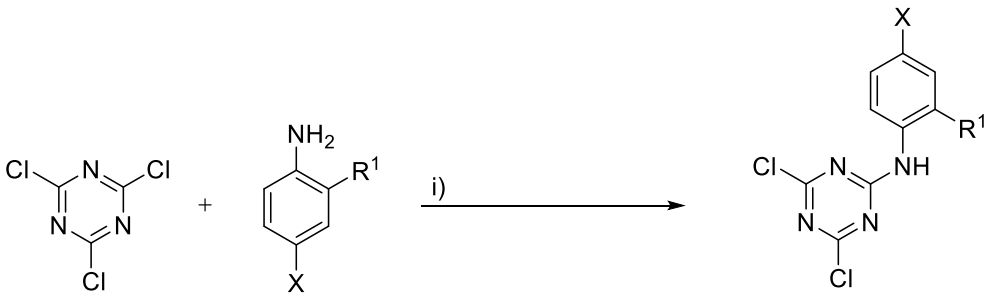

30 **31a-e** **32a-e**

Reagents and conditions: i) Acetone, NaOH (aq) 0-5° C, 4-5 h

Scheme 12: Reaction of cyanuric chloride with amine-bearing nucleophiles

The desired compounds (**Table 1**) were successfully synthesized in moderate to excellent yields of 54-90 % as shown in **Figure 13**.

Table 1: Substituents of synthesized compounds **32a-e**

	X	**R^1**
32a	F	H
32b	Br	H
32c	Cl	H
32d	NO_2	H
32e	Cl	CH_3

An unexpected result was noted from the percentage yields of the desired products obtained wherein the reaction with *p*-nitroaniline afforded a product with the best yield.

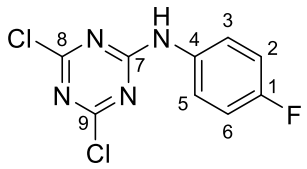

32a: 82 %

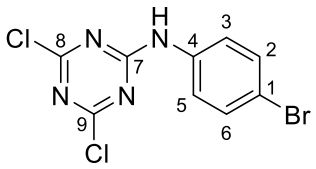

32b: 59 %

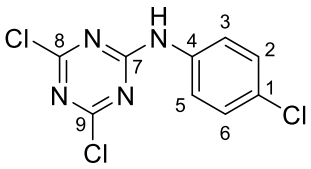

32c: 54 %

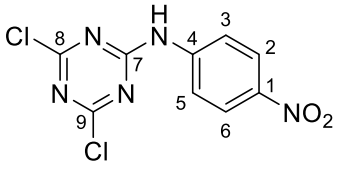

32d: 90 %

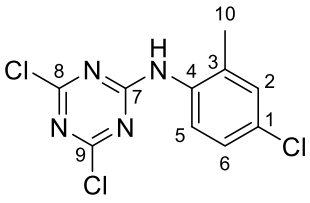

32e: 78 %

Figure 14: Synthesized amine bearing 4,6-dichloro-1,3,5-triazine derivatives and their isolated yields.

The nitro group is a strong electron-withdrawing group (EWG) and this would be expected to cause a reduction in the electron density of the aromatic ring system thereby decreasing the nucleophilicity of the aniline. The nitro group in the *para* position deactivates the amino group.[84] The halogen substituents are also expected to be deactivating agents and reduce electron density of the aniline ring, but not to the same extent as the nitro group. We therefore expected to see the results of the *p*-nitroaniline reaction the least favorable of all the anilines bearing different substituents as seen in **Figure 14**. However, the yields were not a direct or necessarily accurate indication of the reactions reaching completion or efficiency as there were challenges in isolation of compounds **32b**, **32c** and slightly for **32e**. The purification steps using column chromatography resulted in the products being bound to the solid phase (silica gel) and numerous solvent systems were utilized in an attempt to improve the elution of the desired products. For some of the compounds this effort was not highly successful and products were lost, subsequently leading to low yields being obtained.

Compounds **32a-32e** have been previously reported in literature; these compounds were synthesized under similar conditions with slight modifications to improve reaction times. The data reported shows that these reactions involving aniline derivatives give good yields which was comparable to the information we obtained upon characterization of these synthesized products.[85-87]

The first nucleophile applied in these reactions was 4-fluoroaniline and the product **32a** was isolated in a good yield of 82 %. ^{1}H NMR and ^{13}C NMR data was vital in the characterization of the synthesized products, due to the fact that cyanuric chloride (**30**) does not possess any protons, the presence of any signals in the aromatic region of the ^{1}H NMR spectrum confirms that a substitution has occurred.The data observed for compound **32a**

showed signals for 2 protons at δ 7.65-7.54 and 2 protons at δ 7.28-7.20, which supports the presence of aromatic protons. The signals for H-3 and H-5 appear as multiplets and due to symmetry, these protons are equivalent and appear as 1 signal and the same was observed for protons at H-2 and H-6. The N-H signal appears downfield as a singlet at δ 11.14, as the proton is directly attached to a nitrogen atom which is electronegative, the proton is deshielded. The triazine ring is electron poor and so there is delocalisation of the nitrogen lone pair electrons of the NH into the triazine ring, which leaves the proton of the N-H electron deficient, leading to the downfield chemical shift.

The ^{13}C NMR spectrum was interesting for the quaternary carbons in the triazine ring. We expected to see one signal for C-8 and C-9 as they are chemically equivalent, but instead there were two signals at δ 169.7 and 168.8. The carbon atoms are deshielded as they are attached to one chlorine atom and two nitrogen atoms. There were 2 signals observed for C-7 with a major signal at δ 163.8 and a minor signal at δ 163.7 which confirmed the presence of conformers. The C-F coupling constants observed in the ^{13}C NMR spectrum confirmed the presence of the aromatic compound bearing a fluorine substituent and this also assisted in the assignment of the carbon atoms in the synthesized product. The signal for C-1 was observed at δ 159.2 and was identified as the carbon directly attached to the fluorine atom, due to the downfield shift and a large carbon-fluorine coupling constant, $^{1}J_{C\text{-}F}$ = 242.2 Hz. We observed a major conformer for C-2 and C-6 at δ 115.6 and a minor conformer at δ 115.0 and they both showed a $^{2}J_{C\text{-}F}$ = 22.6 Hz coupling constant. Similarly for C-3 and C5 minor and major signals were observed at δ 124.0 and 123.6 respectively, they exhibited a $^{3}J_{C\text{-}F}$ = 8.3 Hz coupling constant. The carbon furthest from the fluorine had the smallest coupling constant which was

identified to be C-4 which was observed at δ 133.2 with $^{4}J_{C\text{-}F}$ = 2.7 Hz which is supported by literature values for C-F coupling constants.[88]

We then moved on to react different nucleophiles with cyanuric chloride **30** to yield compounds **32b-32e**. All the compounds prepared were characterised using NMR, IR and mass spectrometry and the results were as expected. Afonso and his colleagues were able to prove that substitution reactions involving aliphatic primary amines were successful with high yields as compared to utilizing secondary amines which proved to be more complex to work with, resulting in unfavorable results.[83] This is consistent with the results we obtained as we synthesized products using primary amines with good yields as reported earlier. Secondary amines are bulky and more hindered as compared to primary amines and based on the reactivity profile of cyanuric chloride their reactions require more vigorous conditions to obtain the desired products in good yields.

The presence of conformers in some of the synthesized compounds was observed in the ^{13}C NMR spectra. Conformational isomers are observed when a molecule is able to exhibit different spatial arrangements as a result of restricted rotation about certain bonds. In compound **32d**, as shown in **Figure 15**, major and minor peaks for the same carbon atom confirmed the presence of conformers. Conformers of this molecule are seen when some carbon atoms have more than 1 signal in the NMR spectrum as the different conformers experience distinct chemical environments. The chemical shifts at δ 143.6 & δ 144.3 (C-4), δ 143.4 & δ 142.9 (C-1), δ 121.2 & δ 120.6 (C-3 and C-5) all represented the major and minor conformers, respectively, of compound **32d**.

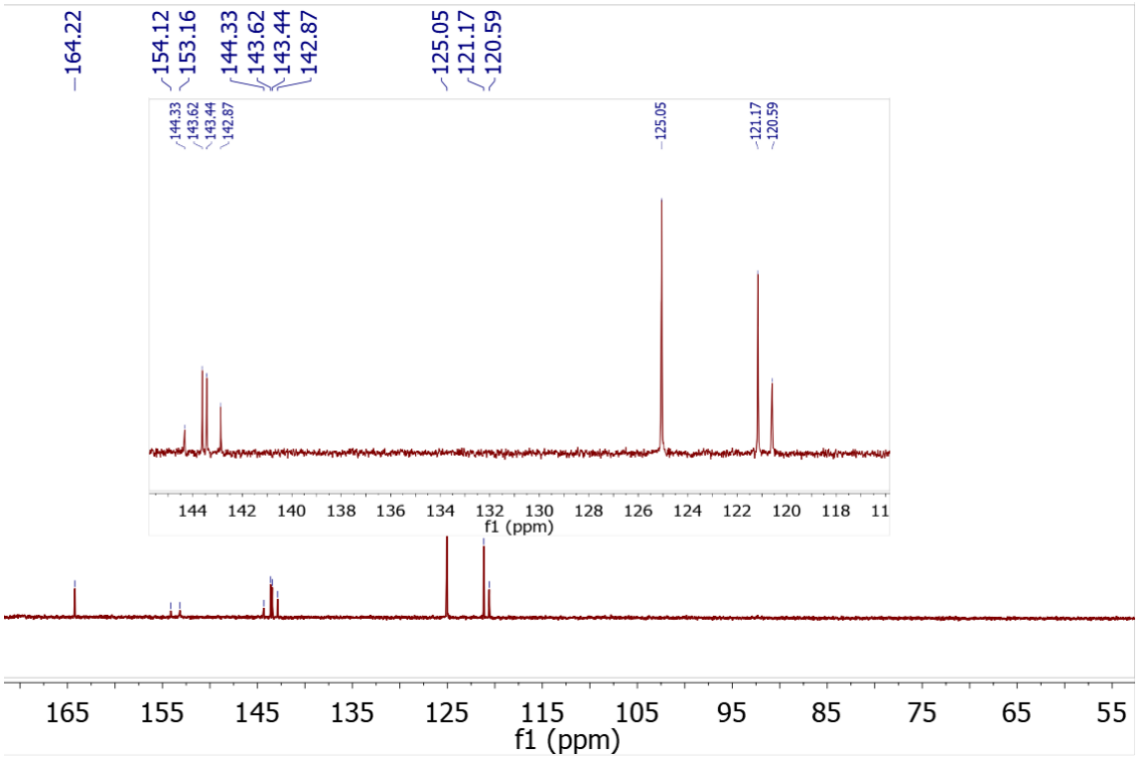

Figure 15: ^{13}C NMR Spectrum (101 MHz, DMSO- d_6) of **32d**.

The signal in the ^{13}C NMR spectrum of **32e** at δ 17.5 confirmed the presence of the methyl group C-10 attached to the C-3 of the aromatic ring. This shift value is consistent with where it is expected to be seen for a primary carbon attached to an aromatic ring. The methyl group attached to C-3 in compound **32e** is electron donating and effectively increases the electron density in the aromatic ring via the inductive donating effect which may have led to a shielding effect on the NH proton. The chemical shift for this NH proton was observed at δ 10.70 as compared to the range of δ 11.14-11.60 for compounds **32a-32d. Table 2** shows selected chemical shifts for compounds **32b-e**. In comparison the signal for C-1 in compound **32b** is more upfield as compared to **32a**, **32c** and **32d**. C-1 in **32b** is attached to a Br-atom which is less electronegative, and the carbon atom is more shielded than when attached to Cl or NO_2 which are more electronegative or electron-withdrawing. This reduces the electron density and results in a deshielded environment around the carbon nucleus. It is also well known that the

chemical shift values of aromatic carbon atoms bearing bromine or iodine are far more shielded than for the equivalent compounds bearing chlorine or fluorine.[82]

Table 2: Selected ^{1}H and ^{13}C NMR shifts for compounds **32a-e.**

	NH	**C-1**	**C-4**
32a	11.14	159.2	133.2
32b	11.23	116.9	136.4
32c	11.24	136.0	141.5
32d	11.60	142.9	143.6
32e	10.70	133.6	136.2

The IR spectroscopic data confirmed the presence of the NH group in all compounds synthesized (**32a-e**), with the peaks being recorded in the ranges of 3152-3406 cm^{-1}. The presence of the nitro group in **32d** was confirmed by a strong stretch at 1490 cm^{-1}.

HRMS (m/z) results of the synthesized compounds further confirmed formation of the products as the masses obtained were as expected, the mass $(M-H)^-$ found for **32c** was 272.9512 which is close to the expected mass $(M-H)^-$ of 272. 9507. Similarly, the masses found for the other synthesized compounds supported the identity of the products formed.

2.1.2 Synthesis of thiol-bearing 4,6-dichloro-1,3,5-triazine derivatives

In the following set of reactions, 4-bromothiophenol **33a** and 4-methoxythiophenol **33b** were used as nucleophiles in the aromatic substitution of one Cl atom of compound **30** as shown in **Scheme 13.**

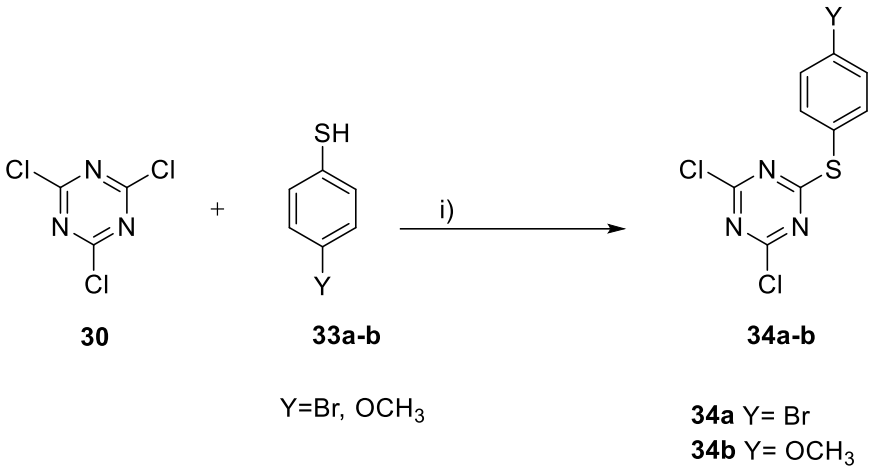

Reagents and conditions: i) acetone, NaOH (aq), 0-5 °C, 4-5 h

Scheme 13: Reaction of cyanuric chloride and substituted thiols to yield thiol-bearing 4,6-dichloro-1,3,5-triazine derivatives.

The methoxy group is electron-donating which increases the electron density in the aromatic system thereby making 4-methoxythiophenol a stronger nucleophile than the 4-bromothiophenol used in a similar reaction. Conversely bromine is electron-withdrawing and reduces the electron density in the conjugated system resulting in a weaker nucleophile. The reaction with 4-methoxythiophenol was expected to give a better yield as a result of it being more favorable due to its increased nucleophilicity.[83] However, the laborious compound isolation process during purification caused a significant loss in the yield of the synthesized product. The reaction itself was repeated several times at higher scale in an attempt to obtain higher yields. Complications such as co-elution of compounds led to a switch from the use of gravity silica gel to flash silica gel and varying the solvent systems from 1-10 % EtOAc/Hexane during the purification. Purification via recrystallization using ethyl acetate was also attempted with a satisfactory result. The synthesized compounds **34a** and **34b**[89] afforded yields of 88% and 28 %, respectively, as shown in **Figure 16**.

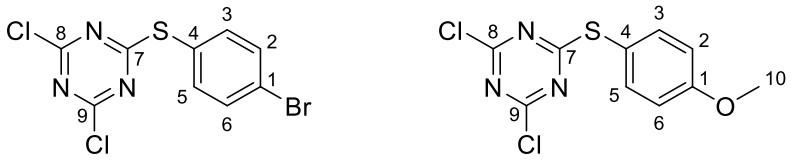

34a: 88% **34b: 28%**

Figure 16: Thiol-bearing 4,6-dichloro-1,3,5-triazine derivatives synthesized and their yields.

An intensive amount of time was spent analyzing the NMR data of these compounds and multiple NMR sample preparation procedures were tried due to an observation in the ^{1}H NMR spectra that we were initially unable to explain. An examination of the NMR spectra for compounds **34a** and **34b** exhibited signals which were observed at around δ 11.15-11.20 and these were surprising as this is where the NH signal was observed previously for compounds **32a**-**e**, but these compounds did not possess an NH group. This observation led us to believe that possibly the reaction hadn't occurred successfully, and we were observing the starting material or there was some kind of contaminant. Several investigations were conducted, which included carrying out the reactions using various solvents such as 1,4-dioxane and THF as well as increasing the temperature of the reaction to about 40 °C. We also increased the reaction time up to 26 hours in an attempt to complete substitution reaction, but surprisingly we eventually discovered that the anomaly was due to the NMR solvent choice. Upon changing the solvent used for the NMR analysis from DMSO-d_6 to acetone-d_6 the proton signals positioned between δ 11-11.50 were no longer observed in the ^{1}H NMR spectra (**Figure 17 & Figure 18**).

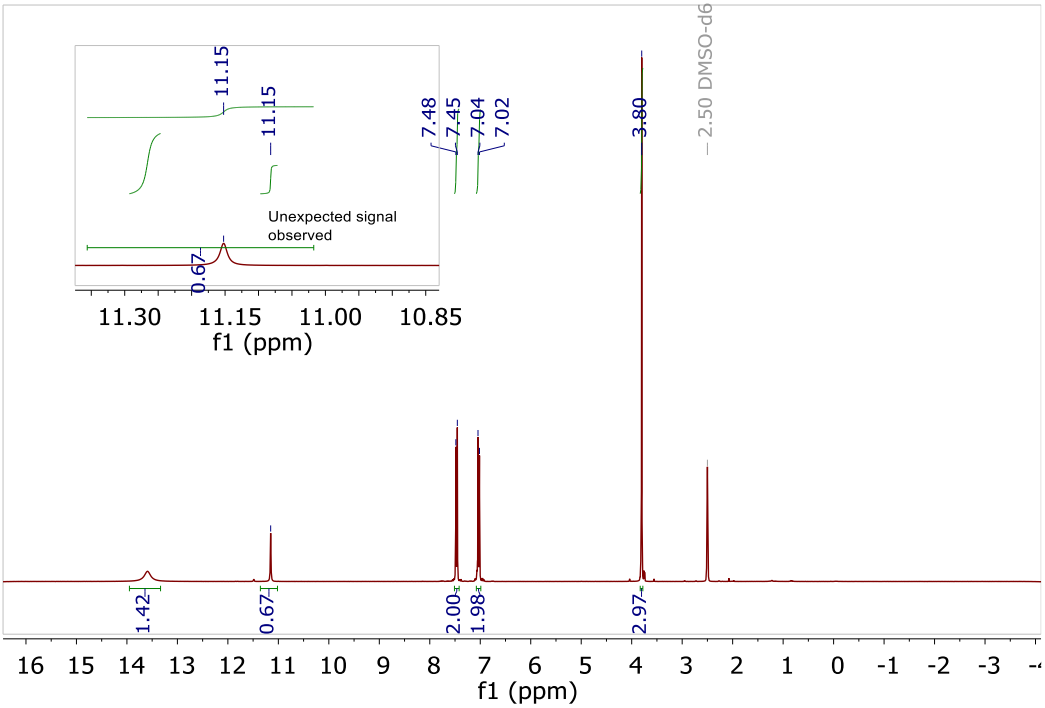

Figure 17: ^{1}H NMR spectrum of compound **34b** using DMSO-d_6 as a solvent.

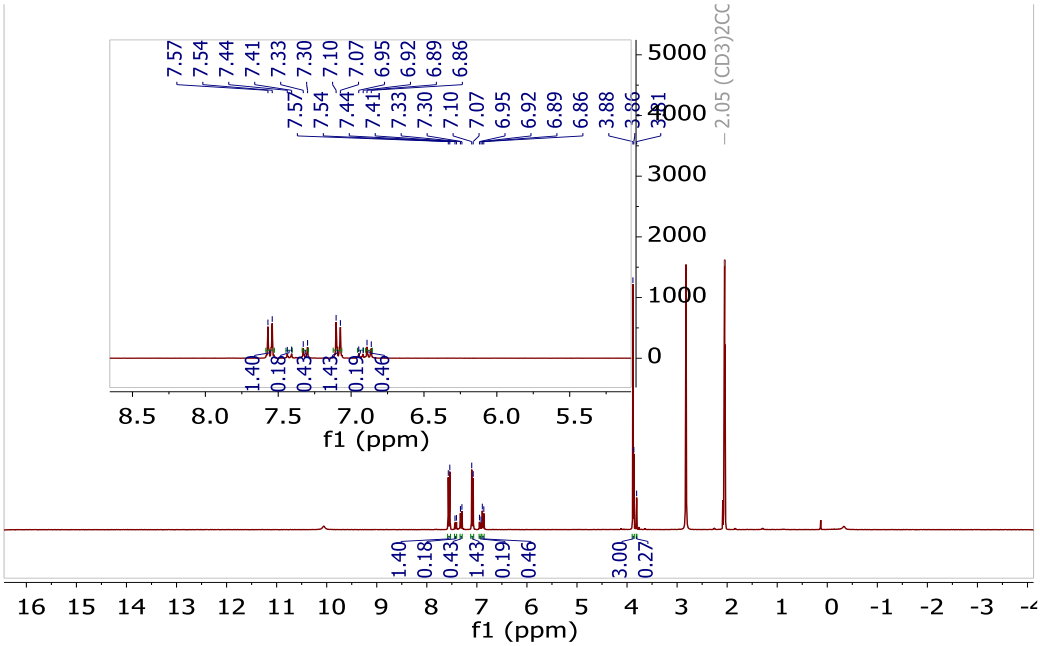

Figure 18: ^{1}H NMR spectrum of compound **34b** using acetone-d_6 as a solvent.

We examined the literature for a possible explanation of our observation. Based on literature information relating to the Swern oxidation mechanism, we hypothesize that a displacement of one of the Cl atoms by DMSO occurs to form compound **35a/35b**, where one of the Cl atoms

has been replaced by an OH group (**Scheme 14**). The intermediate **35a/35b** would give rise to a downfield signal in the ^{1}H NMR as expected for protons attached to an oxygen or nitrogen atom This is in line with what occurs under the Swern oxidation conditions wherein DMSO activated by cyanuric chloride is used for the conversion of alcohols to their corresponding carbonyl compounds (**Scheme 15**).[90]

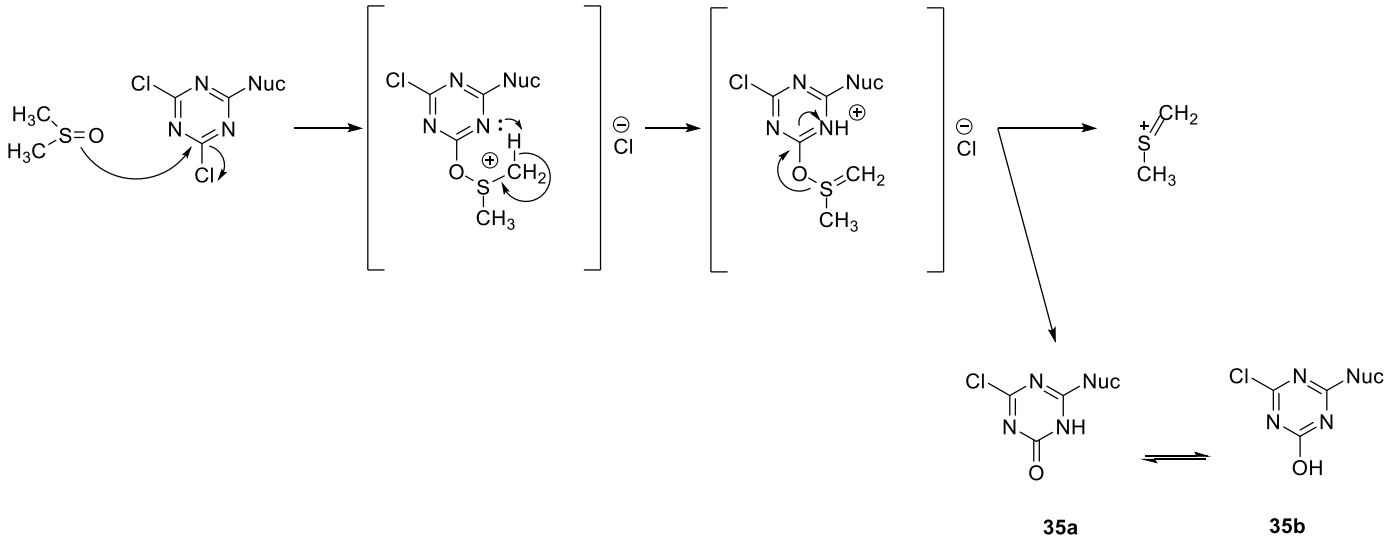

Scheme 14: Proposed formation of **35a/b** by reaction between DMSO and chlorinated triazine derivatives.

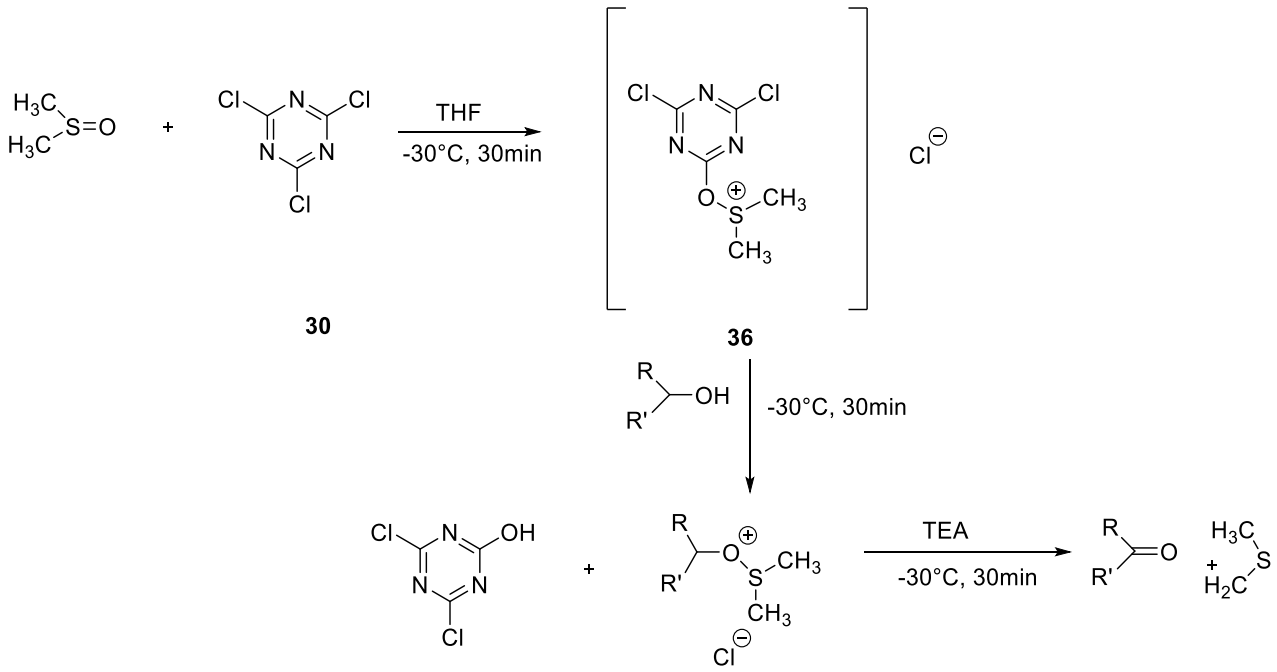

Scheme 15 Conversion of alcohols into carbonyls under Swern oxidation conditions using DMSO activated by **30.**

The presence of three conformers of triazine **34b** is clearly demonstrated in the ^{1}H NMR spectra acquired in acetone-*d*$_6$ (**Figure 15**). The signals for the equivalent aromatic protons appear in three sets as multiplets which integrate for a total of 2 protons, as expected. The proton signals for H-3 and H-5 are seen at δ 7.59-7.52 (1.39H), 7.45-7.40 (0.14H) and 7.34-7.29 (0.43H) while those for H-2 and H-6 are observed at δ 7.12-7.06 (1.43H), 6.95-6.91 (0.19H) and 6.90-6.85 (0.43H). It is clear that under certain conditions the effects of restricted internal rotations about bonds in triazine systems gives rise to the observation of conformers. [85] **Figure 14** shows the NMR spectrum of compound **34b** using DMSO-*d*$_6$ as a solvent and under these conditions, conformers were not observed. This is in stark contrast to what was observed when NMR data for the same thiol derivative was acquired using acetone-*d*$_6$ as a solvent. (**Figure 15)**.

For compound **34b** the protons at H-10 were observed at δ 3.80, which is expected, and the signal integrates for the 3 protons attached to C-10 in the methoxy group, which also confirms

its presence in the synthesized product. In the ^{13}C NMR spectrum the signal for C-10 was seen as a singlet at δ 55.5. This carbon is directly attached to an electronegative oxygen atom which tends to attract electron density towards itself thus reducing the electron density around the carbon nucleus. A net deshielding effect results in the signal for C-10 having a higher chemical shift as compared to a methyl group attached to a carbon atom.

2.1.3 Synthesis of 2,4-dichloro-6-(4-nitrophenoxy)-1,3,5-triazine 38.

The S_NAr reaction shown in **Scheme 16** to generate compound **38** was carried out by the slow addition of aqueous sodium phenoxide **37** to cyanuric chloride **30** dissolved in acetone in a similar fashion to what was demonstrated by Delia and colleagues whilst working with 2,4,6-trichloropyrimidine reacting with substituted phenolate ions.[91] Sodium phenoxide **37** was prepared by reacting 4-nitrophenol dissolved in acetone with aqueous sodium hydroxide solution in a 1:1 molar ratio. This reaction mixture was stirred at room temperature for 30 minutes while monitoring via thin layer chromatography, the phenoxide generation was carried out to favor a stronger nucleophilic attack as the phenoxide oxygen anion is a stronger nucleophile that the -OH from the 4-nitrophenol.

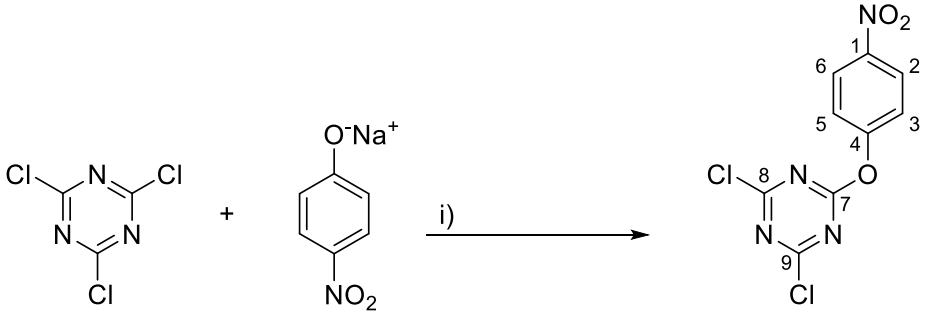

30 **37** **38**

Reagents and condirions i) Acetone, 0-5 ° C, 4-5 h

Scheme 16: The nucleophilic substitution of sodium phenoxide and cyanuric chloride**.**

Compound **38** was obtained in a yield of 69 % and the ^{1}H NMR spectrum showed the presence of two aromatic proton signals. The signal for H-2 and H-6 which are chemically equivalent appears as a multiplet at δ 8.32-8.23 and these protons were bonded to carbon atoms giving a signal at δ 126.8 as seen in the HSQC spectrum. Similarly, the signal for H-3 and H-5 appears upfield at δ 7.53-7.46 and these protons were directly bonded to carbon atoms giving a signal at δ 116.4. As stated previously in our discussion, compound **30** doesn't possess any protons so the presence of aromatic proton signals confirms the successful synthesis of the desired product as well as other supporting evidence obtained from the ^{13}C NMR data and the DEPT 135 experiment. Comparing the signals observed in the ^{13}C NMR spectrum and the DEPT 135 spectrum assisted in identifying the quaternary carbons, all of which were observed downfield as compared to the aromatic carbons which have a proton attached to them. The signal for C-7 was the most deshielded, appearing at δ 164.6 while the signal for C-8 and C-9 appears as one peak at δ 154.7.

2.1.4 Summary of characteristics derived from synthesized derivatives substituted with one aromatic ring.

The compounds in **Figure 19** were analyzed to compare the differences in chemical shift values in the NMR spectra of the carbon atoms attached to the different linkers of the incoming nucleophile.

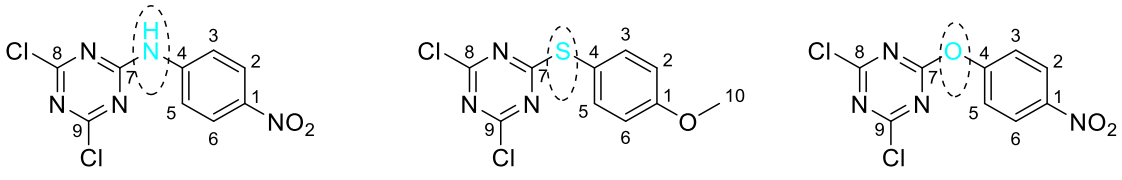

32d **34b** **38**

Figure 19: Triazine derivatives bearing an aromatic ring with different linkers.

Compounds **32d**, **34b** and **38** each contain either an N-, S-, or O linker. **Table 2** shows the different chemical shift values exhibited by the carbon atoms attached to the nucleophile and this illustrates the nature of the chemical environment surrounding the carbon nucleus. The triazine ring has a conjugated system due to alternating single and double bonds thereby creating delocalization of π-electrons within the ring system. It has been identified that the 1,3,5-triazine has π electron deficiency and is more susceptible to nucleophilic substitution as compared to other six-membered heteroaromatic ring compounds bearing nitrogen atoms.[92-93] The chlorine atoms attached to the ring which are electron withdrawing contribute to the electrophilicity of the carbon atoms within the ring as they further reduce the electron density around them. The carbon atoms are susceptible to nucleophilic attack as they are electron deficient leading to the ability of nucleophilic substitution reactions to occur. The chlorine atoms in cyanuric chloride also act as good leaving groups in the substitution reactions. We compared the success of the reactions using aromatic nucleophiles bearing the N-, S- and O atoms with substituents in the *para* position which were EWG and EDG. From previous studies we deduced that aromatic nucleophiles that possess *para*-substituents would act as good nucleophiles as they have low steric hinderance thereby approaching the electrophilic carbon atom with greater ease.[94]

Sharma and co-workers proved that bulky, sterically hindered nucleophiles give unsatisfactory results with low yields in the nucleophilic substitution reactions. [95] Electron donating substituents in the *para*-position of the aromatic ring increase the electron density by donating electrons through resonance and inductive effects. The negative charge is distributed across the conjugated system resulting in a stronger electron cloud which results in an overall stronger nucleophile with a greater capacity to attack the electron deficient carbon in the triazine ring.[95]

Conversely, electron withdrawing substituents reduce the electron density by attracting electrons towards themselves, thereby reducing the overall electron cloud around the aromatic ring system making the nucleophile weaker as the strength of the lone pair/s of electrons are pulled away from attacking the electrophile. This led us to expect successful reactions with higher yields of nucleophiles with EDG as substituents as compared to those with EWG, however, we observed varying results as discussed earlier with justifiable reasoning as to the low yields in some instances.

With respect to electronegativity of the three atoms that are the linkers to the triazine ring on the incoming nucleophile, oxygen is the most electronegative and an electronegativity scale between all three shows O>N>S. Spectroscopic data obtained from the AIST database shows that ^{13}C NMR chemicals shifts of the carbon atoms bearing the heteroatom directly follow the electronegativity order, where these groups are attached to a benzene ring. The chemical shift values obtained have been reproduced in **Figure 20** and this shows that the carbon C-1 attached to the OH group is the most deshielded appearing at δ 155 while the signal for C-1 attached to the NH_2 group appears at δ 146. The signal for C-1 attached to the SH group is the least deshielded, appearing at δ 130.[96] From our own observations and other literature values, the same sequence is not observed when these heteroatoms are attached to the triazine ring as compared to the benzene ring.

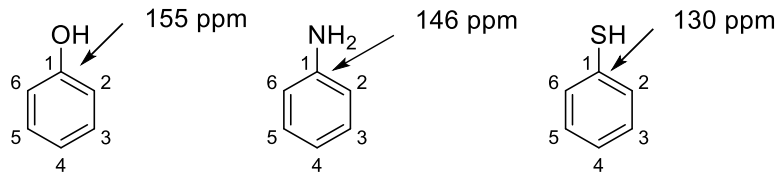

Figure 20: ^{13}C NMR chemical shift values observed for substituted benzene rings bearing heteroatoms.

In the case of triazine compounds the substituents attached to the triazine ring play a significant role in the chemical environment surrounding the carbon atoms. Nucleophiles with nitrogen and oxygen linkers can directly increase the electron density surrounding the carbon nucleus. Oxygen and nitrogen have lone pairs of electrons that can be donated to the triazine ring through resonance, thus increasing the electron density. The size of the 2p donor orbitals of nitrogen and oxygen are relatively similar to the size of the 2p acceptor orbital of carbon which greatly favors the electron donating capability and effectiveness. Conversely, the size of the 3p orbital of sulfur differs from that of the carbon orbital thereby limiting the electron donating effect of the sulfur atom to the carbon in the triazine.

Table 2: Selected ^{13}C NMR chemical shift values of compounds **32d**, **34b** and **38.**

32d	**34b**	**38**
C-4 143.6	C-4 150.0	C-4 150.7
C-7 153.2	C-7 180.1	C-7 164.6

The ^{13}C NMR data we obtained is shown in **Table 2** for compounds **32d**, **34b** and **38**, with specific focus on the chemical shift values of the carbon atoms directly attached to oxygen, nitrogen, and sulfur atoms.

The thiol-bearing triazine derivative **34b** exhibited the most deshielded carbon atoms with the signal for C-7 with 2 nitrogen atoms and 1 sulfur atom attached to it appearing at δ 180.1. The methoxy substituent in the *para*-position of the aromatic ring plays a significant role in

donating electrons within the ring via resonance and inductive effects. This subsequently generates a greater electron density around C-7 which appears at a higher chemical shift value than that of C-7 for compounds **32d** and **38**. In studies carried out by Grate and his colleagues wherein they designed a new class sequence-defined polymers via nucleophilic substitution reactions of cyanuric chloride as a building block they demonstrated that carbon atoms in the triazine ring attached to sulfur are more deshielded than those attached to nitrogen.[97] This supports the NMR spectroscopic data we obtained from a number of structurally similar compounds we synthesized. **Figure 21** presents information reproduced from Grate *et al.*[97] illustrating specific chemical shift values they obtained from selected compounds that were successfully synthesized and these are consistent with data we are reporting here. From the spectroscopic data we obtained from our ^{13}C NMR spectra the chemical shift values for C-7 of compound **38** at δ 180.1 and that of **32d** at δ 153.2 correlates with literature values for carbon atoms in similar chemical environments.[96-97]

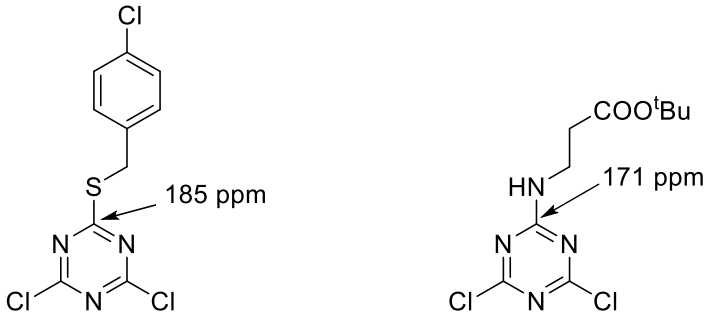

Figure 21: ^{13}C NMR chemical shift values of specific carbon atoms attached to a heteroatom.

2.2 Second nucleophilic substitution reaction on the triazine ring.

Successive displacement of the second chlorine atom from the s-triazines synthesized in Section 2.1 was carried out as illustrated in **Scheme 17**.

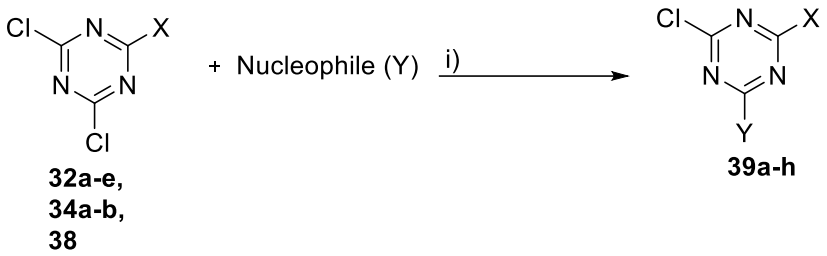

32a-e, 34a-b, 38

39a-h

Reagents and conditions: i) Y, Acetone/THF, NaOH (aq), 0 °C-RT, 5-24 h

Scheme 17: Nucleophilic substitution reaction of the second chlorine atom to synthesize triazine derivatives with two aromatic substituents.

Table 3: Various nucleophiles attached to the triazine ring of compounds **39a-h**.

	X	**Y**
39a	4-fluoroaniline	4-nitrophenol
39b	4-bromoaniline	4-chlorophenol
39c	4-nitroaniline	p-anisidine
39d	4-chloroaniline	4-nitrophenol
39e	4-nitroaniline	4-fluorophenol
39f	4-methoxythiophenol	4-nitrophenol
39g	4-chloro-2-methylaniline	4-nitrophenol
39h	4-nitrophenol	4-nitroaniline

Compounds **32a-e, 34a-b** and **38** were used as the starting materials with various nucleophiles as shown in **Table 3** yield the triazine derivatives **39a-h**. The bulk of the synthesized compounds **39a-h** gave very good yields of between 76-91 % (**Figure 22**).

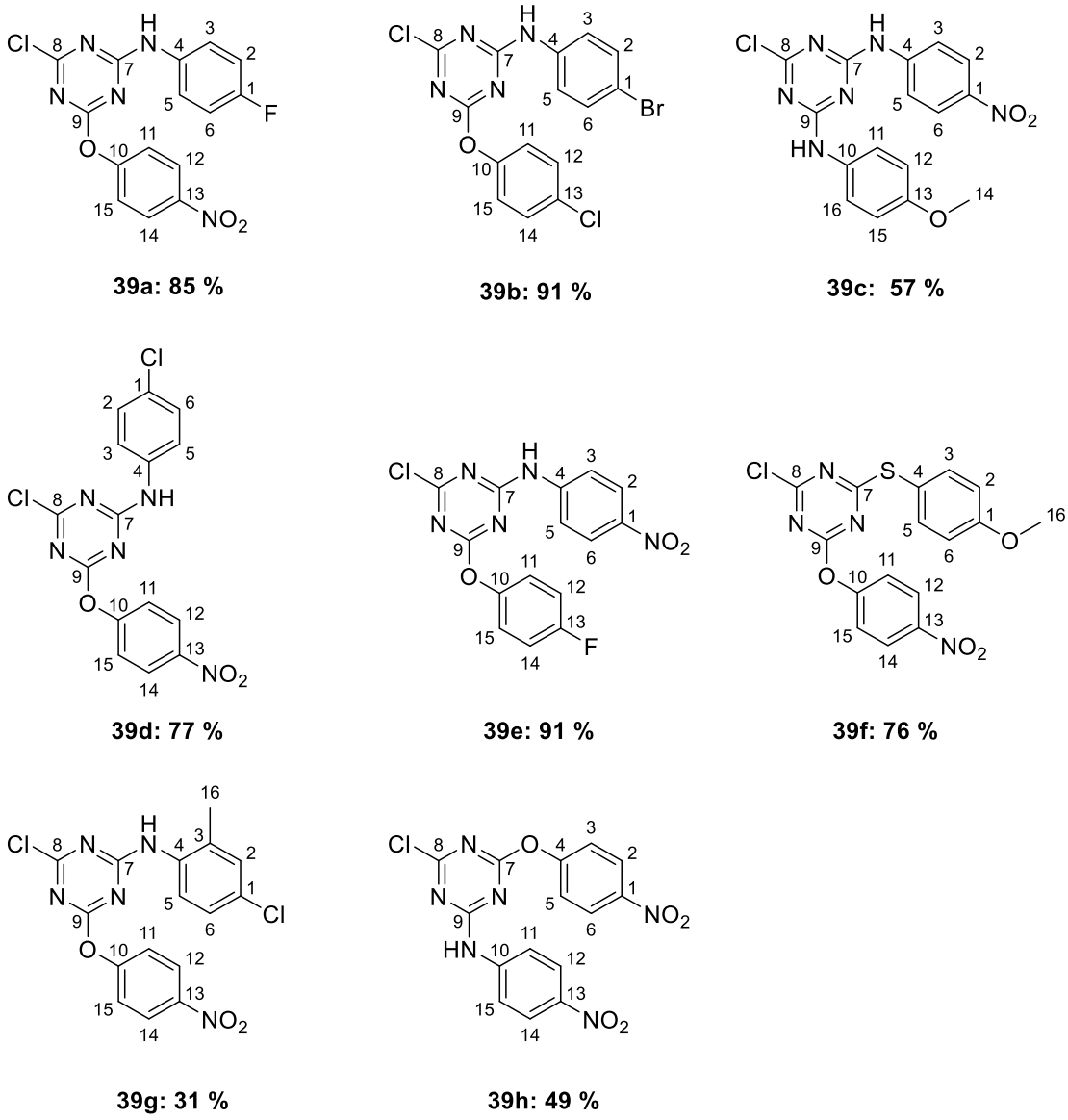

Figure 22: Triazine derivatives bearing two aromatic substituents and their isolated yields.

The displacement of the second chlorine atom in the nucleophilic substitution reactions was carried out at room temperature up to about 30 °C. The presence of a substituent on the triazine core altered the reactivity and its susceptibility to a nucleophilic attack compared to the first chlorine displacement. Reaction conditions had to be altered in order to achieve the desired results, however, some reactions yielded compounds that were tri-substituted with aromatic substituents instead of the desired di-substituted triazine derivatives at higher temperatures. For

these reactions the temperatures were altered back to between 0-5 °C and the resultant reaction completion time was very lengthy with reaction times of up to 26 h as compared to reactions where the temperature was raised which were complete within 4-5 h.

Information obtained from the ^{1}H and ^{13}C NMR spectra was used to confirm the synthesis of the desired triazine derivatives with various aromatic substituents attached to the triazine ring. Novel compounds **39a**, **39b**, **39d**, **39e**, **39g** and **39h** all have anilines and phenols as nucleophiles attached to the triazine ring and we expect to see 1 proton signal that would appear downfield in the ^{1}H NMR spectrum between 9.00-12.00 ppm as compared to **39c** which would exhibit 2 NH signals. Novel compound **39f** has no protons attached to the sulfur and oxygen which would appear in the downfield region. The NH signal was split into two for compound **39a** whilst for **39b** and **39d** it was split into three signals, indicating the presence of a number of different conformational isomers.[98] Preparation of samples for NMR analysis of compounds **39g** and **39h** was extremely difficult as they were insoluble in most of the available deuterated solvents. After a number of trials, a solvent mixture of methanol-d_4 and acetone-d_6 was found to be suitable to dissolve these compounds when used together with heating and ultra-sonication processes. The NH proton for compound **39g** was not observed in the ^{1}H NMR spectrum while for compound **39h** the signal was very weak and integrated for 0.09 H and this was owing to the exchange of protons with the deuterium atoms in the methanol- d_4 solvent used for the analysis. All the other observed signals confirmed the successful coupling reaction as shown in **Table 4**.

Table 4: Selected ^{1}H and ^{13}C NMR shift values for some of the synthesized compounds.

	NH	C-7	C-8	C-9	C-10
39a	δ 10.90 (s, 0.63H), δ 10.64 (s, 0.31H)	δ 163.9	δ 170.2 & δ 169.9	δ 164.7	δ 156.3
39b	δ 10.92 (s, 0.50H), δ 10.79 (s, 0.22H), δ 10.65 (s, 0.25H)	δ 156.3	δ 170.7 & δ 169.9	δ 164.5	δ 150.4
39d	δ 11.26 (s, 0.13H), δ 11.02 (s, 0.60H), δ 10.76 (s, 0.29H)	δ 164.6	δ 170.3	δ 170.1 & δ 169.9	δ 156.2
39e	δ 10.87 (s, 1H)	δ 164.9	δ 170.8, δ 170.4	δ 166.1	δ 147.7
39g	NOT OBSERVED	δ 167.7	δ 172.6	δ 172.0, δ 171.6	δ 157.6
39h	δ 9.98 (s, 0.09H)	δ 172.9	δ 174.2, δ 174.1	δ 157.7	δ 157.1, δ 156.9

The aromatic proton signals were observed in the aromatic region of 7.50-8.50 ppm as expected for all of the synthesized compounds, albeit there were complexities in assigning the signals as they appeared as broad multiplets that overlapped. Because of the presence of conformers, individual signals integrated for odd fractional values, however, when these fractional values were added together, they gave the accurate total number of expected protons.

When comparing the C-H signals observed in the HSQC spectrum for **35d** and the number of C-H signals observed for compound **39a** we observed an increased number of signals. This confirmed the successful coupling reaction as the presence of these signals arose from the incoming nucleophile bearing an aromatic ring.

The synthesis of di-aminosubstituted triazines such as compound **39c**[97] required elevated temperatures and these compounds exhibited interesting spectroscopic characteristics and these are described in the discussion that follows. Synthesis of 6-chloro-N^2-(4-methoxyphenyl)-N^4-(4-nitrophenyl)-1,3,5-triazine-2,4-diamine **39c** was carried out by the substitution of the second chlorine atom by *p*-anisidine **40** from compound **32d** as illustrated in **Scheme 18** using similar protocols as adopted by Bhat and his colleagues.[97] This compound has been reported This reaction reached completion within 5 h while monitoring via TLC. Under UV light a new spot was observed, and the absence of the reactant spots confirmed the formation of a new compound with different chemical properties from the reactants.

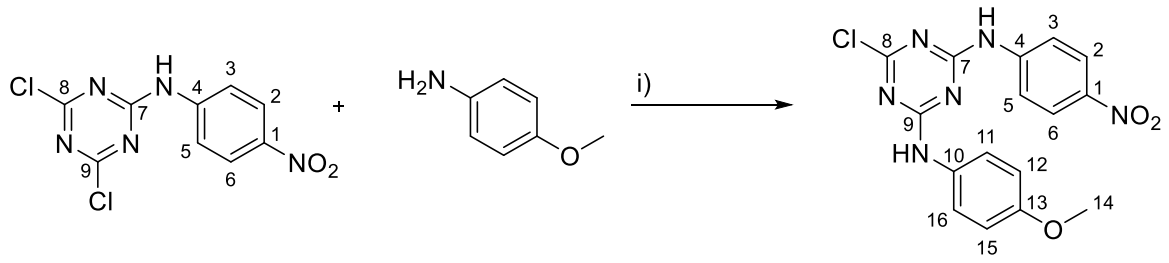

32d **40** **39c**

Reagent and conditions: i) *p*-Anisidine, Acetone, NaOH (aq), RT, 5 h

Scheme 18: Synthesis of 6-chloro-N^2-(4-methoxyphenyl)-N^4-(4-nitrophenyl)-1,3,5-triazine-2,4-diamine.

Successive substitutions of the chlorine atoms by nucleophiles deactivates the remaining sites making them less susceptible to nucleophilic attacks, but higher temperatures alleviate this challenge. **Scheme 18** illustrates this reaction being carried out at room temperature which is moderately elevated as compared to the reactions to synthesize triazine derivatives substituted with a single aromatic ring. At higher temperatures the reactant molecules have increased kinetic energy which favours a nucleophilic attack and the breaking of the C-Cl bond, and these factors contributed to the success of the reaction. The strength of *p*-anisidine **40** as a nucleophile is attributed to the lone pair of electrons attached to the amino group which initiates the attack on the electron deficient carbon atom of the triazine ring. The methoxy group is an electron donating substituent which increases the electron density via resonance effects, thereby increasing the nucleophilicity of the amine group yielding a stronger nucleophilic attack. Considering the abovementioned attributes, we expected a fairly good yield for this particular reaction, however, our results were not very satisfactory as we obtained a yield of 57%. The purification process resulted in the loss of a significant amount of the synthesized compound. We deduced that the greater interactions between the solid phase silica gel and the solute lead to adsorption of the solute onto the stationary phase resulting in difficulties of solute movement into the mobile phase even with a change in the solvent polarity.

Observing the ^{1}H NMR spectrum confirmed the presence of 2 downfield signals as singlets at δ 10.37 for the NH from the 4-nitroaniline and δ 9.82 owing to the NH from the 4-methoxyaniline. The nitrogen and oxygen atoms within the nitro group are electronegative and reduce the electron density from the aromatic ring via sigma bonds. This electron withdrawing effect causes the proton attached to the nitrogen atom to be deshielded and the signal appears downfield as compared to the NH proton attached to the methoxyaniline. The absence of carbon correlations for these signals in the HSQC spectrum confirmed that these were the NH protons.

The signal for the aromatic protons H-2 and H-6 appears as a multiplet at δ 8.19-7.79. Assigning the signals that appear as multiplets at δ 7.60-7.48 and at δ 7.36-7.28 was complex due to the fractional integration values obtained that could result from the dynamic system of the compound where conformers are exhibited, as mentioned previously. Multiple conformers can be present in solution at any given time and at the NMR time scale the protons of different conformations may appear at different shift values, giving rise to fractional integration values. When these fractional values were added together, they gave the total number of expected protons. The signal for H-12 and H-15 appeared as a multiplet at δ 7.02-6.73 while the signal for H-14 was seen upfield as a singlet at δ 3.75 which confirmed the presence of the methoxy group.

The ^{13}C NMR spectroscopic signal for C-8 appears at δ 165.3. It is attached to one electronegative chlorine atom and 2 nitrogen atoms hence it appears downfield as compared to the signal for C-7 which appears at δ 154.8 and C-9 which appears at δ 151.0, both of which are attached to 3 nitrogen atoms. The signal for C-1 appears at δ 141.3; it is directly attached to the electron withdrawing nitro group while the signal for C-13 appears at δ 131.5. C-14 which is the carbon atom in the methoxy group of compounds **39c** was observed on the ^{13}C NMR spectrum at δ 55.2 and this signal was also observed in the HSQC spectrum attached to the protons for H-14 at δ 3.75 which confirmed the synthesis of the desired product. The signal for C-14, which is from the methoxy group, was also observed at δ 55.2 in the ^{13}C NMR spectrum. The signals for the other quaternary carbons which were confirmed by their absence from the DEPT 135 spectrum appear at δ 129.6 for C-4 and δ 124.1 for C-10. The signal for C-11 and C-16 which are chemically equivalent appear at δ 129.4 which closely overlapped with the signal for C-4. The signals for C-2 and C-6, C-3 and C5, C-12 and C-15 appear at δ

124.5, 119.3 and 113.7 respectively, with these pairs representing chemically equivalent carbon atoms.

The NH signal for compound **39e** appeared downfield, as expected, as a singlet at δ 10.87. Due to symmetry the protons at H-2 and H-6 are equivalent; this is also the case for the protons at H-3 and H-5 and therefore they appear as a single signal. We expected to see the signal for H-2 and H-6 as a doublet, as well as for H-3 and H-5 but they appear as multiplets at δ 8.07-8.02 and 7.75-7.69, respectively. These protons appear as multiplets due to the fact that they are magnetically inequivalent, and they experience differences in the magnetic field generated by the neighbouring protons.

Two signals for C-8 were observed in the ^{13}C NMR spectrum at δ 170.8 and 170.4, with the signal at δ 170.4 almost double the size of the signal at δ 170.8. Such splitting of signals of carbon atoms in the triazine ring was observed often during our analysis and is an inherent complexity in the NMR analysis of triazines due to the presence of multiple conformers. [98-99] To further confirm the formation of the newly synthesized compound C-F coupling was observed for carbon atoms of the 4-fluorophenol ring that substituted the second chlorine atom in **34d.** The signal for C-13 which is directly attached to the fluorine atom appears as a doublet at δ 159.9 and has a coupling constant of $^{1}J_{C\text{-}F}$ = 241.8 Hz. The signal for C-10 which is 4 bonds away from the fluorine atom appears at δ 147.7 with a coupling constant of $^{4}J_{C\text{-}F}$ = 2.4 Hz. In the position *meta* to fluorine the signal for C-11 and C-15 appears as a doublet at δ 123.6 with a coupling constant of $^{3}J_{C\text{-}F}$ = 8.7 Hz as it is 3 bonds away from the fluorine atom. The signal for C-12 and C-14 was observed as a doublet at δ 116.5 with a coupling constant of $^{2}J_{C\text{-}F}$ = 23.7 Hz.

Observing the NMR spectra for 4-chloro-*N*-(4-chloro-2-methylphenyl)-6-(4-nitrophenoxy)-1,3,5-triazin-2-amine **39g** with a methyl group attached to one of the aromatic rings the signal for C-16 appears upfield at δ 17.9 and the corresponding protons were also observed in the HSQC spectrum attached to this carbon at δ 2.22. In the ^{1}H NMR spectrum of **39g** the signal for the protons for H-16 appears as a singlet integrating for 3 protons as expected as the carbon attached to this methyl group which is C-3 is a tertiary carbon without any protons attached to it. The ^{13}C NMR spectrum for compound **39g** was extremely complex (**Figure 23**) to analyze as there was an abundance of signals arising from conformational isomerism with relative signal heights of 2:1 and for some signals the ratio was 3:2:1. The signal for C-9 had a major peak at δ 171.6 and a minor peak at δ 172.0. The signal for C-4 appears as a major peak at δ 136.4 and a minor peak at δ 137.4. A similar pattern was observed for the signals for C-3, C-1, C-5, C-12 and C-14 which are chemically equivalent as well as C-11 and C-15. We observed 3 different signals for C-2 with chemical shift values at δ 132.2, 132.7 and 133.0 which was interesting to note that a possible 3 rotamers of this compound were exhibited. From literature it has been reported that if some conditions are changed such as temperature or solvent then more conformations can be observed for the same compound.[99-100]

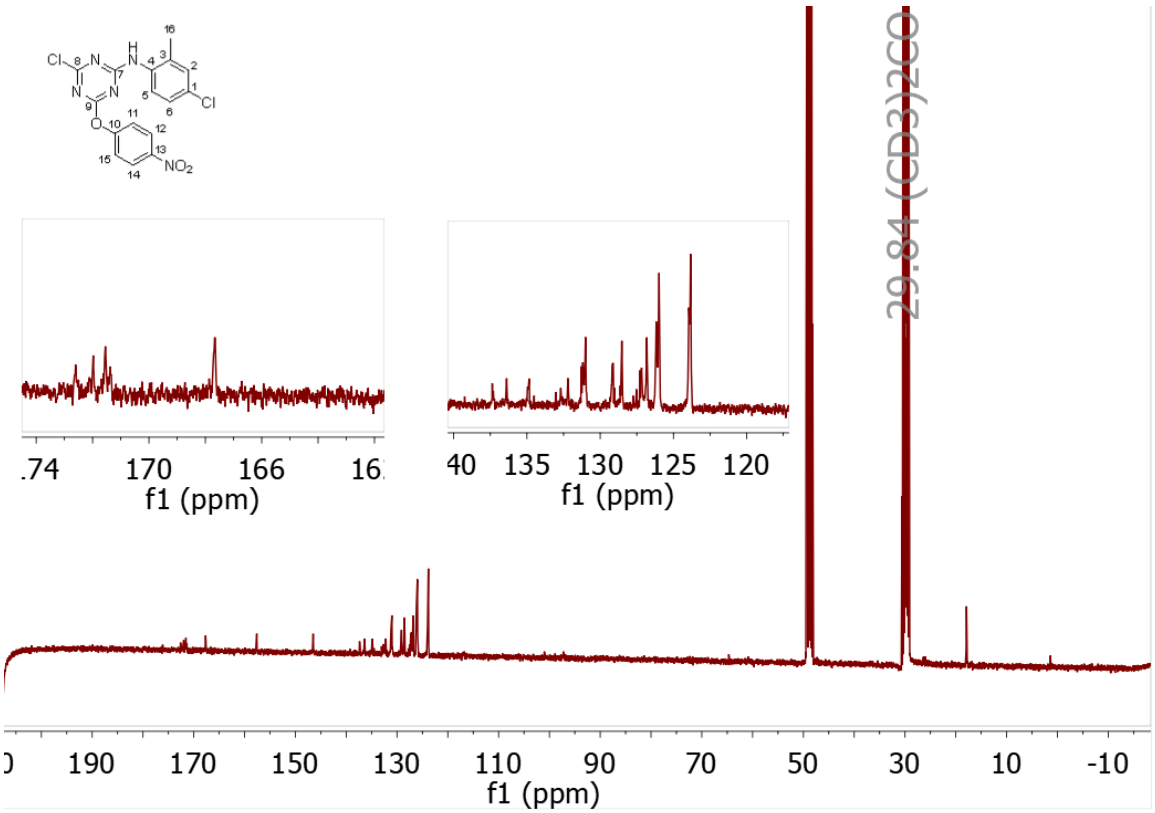

Figure 23: ^{13}C NMR spectrum of triazine **39g** in a mixture of methanol-d_4 and acetone-d_6. Inserts show regions where complex split signals were observed.

Compound **39f** was synthesized by reacting **35b** with the sodium phenoxide **37** at room temperature for 5 h as shown in **Scheme 19** giving a yield of 76 %.

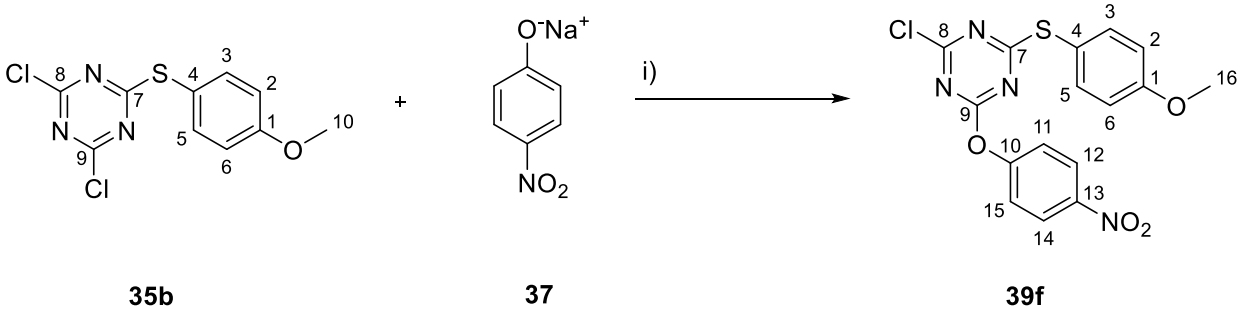

35b **37** **39f**

Reagents and conditions i) Acetone, RT, 5 h

Scheme 19 Synthesis of compound **39f**

In the ^{1}H NMR spectrum the signals for the aromatic protons appear in the region expected for aromatic protons as multiplets at δ 8.30-8.13, δ 7.52-7.22 and δ 7.00-6.84 as discussed earlier. Assigning these protons was not feasible as they integrated for fractional values and the peaks overlapped, which proved to be a challenge when analysing the NMR data. The signal for H-16 appeared as a multiplet at δ 3.80-3.69 and integrated for 3 protons.

In the ^{13}C NMR spectrum the signal for C-7 appears downfield at δ 186.3; this observation is similar to previous examples where the carbon atom attached to the sulfur atom is the most deshielded. The presence of conformational isomers was also observed from the signals that appear at δ 160.7 and 160.4 for C-9 and a similar pattern was noted for C-2 and C-6 with signals that appear at δ 136.9 and 136.5. Interestingly, the signals that appear at δ 125.3 and 124.8 for C-11 and C-15 showed that the major conformer gave a signal double the size of that of the minor conformer. The same was true for the signals that appear at δ 123.0 and 122.8 for C-12 and C-14. Furthermore, the presence of a signal upfield at δ 55.2 for C-16 confirmed the presence of the methoxy group which supported the successful synthesis of the desired product. IR spectroscopy exhibited some characteristic peaks**,** for example we observed 2 medium peaks at 1546 cm^{-1} and 1515 cm^{-1} which confirmed the presence of the nitro group present in the synthesized product. There was also a sharp peak at 1336 cm^{-1} which was assigned to the methyl group and further confirmed the synthesis of the desired product. Similar observations were made for the rest of the synthesized triazine derivatives with two aromatic substituents to support the successful synthesis of the desired products.

HRMS was used to determine the exact masses of the synthesized products and the results obtained closely matched the expected results for the tested products as seen in **Table 5** for selected compounds.

Table 5: HRMS results for selected compounds.

	39a ($C_{15}H_8ClFN_5O_3$)	**39c** ($C_{16}H_{11}ClN_6O_3$)	**39e** ($C_{15}H_8Cl\,FN_5O_3$)
Expected Mass $(M-H)^-$	360.0305	373.0810	360.0305
Found Mass $(M-H)^-$	360.0309	373.0874	360.0306

Some reactions that were attempted were not successful even following several changes to the reaction conditions. For example, in the attempted preparation of triazine **39a**, the order of the reactions was to substitute the first chlorine atom of compound **30** with *p*-nitrophenol to yield 2,4-dichloro-6-(4-nitrophenoxy)-1,3,5-triazine **39**. The subsequent step would be to react the 2,4-dichloro-6-(4-nitrophenoxy)-1,3,5-triazine with 4-fluoroaniline to yield the desired product as illustrated in **Scheme 20**, however this reaction failed. Reaction temperature was increased from room temperature to 40 °C and the results observed from NMR as well as TLC analysis indicated that only the starting material was present. The reaction time was also adjusted from 5 h to 24 h, and 2 different spots were observed on the TLC plate, however the NMR data didn't support the successful synthesis of the desired product.

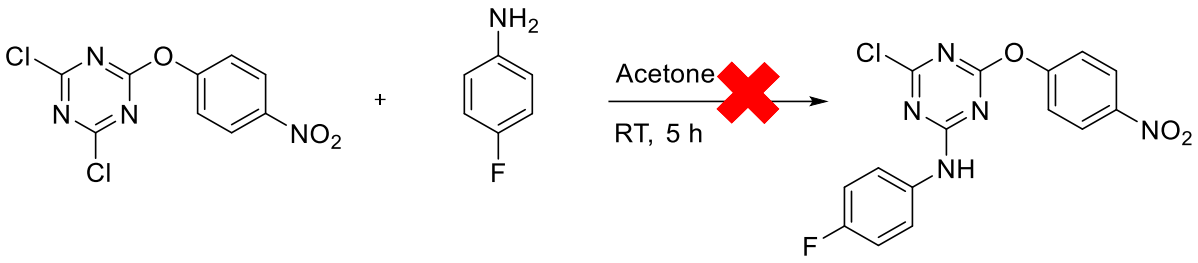

38 **39a**

Scheme 20: A failed attempt to synthesize compound **39a**.

Interestingly, when the order of the reaction was switched, with the reaction of the fluoroaniline with cyanuric chloride being carried out first, followed by the reaction with the phenoxide **37**, compound **39a** was successfully obtained, as previously described (see **Scheme 15**). The nitro group and the fluoro group are both electron-withdrawing groups which reduce the nucleophilicity of the aromatic compounds they are attached to, albeit the phenoxide **37** acted as stronger nucleophile than the fluoroaniline. The phenoxy group is a better nucleophile than the amino group as the negatively charged oxygen would have a stronger nucleophilic nature than the neutral nitrogen. We concluded that the reactions were determined by the strength of the incoming group as a nucleophile and the effects of the substituents already attached to the aromatic ring. Therefore, we had to identify the properties of each compound to ascertain the most favourable order in which to carry out the substitution reactions.

2.3 Third nucleophilic substitution reaction on the triazine ring.

The final step in the nucleophilic substitution reactions was the replacement of the third chloro-substituent in the triazine system by an aromatic nucleophile. The reactions were carried out under reflux conditions in suitable solvents in an attempt to obtain better yields as compared to microwave irradiation methods. Other groups have carried out this reaction via microwave irradiation techniques with shorter reaction times.[100-101]

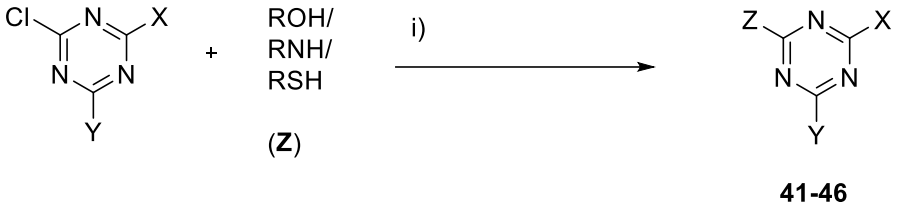

Reagents and conditions: i) Z,THF/1,4- dioxane, K_2CO_3 (aq) /NaOH (aq), Reflux 80- 100 °C

Scheme 21: Last nucleophilic substitution reaction to synthesize tri-substituted triazines.

Various nucleophiles (**Table 6**) were reacted with synthesized triazines bearing two aromatic substituents for up to 48 h at temperatures of between 80-100 °C to yield novel triazines **41**-**46** as illustrated in **Scheme 21**. This final step was extremely challenging as the high temperature conditions caused decomposition of some products which were irrecoverable thereby resulting in the compounds being resynthesized.

Table 6: Substituents attached to the triazine ring for compounds **41-46**

	X	Y	Z
41	4-fluoroaniline	4-nitrophenol	4-Hydroxybenzonitrile
42	4-bromoaniline	4-chlorophenol	4-Hydroxybenzonitrile
43	4-chloroaniline	4-nitrophenol	4-fluorophenol
44	4-nitroaniline	4-fluorophenol	*p*-Anisidine

45	4-methoxythiophenol	4-nitrophenol	4-aminobenzonitrile
46	4-chloro-2-methylaniline	4-nitrophenol	4-methoxythiophenol

Another complexity that was experienced when handling these compounds was low solubility. This has been discussed earlier, however, the loss of starting materials at each synthesis step resulted in only small-scale reactions towards the tri-substituted compounds being possible and therefore we had to be very cautious to preserve as much of the product as feasible during sample preparation for characterization. Information from literature suggests that the intermolecular hydrogen bonding and π-stacking between the aromatic rings could initiate strong interactions between molecules thereby leading to the formation of insoluble assemblies.[93,99]

Analysis and characterization via NMR spectroscopy proved to be a mammoth task as the compounds didn't readily dissolve in the commonly available deuterated solvents and we had to explore solvent mixtures. Similar complexities were experienced when preparing these samples for mass spectrometry. We resorted to heating some of these samples in the deuterated solvent/solvent mixtures to temperatures of about 50-60 °C as well as ultrasonication which proved to be successful in solubilizing these trisubstituted triazines. The task of analyzing the NMR spectra for these compounds was extremely time-consuming as they were very complicated which made it very difficult to assign certain signals. As mentioned previously, the complexity of the NMR spectra is hypothesized to arise from the probability that these compounds exist as tautomers in equilibrium.

Table 7 shows tri-substituted triazine compounds that were synthesized successfully and their corresponding yields which varied from 11%-83%.

Table 7: Synthesized tri-substituted triazine compounds and their yields.

Compound	Yield (%)
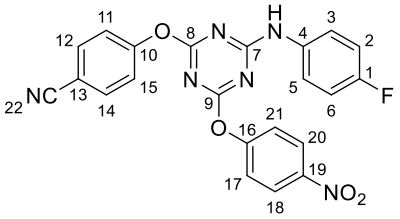 **41**	91
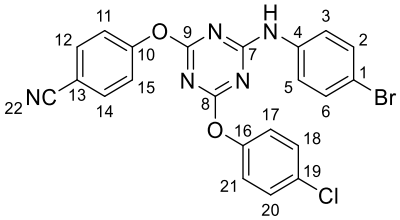 **42**	54
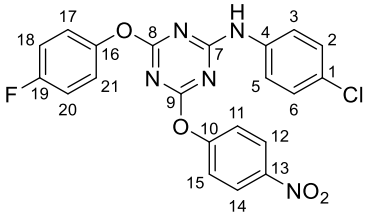 **43**	25
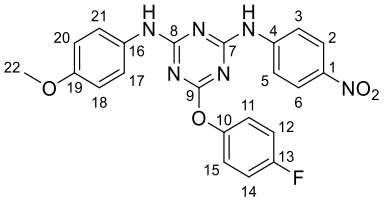 **44**	11

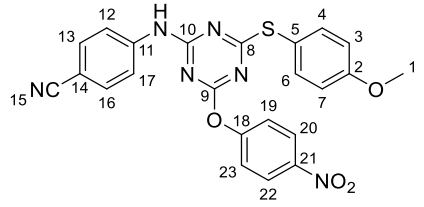 **45**	77
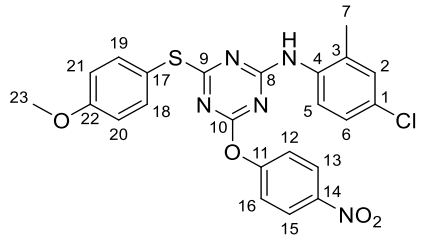 **46**	83

The tri-substituted triazine derivative **41** was synthesized by reacting 4-hydroxybenzonitrile with compound **39a** in a 1:1 ratio under reflux conditions as illustrated in **Scheme 16**, in a very good yield of 91 %.

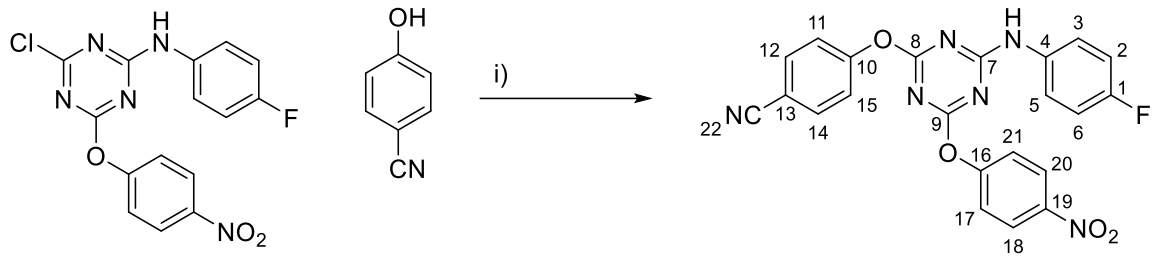

39a **41**

Reagents and conditions: i) THF, NaOH (aq), Reflux, 40 h

Scheme 22: Reaction carried out under reflux to prepare 4-((4-((4-fluorophenyl)amino)-6-(4-nitrophenoxy)-1,3,5-triazin-2-yl)oxy)benzonitrile (**41**)

Figure 24 shows the ^{1}H NMR spectrum of triazine **41** some signals which integrate for fractional values make it very difficult to accurately assign these protons, however due to the downfield chemical shift value for the NH proton it effortlessly recognized. The signal for this proton is split into three peaks that appear in the downfield region between 10.35-10.45 ppm which contributed to a total integration of one proton as expected. The signal at δ 8.33 appears as a doublet with a J coupling constant of 8.9 Hz, however, it integrated for a fractional value of 1.38H and we were unable to accurately assign this signal. The signal at δ 7.04 appears as a triplet and this was assigned to H-2 and H-6. The other signals were observed as broad multiplets at δ 8.00-7.94, δ 7.60-7.55, δ 7.53-7.49 and δ 7.47-7.40 (**Figure 24**) and similar to the previous signal these all integrated for fractional values. The signal observed at δ 7.47-7.40 was assigned to H-3 and H-5 The complexity of this fractional integration led to the conclusion that these signals arose from the aromatic protons and these are supported by chemical shift values reported in literature.[103-104]

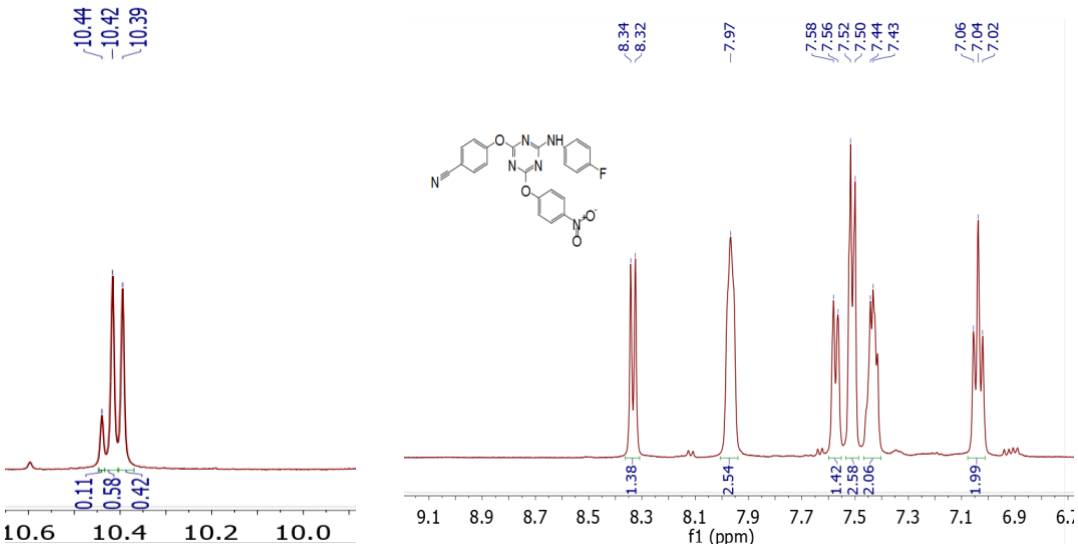

Figure 24: Segments of ^{1}H NMR spectrum of compound **41**

Analyzing the correlation spectrum (COSY) (**Figure 25**) of compound **41** gave minimal though useful information in relation to the spin-spin coupling within this molecule, this is due to the

integration complexity discussed above. Three spin systems were identified which were relevant in confirming these proton interactions which correspond to 3 aromatic rings present in the synthesized product. One of the spin systems' correlation signals had chemical shift values at δ 7.06 (H2 and H6) and δ 7.40-7.47 (H3 and H5) which corresponds to the aromatic protons arising from the aniline moiety of the compound, confirming the assignments from the ^{1}H NMR spectrum. The corresponding chemical shift values are slightly upfield as compared to the more downfield values of the protons on the cyano- and nitro- bearing aromatic substituents.

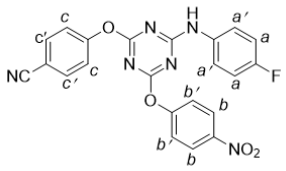

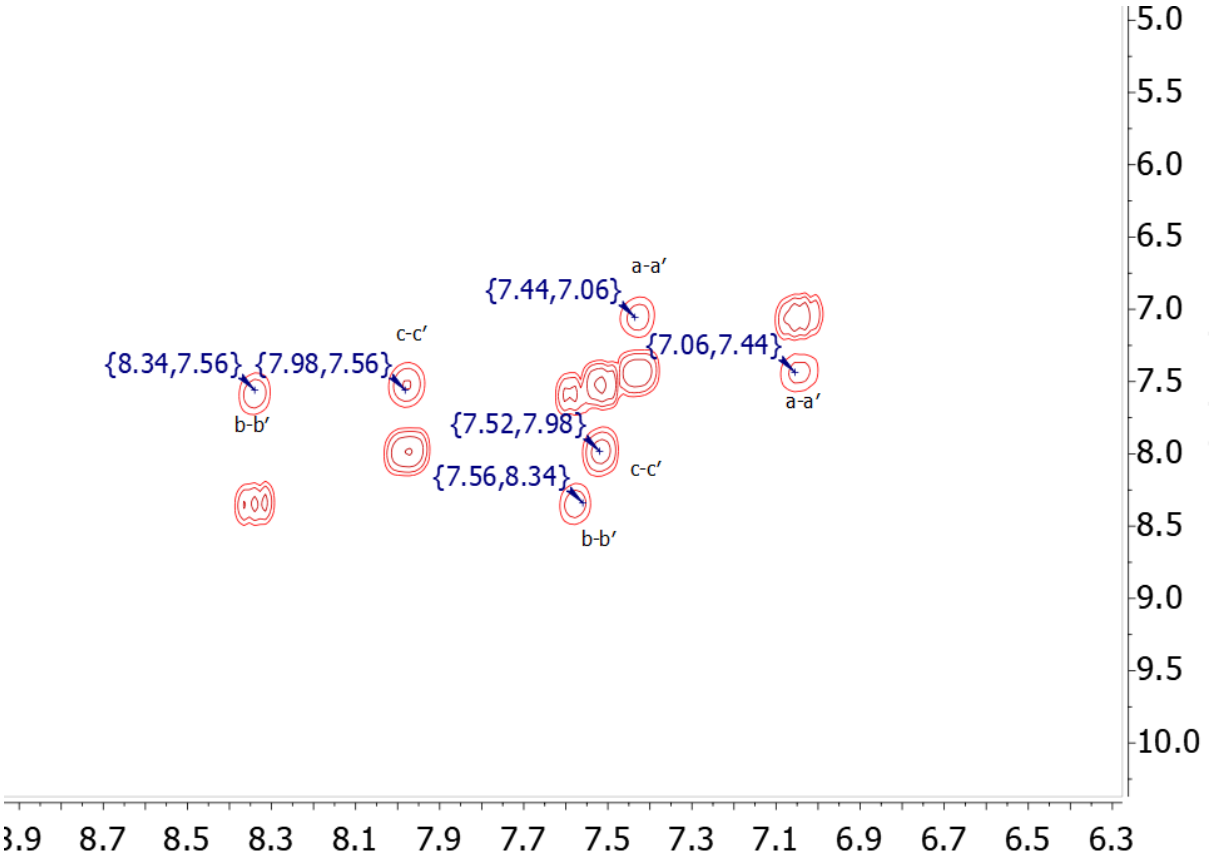

Figure 25: COSY spectrum of triazine **41**, the assigned correlated signals are labelled as *a-a′*, *b-b′* and *c-c′*

Information obtained from the ^{13}C NMR and HSQC spectra was very useful in the characterization of the synthesized triazine **41**. The presence of a fluorine atom attached to the aniline moiety was useful in identifying the carbon atoms in close proximity to fluorine with the guidance of the C-F coupling constants. The signal for the carbon attached directly to the fluorine, C-1, appears at δ 158.4 with the largest C-F coupling constant of $^{1}J_{C\text{-}F}$ = 240.9 Hz. The signal for C-2 and C-6 appears as a doublet at δ 115.0 with a coupling constant of $^{2}J_{C\text{-}F}$ = 22.3 Hz; this confirmed that these are 2 bonds away from the fluorine atom. The C-3 and C-5 signal which is 3 bonds away from the fluorine appears at δ 122.7, with a coupling constant of $^{3}J_{C\text{-}F}$ = 7.9 Hz. The signal for C-4 which is the farthest from the fluorine atoms and is 4 bonds away appears as a doublet at δ 134.2 with a coupling constant of $^{4}J_{C\text{-}F}$ = 3.2 Hz. Information from the HSQC spectrum confirmed that the signal for C-2 and C-6 at δ 115.0 is bonded to the proton at 7.06 ppm which affirms the accurate assignment of these chemical shift values in the characterization of compound **41**. The carbon atoms in the triazine ring were the most deshielded and they appear at δ 171.6, δ 171.1 and δ 165.8 for C-9, C-8 and C-7 respectively. The signal for C-16 appears at δ 156.6 while the signal for C-10 appears at δ 155.1. Both these carbon atoms are attached to an oxygen atom and are part of an aromatic ring system, however, they differ by the substituent in the *para*-position, a nitro group is the substituent in the *para*-position to C-16 while a nitrile group is the substituent in the *para*-position to C-10.

The signals for the nitrile functional group appear at δ 118.4 for **41**, δ 118.3 for **42** and δ 115.6 for **45** and the signals for the carbon atom directly attached to the nitrile functional groups for these synthesized compounds, C-13, appear at δ 108.6 for **41** and δ 108.7 for **42**. Interestingly for **45** the carbon attached to the nitrile group exhibited 2 signals observed with the major signal

C-14 at δ 121.2 and the minor signal C-14 ′ at δ 120.6, indicating the presence of conformers. The ^{13}C NMR spectrum shown in **Figure 26** shows an increased number of signals when deuterated acetone or a mixture of solvents including deuterated acetone was used, as a result this made it very complicated to differentiate these extra signals and signals arising from conformers. The presence of a methoxy group was confirmed by the signal that appears at δ 55.7 in the ^{13} C NMR spectrum of compound **45**, additionally the HSQC spectrum confirms that C-1 is bonded to 3 protons that appear in the ^{1}H NMR spectrum as a singlet at δ 5.08.

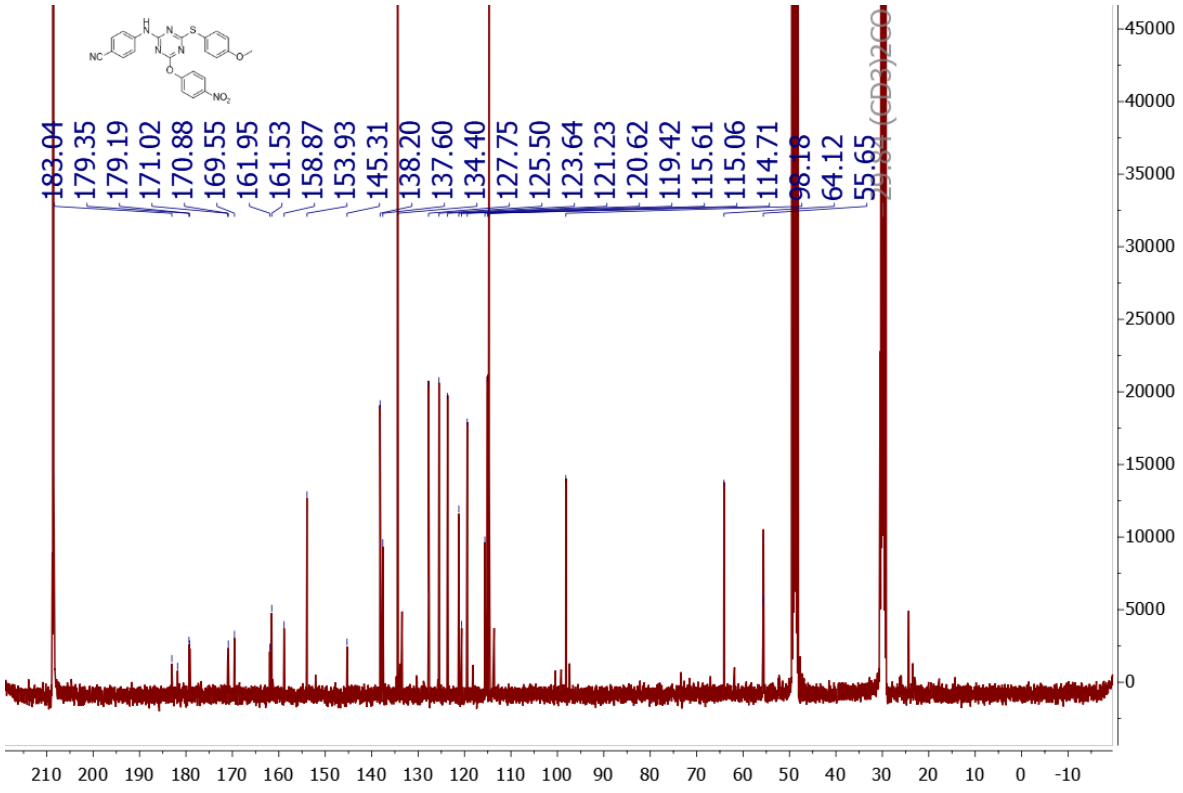

Figure 26: ^{13}C NMR spectrum for trisubstituted triazine derivative **45** in MeOD-d_4 + Acetone-d_6

The ^{13}C NMR spectrum of compound **45** was a challenge to interpret due to the above-mentioned occurrences and this was also observed in the ^{1}H NMR spectrum. The signals indicated the possibility of 2 or more conformers being exhibited due to multiple spatial arrangement of atoms of this molecule that arise from restricted rotation about a single bond.[93,99] The C-N bond between the triazine and the amine is expected to have partial double bond character, leading to the existence of "*cis*" and "*trans*" isomers (**Figure 27**).

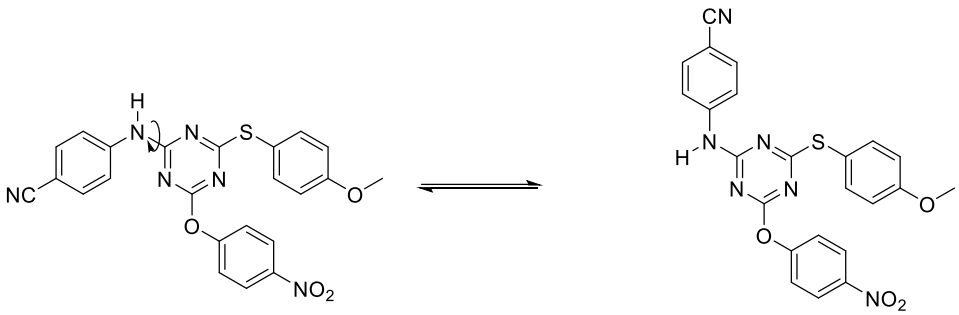

45 **45**

Figure 27: Conformational equilibrium arising from restricted rotation about the amine-triazine linkage.

Previous studies have reported interesting data on prototropic tautomerization. This phenomenon arises when the repositioning of a hydrogen atom between the ring nitrogen atom and the atom adjacent to it occurs. **Figure 28** shows NH, O and S bearing triazine molecules and their multiple tautomer forms that have been investigated where amine-imine, iminol-amide and thioiminol-thioamide tautomerisms were exhibited.[105]

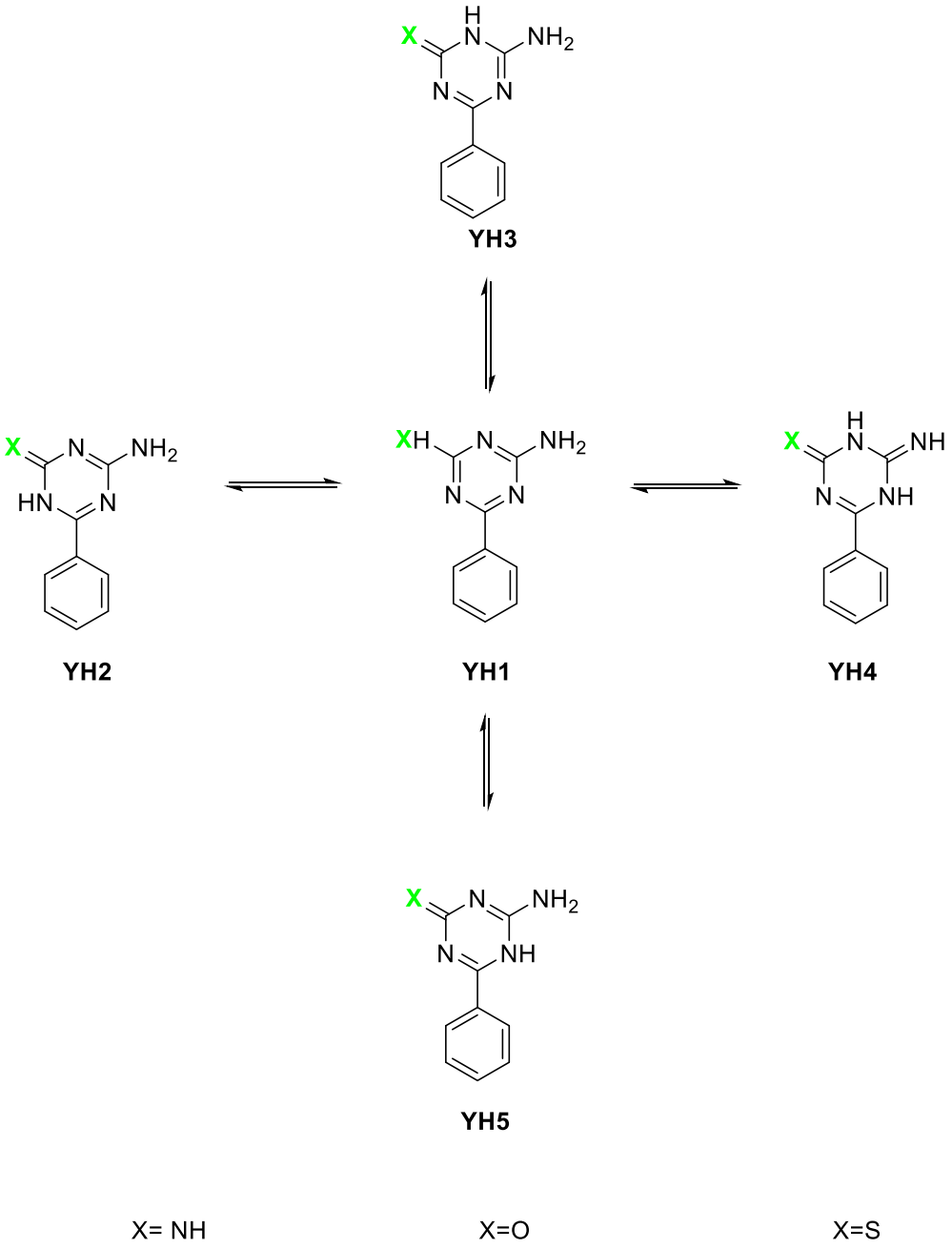

Figure 28: Different tautomeric forms of molecules with NH, O and S attached to the triazine ring.

Characterization of the synthesized tri-substituted triazine compounds **42**, **43**, **44** and **46** was carried out using the information obtained from NMR spectra to confirm successful coupling reactions in the same fashion as described for triazine **41**.

IR spectroscopy was used to confirm the presence of some of the functional groups that can be distinguished using this technique. The NH group in these compounds was confirmed by the appearance of peaks in the range of 3265 cm^{-1} – 3368 cm^{-1}. Peaks identified at 2233 cm^{-1}, 2234 cm^{-1} and 2213 cm^{-1} for compounds **41**, **42** and **45**, respectively, confirmed the presence of the nitrile functional group in these products. The presence of a nitro group in compounds **41**, **43**, **44**, **45** and **46** was confirmed by strong stretching peaks in the range of 1510 cm^{-1}- 1564 cm^{-1}.

HRMS (m/z) results confirmed the identity of the synthesised products as shown in **Table 8**.

Table 8: HRMS results for selected trisubstituted triazine derivatives.

	41 ($C_{22}H_{12}FN_6O_4$)	**42** ($C_{22}H_{14}{}^{79}BrClN_5O_2$)	**43** ($C_{21}H_{14}ClFN_5O_4$)	**44** ($C_{22}H_{16}FN_6O_4$)
Expected Mass $(M+H)^+$		494.0014	454.0713	447.1223
Found Mass $(M+H)^+$		494.0005	454.0703	447.1225
Expected Mass $(M-H)^-$	443.0910			
Found Mass $(M-H)^-$	443.0912			

The synthesis of the trisubstituted triazine derivatives was lengthy due to changes in the triazine ring system and the reduced reactivity which required higher activation energies for the reactions to progress. The challenges of solubility of some of these compounds introduces room for further modifications that would be required to incorporate these compounds as active substances in medicines such as NNRTIs.

2.4 Antiviral activity and toxicity studies of synthesized compounds.

With the aim to ascertain if the compounds synthesized would yield positive results in the interactions with the RT enzyme to slow down or stop its replication of the wild type HIV, anti-HIV assay studies were conducted by a collaborator, Dr Adriaan Basson, in the Faculty of Health Sciences, Wits University. A selected number of compounds with at least one from each step of the nucleophilic substitution reactions, were evaluated against HIV-1 pseudoviruses and two of the eight compounds tested showed activity. The values of the CC_{50} (cytotoxicity), IC_{50} (anti-HIV potency) and SI (selectivity index, CC_{50}/IC_{50} ratio) of the target compounds are illustrated in **Table 9**. Nevirapine was used as the control during these tests.

Novel compound **42** was the most toxic to the Human embryonic kidney 293 T-cells (HEK293T) with an average CC_{50} of 9.2 µM after duplicate tests. However, this compound exhibited a good micromolar activity against HIV-1 with an IC_{50} average value of 0.53 µM which can be improved to give better results as the control used Nevirapine with an IC_{50} average value of 0.01 µM. These results proved that the novel target **42** has a high affinity and binding interactions with HIV-1 RT. Further modifications can be implemented to reduce the cytotoxicity, thus improving the properties of this compound as a possible NNRTI.

Table 9: CC_{50}, IC_{50} and selectivity index values of target compounds from *in vitro* anti-HIV evaluations.

Compound	**Toxicity (CC_{50}, HEK293T cells)**			**Activity (IC_{50}, p8.9MJ4)**		**SI (CC_{50}/IC_{50})**
		Result	%CV	Result	%CV	
32c		>100	-	22.47	3.30	>4.5
32d		>100	-	Inactive		
34a		28.0	6.8	Inactive		
38		>100	-	Inactive		
39a		71.5	2.8	Inactive		
39e		56.5	5.3	Inactive		
42		9.2	0.3	0.53	10.5	17.2
43		28.2	4.3	Inactive		

Compounds for testing were dissolved in dimethyl sulfoxide (DMSO) and serial dilutions were prepared in cell culture medium in the wells of 96-well culture plates. Comparing structure-activity relationship (SAR) study results obtained by other groups we hypothesised how the structure of compound **42** could form interactions with the HIV-1 to yield good activity against the viral strain. **Figure 29** illustrates how novel target **42** could possibly maintain double hydrogen bond interactions with the backbone of the **K101** and the **L180** residues.[106]

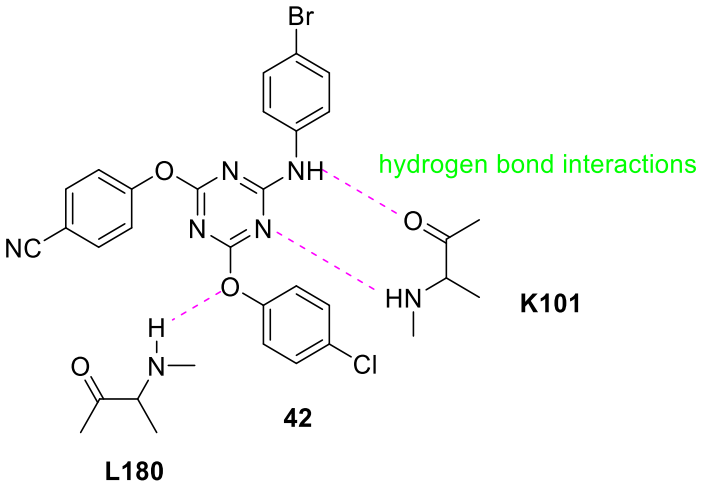

Figure 29: Proposed binding mode of compound **42** with **K101** and **L180** residues

Compound **32c** also exhibited moderate anti-HIV activity with an IC_{50} average value of 22.47 µM from duplicate tests. This compound had a better cytotoxicity profile than compound 43, with no cytotoxicity being shown at the maximum tested concentration of 100 µM. Similarly for compounds **32d** and **39** CC_{50} values were greater than 100 µM. Compounds **32d**, **34a**, **38**, **39a**, **39e** and **43** were all inactive in the HIV-1 pseudovirus assay. It is hypothesized that targets **32d**, **34a**, and **38** did not exhibit any activity due to them bearing a single aromatic substituent on the triazine ring which could not effectively form strong interactions with the enzyme residues. It has been reported that increasing the volume around the triazine ring by additional substituents can promote π-π interactions between the NNRTIs and Tyr188 or Tyr181 of RT.[83]

Chapter 3

3.0 Conclusions and future work

We successfully synthesized an array of triazine derivatives substituted with one, two or three aromatic rings using cyanuric chloride as the starting point of our successive substitution reactions. We determined that the order of the nucleophilic substitution reactions was an important factor in the successes of our reactions owing to the effect of the changes in reactivity of the triazine ring when different substituents are attached to the ring. The strength of the incoming nucleophile alters the electron density within the triazine ring and its susceptibility to a nucleophilic attack hence the necessity to increase the temperature of the reactions at each stage to increase the kinetic energy of the reaction.

In the stepwise nucleophilic substitution reactions, the first step involved the synthesis of compounds **32a-e**, **34a-b** and **38** wherein one of the Cl atoms of the triazine ring was substituted by various nucleophiles (**Figure 30**). The yields of these reactions ranged from 28%-90%, triazine **34b** had the lowest yield of 28% while triazine **32d** displayed the best yield of 90%. These reactions were all carried out under ice-cold conditions with temperatures from 0-5 °C to control the reaction and ensure only one of the Cl atoms from the cyanuric chloride is substituted during this step.

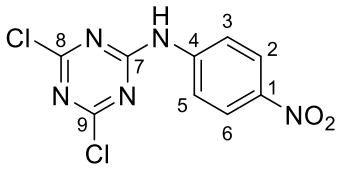

32d: 90 %

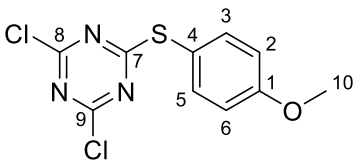

34b: 28%

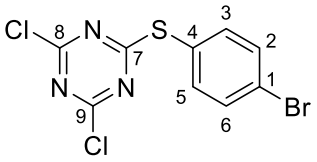

34a: 88 %

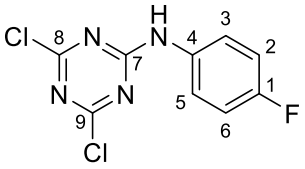

32a: 82 %

Figure 30: Selected triazine derivatives bearing a single aromatic substituent.

The sequential step in the aromatic nucleophilic reactions carried out involved the displacement of a second chlorine atom attached to the triazine ring. This reaction required more kinetic energy as the addition of a new substituent on triazine ring reduced its reactivity and it became less susceptible to a nucleophilic attack. Compounds **39a-g** were successfully synthesized with yields ranging from 31%-91% (**Figure 31**). The reaction times were longer and temperatures were elevated from 0°C -RT for reaction completion to occur based on reasons explained earlier.

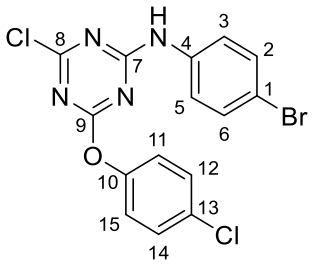

39b: 91 %

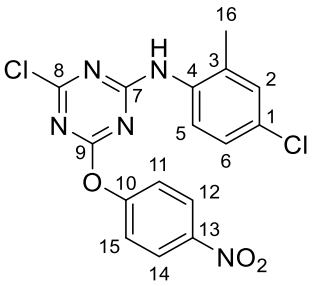

39g: 31 %

Figure 31: Selected triazine derivatives bearing two aromatic substituents.

The final step of these reactions was to substitute the last Cl atom from the triazine ring. This process was the most complex of the three steps and required longer reaction times, higher

temperatures of between 85° C-100 °C under reflux conditions. Compounds **41-46** were synthesized with yields ranging from 11%-83%. The tri-substituted triazine derivatives had very low solubility profiles and their characterization via NMR and mass spectroscopy was extremely difficult due to this. The data obtained from the aforementioned analytical techniques was very useful in confirming the synthesis of the desired compounds. **Figure 32** shows some of the trisubstituted triazine derivatives and their respective yields.

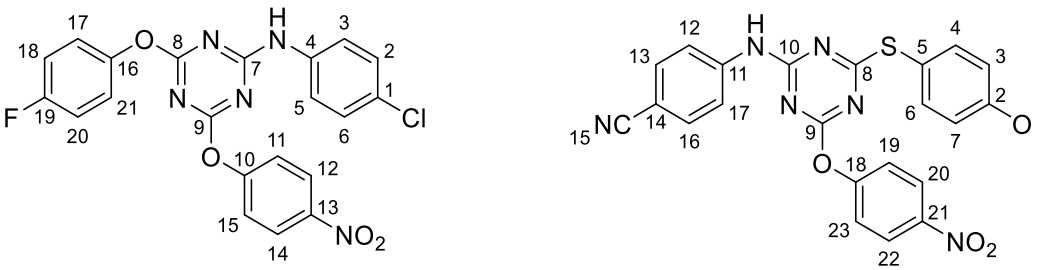

Figure 32: Selected trisubstituted triazine derivatives successfully synthesized.

Conformational isomers were exhibited by most of the synthesized compounds, predominantly those bearing an amine group and some examples are compounds **32d**, **39g**, **41** and **45**. The presence of conformers is most likely due to the restricted rotation of the bond between the triazine ring and the amino substituents. We also noted the presence of rotamers for **34b** and **39f** and these bear thiol substituents which would also suggest that the rotation about the triazine ring and thiol substituents gives rise to conformers. The ability of these compounds to exhibit different spatial arrangements is a vital property for NNRTIs as this enables them to resist multiple mutant strains of HIV-1.

We believe the presence of NH- and O- linkers in compound **42** proved to be beneficial in maintaining hydrophilic interactions via hydrogen bonds with the amino acid residues of the RT. We expected compound **39a** to exhibit some activity toward HIV-1 as its structural

dynamics would fit the profile supporting good binding interactions. The aromatic moieties would promote π-π interactions, while the nitrogen and oxygen atoms are capable of forming hydrogen bonds with the backbone of the amino acid residues of RT. The presence of the fluorine atom which is highly electronegative is known to contribute to biologically active systems through lipophilicity, absorption and transportation. Further modifications on this compound and computational studies can be explored in future work to incorporate substituents that will yield better interactions in the NNRTI-BP.

Future work will involve carrying out anti-HIV evaluation studies on all the synthesized trisubstituted triazine derivatives to identify if any of them based on their chemical structures will have favorable anti-HIV activities as well as a good selectivity index. Molecular modelling will also be beneficial in identifying target binding sites on the amino acid residues for interactions with the NNRTIs. These docking studies can also assist in modifications on the synthesized compounds or even designing new compounds that can maintain multiple hydrogen bonds with the RT enzyme, as well as substituents of sufficient length to go deep into the adjacent sites of the NNRTI-BP. A lot of work has been done and reported with respect to aminosubstituted-1,3,5-triazines and their efficacy as potential NNRTIs but there is a greater need to explore the properties and the contribution thiol substituted-1,3,5-triazines and the role they can play in development of new NNRTIs.

Chapter 4

4. EXPERIMENTAL PROCEDURES

4.1 Materials and general procedures

Commercially available compounds with purity of 95% and above obtained from Sigma Aldrich were used for the experiments carried out and all handling and storage protocols were observed.

Solvents such as hexane, ethyl acetate, dichloromethane and ethanol used for column chromatography to purify products were all distilled prior to use. Other solvents used such as THF and acetonitrile were distilled under nitrogen before use.

Gravity normal silica gel (particle size 0.063-0.200 mm) or flash silica gel (0.040-0.063 mm) purchased from Merck were utilised as the solid phases in the purification via column chromatography.

AR grade acetone from Minema Chemicals with 99.9% purity was used in reactions. Deionized water was obtained in house for the preparation of aqueous NaOH solutions.

Thin Layer Chromatography was conducted using aluminium-backed Merck silica gel 60 F_{524} plates. Visual determinations were made under UV light at wavelengths of 254 nm.

Nuclear magnetic resonance (NMR) spectra were recorded using a Bruker AVANCE 300, 400 or 500 MHz spectrometer. Deuterated chloroform, dimethyl sulfoxide-d_6 and acetone-d_6 were used to dissolve the compounds for NMR spectroscopic analysis. ^{1}H and ^{13}C NMR spectra were referenced to trimethylsilane at 0.00 ppm for $CDCl_3$ solutions. ^{1}H NMR spectra were referenced with signals at 2.50 ppm for DMSO-d_6 and 2.05 ppm for acetone-d_6. ^{13}C NMR signals were referenced at 39.52 ppm for DMSO-d_6 and 29.84 ppm for acetone-d_6.

In reporting NMR data, the signals for minor conformers were designated with a prime symbol and/or a double prime signal while the signals for the major conformers were not marked with the prime symbol for distinctions.

Some signals were reported together as we were not able to assign the chemical shift values with certainty.

High resolution mass spectra were recorded on a Bruker Compact Q-TOF high resolution Compact mass spectrometer.

Melting points were recorded on a Stuart SMP20 melting point instrument and are uncorrected.

For automated column chromatography the CombiFlash NextGen 300+ was used for purification and separations.

Infrared spectra were recorded on a Bruker Tensor 27 standard system spectrophotometer. The measurements were reported on the wavenumber scale (cm^{-1}).

For the purposes of simplicity and convenience we have not adopted the standard IUPAC numbering system for the structures in the experimental section, but the naming of the compounds is in accordance with the IUPAC convention.

4.2 Experimental procedures

4.2.1 General procedure for the preparation of 1,3,5-triazine derivatives bearing a single aromatic substituent.

Cyanuric chloride (10 mmol, 1 equiv.) was added to chilled acetone (25 ml) in a round bottom flask and placed in an ice bath at 0-5°C to obtain a white slurry while stirring. An appropriately substituted aniline, phenol or thiophenol (10 mmol, 1 equiv.) dissolved in acetone (20 ml) and NaOH (10 ml, 1-2 M) /K_2CO_3 (10 ml, 1 M) /$NaHCO_3$ (10 ml, 10 %)

was added in a dropwise manner to the reaction vessel. Care was taken to ensure that the temperature was kept low to prevent multiple substitutions. The reaction mixture was stirred and monitored via TLC for approximately 3-5 h in the ice bath until reaction completion. Once the reaction was complete it was stopped, poured over crushed ice, washed with deionized water (2 x 50 ml) filtered and dried. Purification was carried out using a CombiFlash NextGen 300+ system, with a RediSep Gold silica gel flash column 12 g or gravity column chromatography using a 10-25% ethyl acetate/hexane solvent as eluent. A rotary evaporator was used to remove the solvent *in vacuo* at a temperature of 45°C, to afford the product.

4.2.1.1 Synthesis of 4,6-dichloro-N-(4-fluorophenyl)-1,3,5-triazin-2-amine (32a)[85-87]

Cyanuric chloride (3.53 g, 19 mmol), 4-fluoroaniline (2.30 g, 21 mmol) and NaOH solution (15 ml, 1.6 M) were reacted in acetone (45 ml) for 4-5 h as described in 3.2.1. The mixture was purified by normal silica gel column chromatography using 10-25% ethyl acetate / hexane as eluent to afford **32a** (4.06 g, 82%) as a yellow solid.

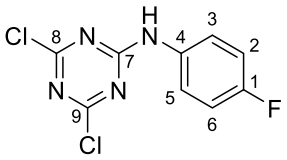

R_f 0.38 (25% EtOAc/Hexane); **mp** 181-190 °C; **IR** (ν_{max}/cm^{-1}) 3152 (N-H), 2099 (C-H), 1080 (C-F); **^{1}H NMR** (400 MHz, DMSO-d_6) δ: 11.14 (s, 1H, NH), 7.65-7.54 (m, 2H, H3 & H5), 7.28-7.20 (m, 2H, H2 & H6); **^{13}C NMR** (101 MHz, DMSO-d_6) δ: 169.7 and 168.8 (C8 & C9), 163.8 (C7), 163.7 (C7′), 159.2 (d, $^1J_{C\text{-}F}$ = 242.2 Hz, C1), 133.2 (d, $^4J_{C\text{-}F}$ = 2.7 Hz, C4), 133.1 (d, $^4J_{C\text{-}F}$ = 2.7 Hz, C4′), 124.0 (d, $^3J_{C\text{-}F}$ = 8.3 Hz, C3′ & C5′), 123.6 (d, $^3J_{C\text{-}F}$ = 8.3 Hz, C3 & C5), 115.6 (d, $^2J_{C\text{-}F}$ = 22.6 Hz, C2 & C6), 115.0 (d, $^2J_{C\text{-}F}$ = 22.6 Hz, C2′ & C6′).

4.2.1.2 Synthesis of 4,6-dichloro-*N*-(4-bromophenyl)-1,3,5-triazin-2-amine (32b)[85-87]

Cyanuric chloride (1.85 g, 10 mmol), 4-bromoaniline (1.72 g, 10 mmol) and NaOH solution (10 ml, 1M) in acetone were reacted for 4-5 h as described in 3.2.1. The mixture was purified

by normal silica gel column chromatography using 10-20% ethyl acetate / hexane as eluent to afford **32b** (1.89 g, 59%) as a white solid powder.

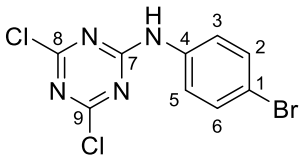

R_f 0.28 (10% EtOAc/hexane); **mp** 174-177 °C; **IR** (ν_{max}/cm^{-1}) 3379 (N-H), 2499 (C-H), 535 (C-Br); **^{1}H NMR** (400 MHz, DMSO-d_6) δ: 11.23 (s, 1H, NH), 7.67 – 7.50 (m, 4H, H2, H3, H5 & H6); **^{13}C NMR** (101 MHz, DMSO-d_6) δ: 169.7 and 168.8 (C8 & C9), 163.7 (C7), 136.4 (C4), 131.8 (C2 & C6), 123.3 (C3 & C5), 116.9 (C1).

4.2.1.3 Synthesis of 4,6-dichloro-*N*-(4-chlorophenyl)-1,3,5-triazin-2-amine (32c)[85-87]

Cyanuric chloride (1.84 g, 10 mmol), 4-chloroaniline (1.28 g, 10 mmol) and K_2CO_3 solution (10 ml, 1 M) in acetone were reacted for 4-5 h as described in 3.2.1. The mixture was purified by normal silica gel column chromatography using 10-20% ethyl acetate / hexane as eluent to afford **32c** (1.47 g, 54%) as a pale-yellow solid powder.

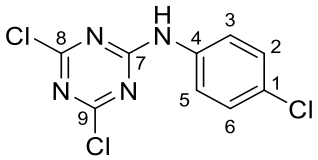

R_f 0.56 (15% EtOAc/hexane); **mp** 182-189 °C; **IR** (ν_{max}/cm^{-1}) 3395 (N-H), 791 (C-Cl); ^{1}H NMR (400 MHz, DMSO-d_6) δ: 11.24 (s, 0.52H, NH), 11.15 (s, 0.28H, NH), 10.87 (s, 0.49H, NH), 7.64-7.59 (m, 2H, H2 & H6), 7.47-7.40 (m, 2H, H3 & H5); **^{13}C NMR** (101 MHz, DMSO-d_6) δ: 169.7 and 168.8 (C8 & C9), 163.8 (C7), 141.5 (C4), 136.0 (C1),128.9 (C2 & C6), 123.0 (C3 & C5); **HRMS** (m/z), calculated for $C_9H_4Cl_3N_4$ $(M-H)^-$: 272.9507, found: 272.9512.

4.2.1.4 Synthesis of 4,6-dichloro-*N*-(4-nitrophenyl)-1,3,5-triazin-2-amine (32d)[85-87]

Cyanuric chloride (1.85 g, 10 mmol) and 4-nitrooaniline (1.39 g, 10 mmol) in acetone were reacted, $NaHCO_3$ solution (10 ml, 10 %) was added to the reaction mixture in a dropwise

manner while maintaining pH at 6-7 for 3 h as described in 3.2.1 The mixture was purified by normal silica gel column chromatography using 10-20% ethyl acetate / hexane as eluent to afford **32d** (2.57 g, 90%) as a yellow solid powder.

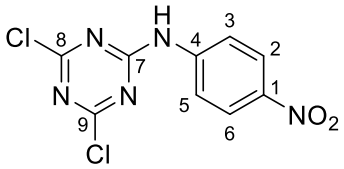

R*f* 0.56 (15% EtOAc/hexane); **mp** 138-142 °C; **IR** (ν_{max}/cm^{-1}) 3347 (N-H), 1490 (N-O); **^{1}H NMR** (400 MHz, DMSO-*d*$_6$) δ 11.60 (s, 0.80H, NH), 10.96 (s, 0.24H, NH), 8.25-8.23 (m, 2H, H2 & H6), 7.87-7.84 (m, 2H, H3 & H5); **^{13}C NMR** (101 MHz, DMSO-*d*$_6$) δ: 164.2 (C8 & C9), 154.1 and 153.2 (C7), 144.3 (C4′), 143.6 (C4), 143.4 (C1), 142.9 (C1′), 125.1 (C2 & C6), 121.2 (C3 & C5), 120.6 (C3′ & C5′); **HRMS** (m/z), calculated for $C_9H_4Cl_2N_5O_2$ (M-H)$^-$: 283.9748, found: 283.9755

4.2.1.5 Synthesis of 4,6-dichloro-*N*-(4-chloro-2-methylphenyl)-1,3,5-triazin-2-amine (32e)[85-87]

Cyanuric chloride (1.34 g, 7.3 mmol), 4-chloro-2-methylaniline (1.06 g, 7.5 mmol) and NaOH solution (10 ml, 1 M) in acetone were reacted for 24 h as described in 3.2.1. The mixture was purified by normal silica gel column chromatography using 10% ethyl acetate / hexane as eluent to afford **32e** (1.63 g, 78%) as a pale yellow solid.

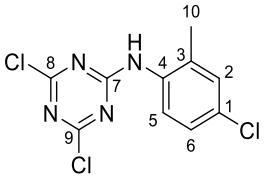

R*f* 0.47 (15% EtOAc/hexane); **mp** 192-197 °C; **IR** (ν_{max}/cm^{-1}) 3406 (N-H), 3074 (C-H); **^{1}H NMR** (300 MHz, DMSO-*d*$_6$) δ 10.70 (s, 1H, NH), 7.42-7.38 (m, 1H, Ar-H), 7.36(s, 0.18H, Ar-H), 7.34-7.30 (m, 1.65H, Ar-H), 7.29-7.28 (m, 0.20H, Ar-H), 3.43 (s,3H, H10); **^{13}C NMR** (101 MHz, DMSO-*d*$_6$) δ: 169.7 and 169.0 (C8 & C9), 165.8 (C7), 136.2 (C4), 133.6 (C1), 131.1 (C3), 130.2 (C2), 128.4 (C5), 126.3 (C6). 17.5 (C10); **HRMS** (m/z), calculated for $C_{10}H_6Cl_3N_4$ (M-H)$^-$: 286.9664, found: 286.9667.

4.2.1.6 Synthesis of 2-((4-bromophenyl) thio)-4,6-dichloro-1,3,5-triazine (34a)

Cyanuric chloride (1.86 g, 10 mmol), 4-bromothiophenol (1.89 g, 10 mmol) and NaOH solution (10 ml, 1 M) in acetone were reacted for 18 h as described in 3.2.1. The mixture was purified by normal silica gel column chromatography using 4% ethyl acetate / hexane as eluent to afford **34a** (2.99 g, 88%) as a white powder.

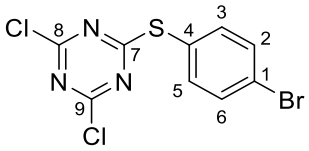

R_f 0.25 (1% EtOAc/Hexane); **mp** >250 °C; **IR** (ν_{max}/cm^{-1}) 3076 (C-H) ; **^{1}H NMR** (300 MHz, DMSO-*d*$_6$) δ 7.76-7.65 (m, 2H, H3 & H5), 7.57-7.48 (m, 2H, H2 & H6); **^{13}C NMR** (101 MHz, DMSO-*d*$_6$) δ: 183.0 (C7), 170.1 (C8 & C9), 151.5 (C4), 137.0 (C2 & C6), 132.4 (C3 & C5),124.3 (C1).

4.2.1.7 Synthesis of 2,4-dichloro-6-((4-methoxyphenyl)thio)-1,3,5-triazine (34b)[89]

Cyanuric chloride (1.87 g, 10 mmol), 4-methoxythiophenol (1.36 g, 9.7 mmol) and NaOH solution (10 ml, 11 mmol) in acetone were reacted for 20 h as described in 3.2.1. The mixture was purified by normal silica gel column chromatography using 4% ethyl acetate / hexane as eluent to afford **34b** (0.81 g, 28%) as a white solid.

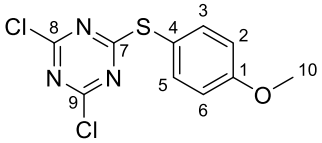

R_f 0.45 (15 % EtOAc/Hexane); **mp** >250 °C; **IR** (ν_{max}/cm^{-1}) 2833 (C-H), 1239 (C-O); **^{1}H NMR** (300 MHz, DMSO-*d*$_6$) δ 7.47 (d, *J* = 8.8 Hz, 2H, H2 & H6,), 7.03 (d, *J* = 8.8 Hz, 2H, H3 & H5), 3.80 (s, 3H, H10); **^{13}C NMR** (101 MHz, DMSO-*d*$_6$) δ: 180.1 (C7), 170.0 (C8 & C9), 161.0 (C1), 160.4 (C1′), 159.7 (C1′′), 152.0 (C4′), 150.0 (C4), 137.7 (C3 & C5), 136.5 (C3′ & C5′), 115.3 (C2′ & C6′), 115.1 (C2 & C6), 114.8 (C2′′ & C6′′), 55.5 (C10); **HRMS** (m/z), calculated for $C_{10}H_6Cl_2N_3OS$ $(M-H)^-$: 286.9614, found: 286.9656.

4.2.1.8 Synthesis of 2,4-dichloro-6-(4-nitrophenoxy)-1,3,5-triazine (38)[87]

Cyanuric chloride (1.86 g, 10 mmol) was added to chilled acetone (20 ml) in an ice bath. 4-Nitrophenol (1.40 g, 10 mmol) in acetone (20 ml) and NaOH solution (10 ml, 1.2 M) were reacted together and stirred for 30 min. The resultant mixture was added in a dropwise manner to the cyanuric chloride and the pH was maintained at pH 7-8 by addition of 10% $NaHCO_3$ solution, after 6 h the reaction was stopped. The mixture was purified by normal silica gel column chromatography using 10% ethyl acetate / hexane as eluent to afford **38** (1.98 g, 69%) as a white solid.

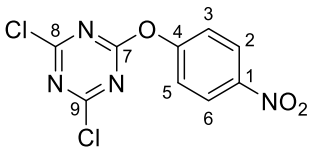

R_f 0.27 (15% EtOAc/Hexane); **mp** >250 °C; **IR** (ν_{max}/cm^{-1}); **^{1}H NMR** (400 MHz, Methanol-d_4, DMSO-d_6) δ 8.32-8.23 (m, 2H, H2 & H6), 7.53-7.46 (m, 2H, H3 & H5); **^{13}C NMR** (101 MHz, Methanol-d_4, DMSO-d_6) δ: 164.6 (C7), 154.7 (C8 &C9), 150.7 (C4), 140.7 (C1), 126.8 (C2 & C6), 116.4 (C3 & C5).

4.2.2 General procedure for the preparation of 1,3,5-triazine derivatives with two aromatic substituents.

A mono-substituted derivative (1 eq.) synthesised as described above in 3.2.1 was dissolved in acetone (10 ml) in a round bottom flask. To this solution an aromatic compound (1 eq.) dissolved in acetone (20 ml) was added in a dropwise manner for approximately 15 min, followed by NaOH solution (10 ml, 0.25-2 M). The reaction was stirred at temperatures from 0-5°C or at room temperature for between 5-24 h while being monitored via TLC for reaction completion. In the case of a phenol being used as a reactant the phenoxide was prepared first by adding the NaOH solution to a substituted phenol dissolved in acetone and stirring at room temperature for 30 min before adding to the reaction vessel. After reaction completion, the

reaction mixture was poured over crushed ice, washed with deionized water (2 x 30 ml), filtered and dried. Purification was carried out using the CombiFlash NextGen 300+ system with a RediSep Gold silica gel flash column 12 g or gravity column chromatography using a 10-25% ethyl acetate/hexane solvent as eluent.

4.2.2.1 Synthesis of 4-chloro-*N*-(4-fluorophenyl)-6-(4-nitrophenoxy)-1,3,5-triazin-2-amine (39a)

4-Nitrophenol (1.99 g, 14 mmol) and NaOH solution (10 ml, 1.7M) were stirred at RT for 30 min to afford the phenoxide which was then reacted with **32a** (3.72 g, 14 mmol) as described in 3.2.2 for 23 h at 0-5°C. The mixture was purified using flash silica gel column chromatography and 10% ethyl acetate / hexane as eluent to afford **39a** (4.42 g, 85 %) as a pale-yellow solid.

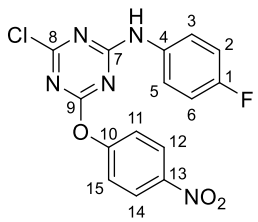

R_f 0.26 (15% EtOAc/Hexane); **mp** >250 °C; **IR** (ν_{max}/cm^{-1}) 3352 (N-H), 1505 (N-O), 1337 (C-O), 1190 (C-F); **^{1}H NMR** (400 MHz, DMSO-d_6) δ 10.90 (s, 0.63H, NH), 10.64 (s, 0.31H, NH), 8.36 (d, *J* = 8.9 Hz, 2H, H12 and H14), 7.61 (d, *J* = 8.6 Hz, 2.77H, Ar-H), 7.45-7.42 (m, 1.39h, Ar-H), 7.21 (t, *J* = 8.2 Hz, 0.77H, Ar-H), 7.06 (t, *J* = 8.6 Hz, 1.36H, Ar-H); **^{13}C NMR** (126 MHz, DMSO-d_6) δ 170.2 and 169.9 (C8), 165.0 (C9′), 164.7 (C9), 163.9 (C7), 158.8 (d, $^1J_{C\text{-}F}$ = 241.3 Hz, C1), 156.3 (C10), 154.3 (C10′) 145.3 (C13), 133.5 (d, $^4J_{C\text{-}F}$ = 2.8 Hz, C4), 126.2 (C12 & C14), 125.4 (C12′ & C14′), 123.8 (d, $^3J_{C\text{-}F}$ = 8.1 Hz, C3 & C5), 122.9 (d, $^3J_{C\text{-}F}$ = 7.9 Hz, C3′ & C5′) 123.2 (C11 & C15), 115.5 (d, $^2J_{C\text{-}F}$ = 22.5 Hz, C2 & C6), 115.2 (d, $^2J_{C\text{-}F}$ = 22.4 Hz, C2′ & C6′); **HRMS** (m/z), calculated for $C_{15}H_8ClFN_5O_3$ $(M\text{-}H)^-$: 360.0305, found: 360.0309.

4.2.2.2 Synthesis of *N*-(4-bromophenyl)-4-chloro-6-(4-chlorophenoxy)-1,3,5-triazin-2-amine (39b)

4-Chlorophenol (0.77 g, 6.0 mmol) and NaOH solution (10 ml, 0.7M mmol) were stirred to afford the phenoxide at RT for 30 min which was reacted with **32b** (1.89 g, 6 mmol) as described in 3.2.2 for 23h at 0-5°C. The mixture was purified by flash silica gel column chromatography and a 10% ethyl acetate / hexane solvent system to afford **39b** (2.28g, 93 %) as a white powder.

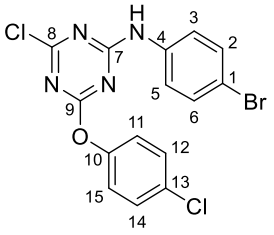

R_f 0.34 (15% EtOAc/Hexane); **mp** >250 °C; **IR** (ν_{max}/cm^{-1}) 3379 (N-H), 1217 (C-O), 716(C-Cl), 616 (C-Br) ; **^{1}H NMR** (500 MHz, DMSO-d_6) δ 10.92 (s, 0.50H, NH), 10.79 (s, 0.22H, NH), 10.65 (s, 0.25H, NH), 7.62-7.51 (m, 3.32H, Ar-H) 7.43-7.34 (m, 3.62H, Ar-H), 7.18 (d, *J* = 8.8 Hz, 0.37H, Ar-H), 6.76 (d, *J* = 8.8 Hz, 0.37H, Ar-H); **^{13}C NMR** (126 MHz, DMSO- d_6) δ 170.7 and 169.9 (C8), 164.5 (C9), 156.3 (C7), 150.4 (C10), 137.0 (C4), 131.6 (C2 & C6), 131.2 (C2′ & C6′), 130.3 (C13), 129.6 (C12′ & C14′), 129.1 (C12 & C14), 123.8 (C11′ & C15′), 123.2 (C11 & C15), 122.4 (C3 & C5) 116.9 (C1).

4.2.2.3 Synthesis of 6-chloro-N^2-(4-methoxyphenyl)-N^4-(4-nitrophenyl)-1,3,5-triazine-2,4-diamine (39c)[97]

p-Anisidine (0.72 g, 5.8 mmol), NaOH solution (10 ml, 0.7 M) and **32d** (1.67 g, 5.8 mmol) were reacted as described in 3.2.2 for 5 h at RT. The mixture was purified using silica gel column chromatography and a 25% ethyl acetate / hexane solvent system to afford **39c** (1.24g, 57%) as a white powder.

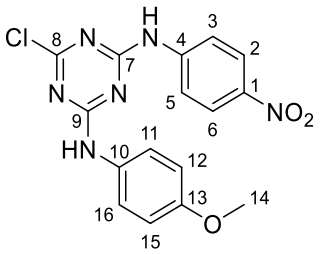

R_f 0.35 (25 % EtOAc/Hexane); **mp** >250 °C; **IR** (ν_{max}/cm^{-1}) 3351 (N-H), 1507 (N-O), 1238 (C-O); **^{1}H NMR** (400 MHz, DMSO-d_6) δ 10.37 (s, 1H, NH), 9.82 (s, 1H, NH), 8.19-7.79 (m, 2H, H2 & H6), 7.60-7.48 (m, 2.76H, Ar-H), 7.36-7.28 (m, 1.74H, Ar-H), 7.02-6.73 (m, 2H, H12 & H15), 3.75 (s, 3H, H14); **^{13}C NMR** (101 MHz, DMSO-d_6) δ 165.3 (C8), 154.8 (C7), 151.0 (C9), 141.3 (C1), 131.5 (C13), 129.6 (C4), 129.4 (C11 & C16), 124.5 (C2 & C6), 124.1 (C10), 119.3 (C3 & C5), 113.7 (C12 & C15), 55.2 (C14); **HRMS** (m/z), calculated for $C_{16}H_{11}ClN_6O_3$ $(M-H)^-$: 373.0810, found: 373.0874.

4.2.2.4 Synthesis of 4-chloro-*N*-(4-chlorophenyl)-6-(4-nitrophenoxy)-1,3,5-triazin-2-amine (39d)

4-Nitrophenol (0.36 g, 2.6 mmol) and NaOH solution (10 ml, 0.7 M) were stirred at RT for 30 min to afford the phenoxide which was then reacted with **32e** (0.71 g, 2.6 mmol) as described in 3.2.2 for 23 h at 0-5°C. The mixture was purified by flash silica gel column chromatography and a 10% ethyl acetate / hexane solvent system to afford **39d** (0.76 g, 77 %) as a white powder.

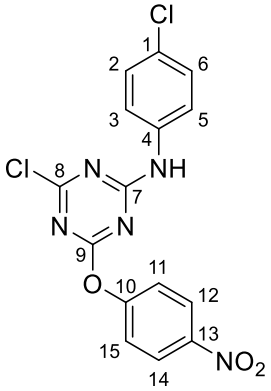

R_f 0.56 (15 % EtOAc/Hexane); **mp** >250 °C; **IR** (ν_{max}/cm^{-1}); **^{1}H NMR** (400 MHz, DMSO-d_6) δ 11.26 (s, 0.13H, NH), 11.02 (s, 0.60H, NH), 10.76 (s, 0.29H, NH), 8.42-8.33 (m, 1.85H, Ar-H), 7.62 (d, J = 8.0 Hz, 2.54H, Ar-H), 7.52-7.38 (m, 2.13H, Ar-H) 7.32-7.24 (m, 1.20H, Ar-H); **^{13}C NMR** (101 MHz, DMSO-d_6) δ 170.3 (C8), 170.1 and 169.9 (C9), 164.6 (C7), 156.2 (C10), 145.3 (C13), 136.4 (C4), 128.4 (C2 & C6), 127.9 (C1), 125.4 (C12 & C14) 123.1 (C11 & C15), 122.2 (C3 & C5).

4.2.2.5 Synthesis of 4-chloro-6-(4-fluorophenoxy)-*N*-(4-nitrophenyl)-1,3,5-triazin-2-amine (39e)

4-Fluorophenol (0.47 g, 4.2 mmol) and NaOH solution (10 ml, 0.5 M) were stirred at RT for 30 min to afford the phenoxide which was then reacted with **35d** (1.16 g, 4.1 mmol) as

described in 3.2.2 for 25 h at 0-5°C. The mixture was purified by silica gel column chromatography and a 15% ethyl acetate / hexane solvent system to afford **39e** (1.33 g, 91 %) as a white powder.

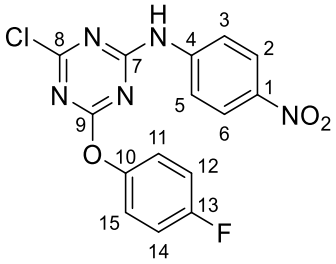

R_f 0.34 (15 % EtOAc/Hexane); **mp** >350 °C; **IR** (ν_{max}/cm^{-1}); **^{1}H NMR** (500 MHz, DMSO-d_6) δ 10.87 (s, 1H, NH), 8.07-8.02 (m, 2H, H2 & H6), 7.75-7.69 (m, 2H, H3 & H5), 7.37-7.30 (m , 4H, Ar-H); **^{13}C NMR** (101 MHz, DMSO-d_6) δ 170.8 (C8′), 170.4 (C8), 166.1 (C9), 164.9 (C7), 159.9 (d, $^1J_{C\text{-}F}$ = 241.8 Hz, C13), 147.7 (d, $^4J_{C\text{-}F}$ = 2.4 Hz, C10), 144.2 (C4), 142.5 (C1), 124.6 (C2 & C6), 123.6 (d, $^3J_{C\text{-}F}$ = 8.7 Hz, C11 & C15), 119.9 (C3 & C5), 116.5 (d, $^2J_{C\text{-}F}$ = 23.7 Hz, C12 & C14); **HRMS** (m/z), calculated for $C_{15}H_8ClFN_5O_3$ $(M\text{-}H)^-$: 360.0305, found: 360.0306.

4.2.2.6 Synthesis of 2-chloro-4-((4-methoxyphenyl)thio)-6-(4-nitrophenoxy)-1,3,5-triazine (39f)

4-Nitrophenol (98 mg, 0.70 mmol) and NaOH solution (10 ml, 0.5 M) were stirred at RT for 30 min to afford the phenoxide **39** which was then reacted with **35b** (202 mg, 0.71 mmol) as described in 3.2.2 for 5-6 h at RT. The mixture was purified by silica gel column chromatography and a 15% ethyl acetate / hexane solvent system to afford **39f** (210 mg, 76 %) as a white powder.

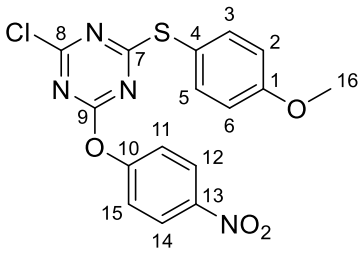

R_f 0.05 (15 % EtOAc/Hexane); **mp** >350 °C; **IR** (ν_{max}/cm^{-1}); **^{1}H NMR** (400 MHz, DMSO-d_6) δ 8.30-8.13 (m, 1.76H, Ar-H), 7.52-7.22 (m,4H, H2, H3, H5 & H6), 7.00-6.84 (m, 2.55H, Ar-H), 3.80-3.69 (m, 3H, H16); **^{13}C NMR** (101 MHz, DMSO-d_6) δ 186.3, (C7), 180.1 (C9), 170.1 (C8), 160.7 (C10), 160.4 (C10′), 155.9 (C13), 145.0 (C1), 136.9

(C3 & C5), 136.5 (C3′ & C5′), 132.1 (C4), 125.3 (C12 & C14), 124.8 (C12′ & C14′), 123.0 (C11 & C15), 122.8 (C11′ & C15′), 114.8 (C2 & C6) , 114.3 (C2′& C6′), 55.2 (C16).

4.2.2.7 Synthesis of 4-chloro-N-(4-chloro-2-methylphenyl)-6-(4-nitrophenoxy)-1,3,5-triazin-2-amine (39g)

4-Nitrophenol (172 mg, 1.24 mmol) and NaOH solution (10 ml, 0.25 M) were stirred at RT for 30 min to afford the phenoxide which was then reacted with **35e** (362 mg, 1.26 mmol) as described in 3.2.2 for 5-6 h at RT. The mixture was purified by aluminium oxide-c neutral column chromatography and a 15 % ethyl acetate / hexane solvent system to afford **39g** (143 mg, 31 %) as a pale-yellow powder.

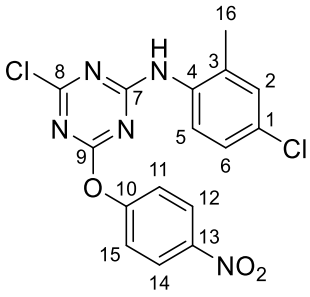

R_f 0.08 (15 % EtOAc/Hexane); **mp** >350 °C; **IR** (ν_{max}/cm^{-1}) 3352 (N-H), 3079 (C-H), 1511 (N-O), 1189 (C-O), 802 (C-Cl); **^{1}H NMR** (400 MHz, Acetone-d_6) δ 8.38-8.22 (m, 2H, H12 &H14), 7.60-7.43 (m, 2H, H11 & H15), 7.37-7.07 (m, 3H), 3.25 (s, 1H, NH), 2.22 (s, 3H, H16); **^{13}C NMR** (101 MHz, Acetone-d_6) δ 172.6 (C8), 172.0 (C9′), 171.6 (C9), 167.7 (C7), 157.6 (C10), 146.5 (C13), 137.4 (C4′), 136.4 (C4), 134.8 (C3) 134.5 (C3′), 133.0 (C2′′), 132.7 (C2′), 132.2 (C2), 131.0 (C6), 129.2 (C1′), 128.5 (C1), 127.2 (C5′), 126.8 (C5), 126.2 (C12′ & C14′), 126.0 (C12 & C14), 124.0 (C11′ & C15′), 123.8 (C11 & C15), 17.89 (C16).

4.2.2.8 Synthesis of 4-chloro-6-(4-nitrophenoxy)-N-(4-nitrophenyl)-1,3,5-triazin-2-amine (39h)

4-Nitroaniline (220 mg, 1.59 mmol), **39** (451mg 1.58 mmol), NaOH solution (10 ml, 0.40 M) were reacted as described in 3.2.2 for 24 h at RT. The mixture was purified by recrystallization using THF/Hexane to afford **39h** (303 mg, 49 %) as a pale-yellow solid.

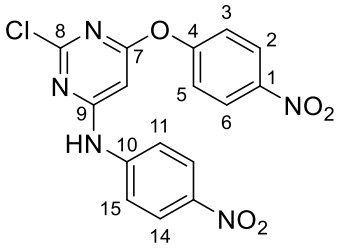

R_f 0.64 (25 % EtOAc/Hexane); **mp** >350 °C; **IR** (ν_{max}/cm^{-1}) 3480 (N-H), 1540 (N-O), 1518 (N-O), 1337 (C-O); **^{1}H NMR** (400 MHz, Acetone-*d_6*) δ 9.98 (s, 0.09H, N-H), 8.46-8.21 (m, 3.26H, Ar-H), 8.16-8.02 (0.39h, Ar-H), 8.01-7.89 (0.97H, Ar-H), 7.87-7.78 (m, 0.28H, Ar-H), 7.64-7.42 (m, 3H, Ar-H), 6.78-6.57 (m, 1H, Ar-H); **^{13}C NMR** (101 MHz, Acetone-*d_6*) δ 174.2 & 174.1 (C8), 172.9 (C7), 157.7 (C9) 157.1 (C4),156.9 (C10), 146.9 (C1), 146.6 (C13), 126.9 (C2 & C6), 126.3 (C12 & C14), 126.1 (C12′ & C14′),124.0 (C3′ & C5′), 123.6 (C3 & C5), 113.5 (C11 & C15).

4.2.3 General procedure for the preparation of 1,3,5-triazine derivatives with three aromatic substituents.

A di-substituted triazine derivative (1 eq.) was reacted with an aromatic compound (1 eq.) in THF or 1,4-dioxane (10-50 ml) and NaOH solution (0.5-2 M) or K_2CO_3 solution (10 %, 10-15 ml) for neutralization of the reaction mixture. The reaction mixture was refluxed for 16-48 h at 80-100°C while the reaction progress was being monitored by TLC. After reaction completion, the reaction mixture was poured over crushed ice, washed with deionized water (2 x 20 ml), filtered and dried. Purification was carried out using flash silica gel/aluminium oxide -c neutral column chromatography and 10-25 % ethyl acetate/hexane as eluent or recrystallization using a suitable solvent or solvent mixture.

4.2.3.1 Synthesis of 4-((4-((4-fluorophenyl)amino)-6-(4-nitrophenoxy)-1,3,5-triazin-2-yl)oxy)benzonitrile (41)

4-Hydroxybenzonitrile (1.29 g, 11 mmol), **39a** (3.94 g, 11 mmol) and NaOH solution (15 ml, 0.9 M mmol) in THF (50 ml) were reacted as described in 3.2.3 for 40 h. The mixture was

purified by silica gel column chromatography using a 25% ethyl acetate / hexane solvent system to afford **41** (4.41 g, 91%), as a white powder.

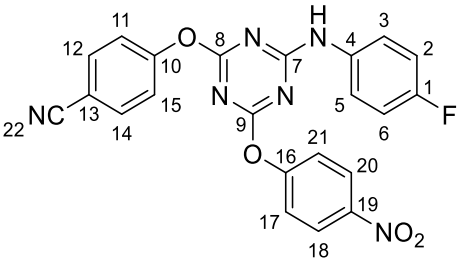

R_f 0.16 (15 % EtOAc/Hexane); **mp** >350 °C; **IR** (ν_{max}/cm^{-1}) 3362 (N-H), 2233 (C≡N), 1613 (C-O), 1510 (N-O), 1217 (C-F); **^{1}H NMR** (500 MHz, DMSO-d_6) δ 10.44 (s, 0.11H, N-H), 10.42 (s, 0.58H, N-H), 10.39 (s, 0.39h, N-H), 8.33 (d, J = 8.9 Hz, 1.38H, Ar-H), 8.00-7.94 (m, 2.54H, Ar-H), 7.60-7.55 (m, 1.39h, Ar-H), 7.53-7.49 (m, 2.58H-Ar-H), 7.47-7.40 (m, 2H, H3 & H5), 7.04 (t, J = 8.6 Hz, 2H, H2 & H6); **^{13}C NMR** (126 MHz, DMSO-d_6) δ 171.6 (C9), 171.1 (C8), 165.8 (C7), 158.4 (d, $^1J_{C\text{-}F}$ = 240.9 Hz, C1), 156.6 (C16), 155.1 (C10), 145.0 (C19), 134.2 (d, $^4J_{C\text{-}F}$ = 3.4 Hz, C4), 134.1 (C12 & C14), 125.3 (C18 & C20), 123.2 (C11 & C15), 122.7 (d, $^3J_{C\text{-}F}$ = 7.9 Hz, C3 & C5), 118.4 (C22), 115.0 (d, $^2J_{C\text{-}F}$ = 22.3 Hz, C2 & C6), 108.6 (C13); **HRMS** (m/z), calculated for $C_{22}H_{12}FN_6O_4$ $(M\text{-}H)^-$: 443.0910, found: 443.0912.

4.2.3.2 Synthesis of 4-((4-((4-bromophenyl)amino)-6-(4-chlorophenoxy)-1,3,5-triazin-2-yl)oxy)benzonitrile (42)

4-Hydroxybenzonitrile (217 mg, 1.8 mmol), **39b** (740 mg, 1.8 mmol) and NaOH solution (10 ml, 0.5 M) in THF (20 ml) were reacted as described in 3.2.3 for 23 h. The mixture was purified by silica gel column chromatography and a 10% ethyl acetate / hexane solvent system to afford **42** (476 mg, 54%), as a white powder.

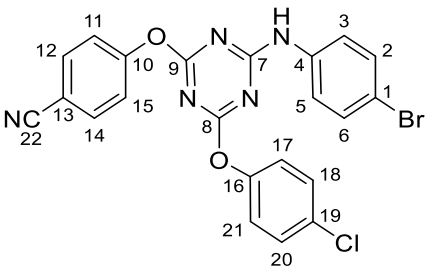

R_f 0.24 (15 % EtOAc/Hexane) ; **mp** >350 °C; **IR** (ν_{max}/cm^{-1}) 3265 (N-H), 2234 (C≡N), 1485 (C-O), 1379 (C-O); **^{1}H NMR** (500 MHz, DMSO-d_6) δ 10.43 (s, 0.50H, N-H), 10.37 (s, 0.41H, N-H), 8.03-7.93 (m, 1.30H, Ar-H) 7.52-

7.51 (m, 4.19, Ar-H), 7.44 – 7.27 (m, 6.61H, Ar-H); **^{13}C NMR** (101 MHz, DMSO-d_6) δ 172.0, (C8), 171.2 (C9), 165.7 (C7), 155.1 (C10), 150.5 (C16), 137.6 (C4), 134.0 (C12 & C14), 131.3 (C19), 131.0 (C2 & C6), 130.0 (C18 & C20), 123.7 (C11 & C15), 123.2 (C17 & C21), 122.3 (C3 & C5), 118.3 (C22), 115.1 (C1), 108.7 (C13); **HRMS** (m/z), calculated for $C_{22}H_{14}{}^{79}BrClN_5O_2$ $(M+H)^+$: 494.0014, found:494.0005.

4.2.3.3 Synthesis of *N*-(4-chlorophenyl)-4-(4-fluorophenoxy)-6-(4-nitrophenoxy)-1,3,5-triazin-2-amine (43)

4-Fluorophenol (196 mg, 1.7 mmol), **39d** (654 mg, 1.7 mmol) and NaOH solution (10 ml, 2.5 mmol) in THF (25 ml) were reacted as described in 3.2.3 for 26 h. The mixture was purified by silica gel column chromatography and a 10% ethyl acetate / hexane solvent system to afford **43** (191 mg, 25%) as a white-yellow powder.

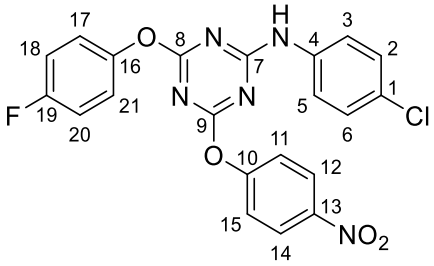

R_f 0.08 (15 % EtOAc/Hexane) ; **mp** >350 °C; **IR** (ν_{max}/cm^{-1}) 3368 (N-H), 1605 (C-O), 1564 (N-O), 1361(C-F); **^{1}H NMR** (500 MHz, DMSO-d_6) δ 10.45 (s, 0.70H, N-H), 10.36 (s, 0.20H, N-H), 8.38-8.32 (m, 1.50H, Ar-H 7.62-7.54 (m, 1.62H, Ar-H), 7.49-7.45 (m, 2.03H, Ar-H), 7.36-7.25(m, 4.89H, Ar-H), 7.24-7.20 (m, 1.86H, Ar-H), 7.19-7.18 (m, 0.22H,Ar-H); **^{13}C NMR** (126 MHz, DMSO-d_6) δ 172.3 (C8), 171.6 (C9), 165.8 (C7), 160.6 (C10), 157.7 (d, $^1J_{C-F}$ = 264.1 Hz, C19), 147.8 (C16), 145.0 (C13), 137.3 (C4), 128.2 (C2 & C6), 127.0 (C1), 125.4 (C12 & C14), 123.7 (C11 & C15), 123.2 (C3 & C5), 121.9 (C17 & C21), 116.2 (d, $^2J_{C-F}$ = 22.9 Hz, C18 & C20); **HRMS** (m/z), calculated for $C_{21}H_{14}ClFN_5O_4$ $(M+H)^+$: 454.0713, found: 454.0703.

4.2.3.4 Synthesis of 6-(4-fluorophenoxy)-*N*^{2}-(4-methoxyphenyl)-*N*^{4}-(4-nitrophenyl)-1,3,5-triazine-2,4-diamine (44)

p-Anisidine (267 mg, 2.2 mmol), **39e** (767 mg, 2.1 mmol) and NaOH solution (10 ml, 2.7 mmol) in THF (25 ml) were reacted as described in 3.2.3 for 44 h. The mixture was purified by recrystallization using acetone as a solvent to furnish **44** (100 mg, 11%) as a light brown solid.

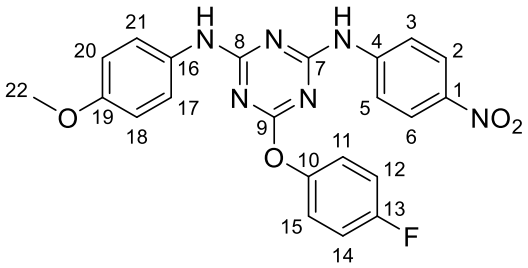

R$_f$ 0.03 (15 % EtOAc/Hexane) ; **mp** >350 °C; **IR** (ν_{max}/cm^{-1}) 3368 (N-H), 1605 (C-O), 1564 (N-O), 1361(C-F); **^{1}H NMR** (400 MHz, DMSO-d_6) δ 10.39 (s, 1H, N-H), 9.82 (s, 1H, N-H), 8.18-7.99 (m, 2.72H, Ar-H), 7.89-7.79 (m, 1H, Ar-H), 7.59-7.46 (m, 1H, Ar-H), 7.46-7.36 (m, 1H, Ar-H), 7.36-7.27 (m, 3.80H, Ar-H), 6.99-6.89 (m, 1H, Ar-H), 6.85-6.70 (m, 1H, Ar-H), 3.85-3.63 (m, 3H, H22); **^{13}C NMR** (101 MHz, DMSO-d_6) δ 170.5 (C7), 165.6 (C9), 165.4 (C8), 161.9 (d, $^1J_{C\text{-}F}$ = 237.0 Hz, C13), 158.3 (C19), 155.1 (C10), 148.4 (C4), 146.3 (C1), 141.1 (C16), 124.5 (C2 & C6), 124.1 (d, $^3J_{C\text{-}F}$ = 8.5 Hz, C11 & C15), 119.0 (C3 & C5), 116.0 (d, $^2J_{C\text{-}F}$ = 23.3 Hz, C12 & C14), 115.0 (C17 & C21), 113.9 (C18 & C20), 55.4 (C22); **HRMS** (m/z), calculated for $C_{22}H_{16}FN_6O_4$ $(M\text{-}H)^-$: 447.1223, found: 447.1225.

4.2.3.5 Synthesis of 4-((4-((4-methoxyphenyl)thio)-6-(4-nitrophenoxy)-1,3,5-triazin-2-yl)amino)benzonitrile (45)

4-Aminobenzonitrile (55 mg, 0.46 mmol), **39f** (139 mg, 0.35 mmol) and K_2CO_3 solution (3 ml, 10%) in 1.4 Dioxane (10 ml) were reacted as described in 3.2.3 for 26 h. The mixture was purified by recrystallization using THF/Hexane solvent mixture to furnish **45** (128 mg, 77 %) as a yellowish-orange solid.

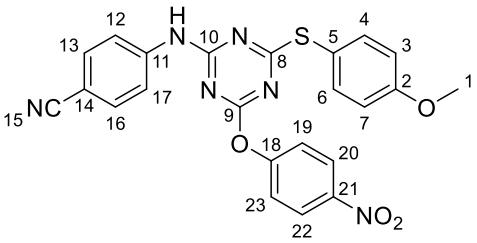

R_f 0.53 (25 % EtOAc/Hexane) ; **mp** >350 °C; **IR** (ν_{max}/cm^{-1}) 3363 (N-H), 2213 (C≡N), 1556 (N-O), 1454 (C-H), 1333 (C-O); **^{1}H NMR** (400 MHz, MeOD-*d*$_4$, DMSO-*d*$_6$) δ 9.35 (s, 0.17H, N-H), 8.93-8.86 (m, 0.77H, Ar-H) 8.71-8.66 (m, 0.73H, Ar-H) 8.17-8.08 (m, 4.09H, Ar-H) 8.07- 8.03 (m, 0.46H, Ar-H), 8.02-7.97,(m,0.73H, Ar-H) 7.74 -7.55 (m, 2.24H, Ar-H), 7.51-7.41 (m, 3.15H, Ar-H), 7.21-7.13 (m, 0.73H, Ar-H), 5.08, (3H, H1).; **^{13}C NMR** (101 MHz, MeOD-*d*$_4$, DMSO-*d*$_6$) δ 183.0 (C8), 181.8 (C8′), 179.4 (C9), 179.2 (C9′), 171.0 (C7), 170.9 (C7′), 169.6 (C18), 1612.0 (C2′), 161.5 (C2), 158.9 (C21), 153.9 (C11), 145.3 (C5), 138.2 (C13 & C16), 137.6 (C13′ & C16′), 134.4 (C20 & C22), 127.8 (C4 & C6), 123.6 (C19 & C23), 121.2 (C14), 120.6 (C14′) 119.4 (C12 & C17), 115.6 (C15), 115.1 (C3′& C7′), 114.7 (C3 & C7), 55.7 (C1).

4.2.3.6 Synthesis of N-(4-chloro-2-methylphenyl)-4-((4-methoxyphenyl)thio)-6-(4-nitrophenoxy)-1,3,5-triazin-2-amine (46)

4-Methoxythiophenol (48 mg, 0.34 mmol), **39g** (103 mg, 0.26 mmol) and K_2CO_3 solution (2 ml, 10%) in 1.4 Dioxane (10 ml) were reacted as described in 3.2.3 for 45 h. The mixture was purified by recrystallization using THF/Hexane solvent mixture to furnish **46** (108 mg, 83 %) as a light brown solid.

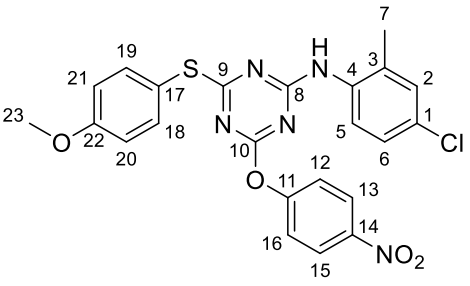

R_f 0.05 (15 % EtOAc/Hexane) ; **mp** >350 °C; **IR** (ν_{max}/cm^{-1}) (N-H), (C-O), (N-O), (C-Cl); **^{1}H NMR** (400 MHz, DMSO-*d*$_6$) δ 8.55 (s, 0.14H, N-H), 7.74-7.68 (m, 1.14H-Ar-H), 7.43-7.38 (m, 3.85H, Ar-H), 7.17-7.16 (m, 0.77H, Ar-H), 7.09-7.05 (m, 1.04H, Ar-H), 7.03-6.98 (m, 0.80H, Ar-H), 6.98-6.92 (m, 3.5H, Ar-H), 5.92-5.86 (m, 1H, Ar-H), 3.79 (3H, H23), 2.13-2.02 (m, 3H, H7); **^{13}C NMR** (101

MHz, DMSO-d_6) δ 180.49 (C9), 168.4 (C10), 161.4 (C8), 160.1 (C11), 159.6 (C22), 145.3 (C14), 136.6 (C2), 134.9 (C17), 132.0 (C13), 129.4 (C12 & C16) , 127.4 (C18 & C19), 126.9 (C3), 125.3 (C6), 122.8 (C4), 119.3 (C20 & C21), 117.8 (C1), 115.0 (C5), 55.3 (C23), 17.7 (C7).

References

(1) JC3032 Aids Data Book-UNAIDS DATA **2021**.

(2) Institute of Medicine (US) Committee on a National Strategy for AIDS. *Confronting AIDS:* Directions for Public Health, Health Care, and Research. Washington (DC): National Academies Press (US); **1986**.

(3) Gallo, R.C; Montagnier, L. *New England Journal of Medicine*, **2003**, 349, 24.

(4) Sharp, P.M; Hahn, B.H. *Cold Spring Harbor Perspectives in Medicine* **2011**, 1, 1.

(5) Justiz, V.A.A; Naik R. *Treasure Island (FL):* StatPearls Publishing; **2021**.

(6) Jamison, D.T; Breman, J.G; Measham, A.R; Alleyne, G; Claeson, M; Evans, D.B; Jha, P; Mills, A; Musgrove, P. *Disease Control Priorities in Developing Countries (2nd edition)*. The International Bank for Reconstruction and Development / The World Bank :Washington (DC): Oxford University Press: New York, **2006**.

(7) Rivat, C; Thrasher, A.J; Gaspar, H.B. *Clinical Immunology (Fourth Edition)*. Elsevier, **2013**.

(8) German Advisory Committee Blood (Arbeitskreis Blut), Subgroup 'Assessment of Pathogens Transmissible by Blood'. *Transfusion, Medicine and Hemotherapy* **2016**, 43, 3.

(9) Berthet-Colominas, C; Monaco, S; Novelli, A; Sibaı, G; Mallet, F; Cusack, S. *The European Molecular Biology Organization Journal* **1999**, 18, 5.

(10) Ciuffi, A. Clinical *Microbiology and Infection* **2016,** 22, 4.

(11) Al-Jabri, A. A. *Journal for scientific research-Medical sciences* **2003,** 5, 1-2.

(12) Abram, M. E.; Parniak, M. A. *Journal of virology* **2005,** 79, 18.

(13) Shaw, G.M; Hunter, E. *Cold Spring Harbor Perspectives in Medicine* **2012**, 2, 11.

(14) Center for Substance Abuse Treatment. *Substance Abuse Treatment for Persons With HIV/AIDS*. Substance Abuse and Mental Health Services Administration (US); Rockville (MD): **2000**.

(15) Mertens, T. E; Low-Beer D. *Bulletin of the World Health Organization* **1996**, 74, 2.

(16) Garnica, A. D.; Chan,W. Y. *Journal of the American College of Nutrition* **1996,** 15, 3.

(17) Douglas, G.C; Fazely, F; Hu, J. *Journal of Reproductive Immunology* **1998**, 41, 1-2.

(18) John-Stewart, G; Mbori-Ngacha, D; Ekpini, R; Janoff, E.N; Nkengasong, J; Jennifer S. Read, J.S; Van de Perre, P; Newell, M. *Journal of Acquired Immune Deficiency Syndromes* **2004,** 35, 2.

(19) Delaney, K.P; Hanson, D.L; Masciotra, S; Ethridge, S.F; Wesolowski, L; Owen, S.M. *Clinical Infectious Diseases* **2017**, 64, 1.

(20) https://hivinfo.nih.gov/understanding-hiv/fact-sheets/stages-hiv-infection.Accessed 01 June 2022.

(21) Yoon, C. I; Park, S: Cha, Y. J: Lee, H.S; Bae, S.J; Cha, C; Lee, D. Y; Ahn, S.G; Jeong, J. *Breast* **2020**, 50.

(22) Marshall, J.S; Warrington, R; Watson, W; Kim, H.L. *Allergy, Asthma & Clinical Immunology* **2018**, 14, 49.

(23) Bousheri, S; Burke, C; Ssewanyana, I; Harrigan, R; Martin, J; Hunt, P; Bangsberg, D.R; Cao, H. *Journal of Acquired Immune Deficiency Syndromes* **2009**, 52, 5.

(24) Luckheeram, R.V; Zhou, R; Verma, A.D; Xia, B. *Clinical and Developmental Immunology* **2012**.

(25) Wilen, C.B; Tilton, J.C; Robert W. Doms, R.W. *Cold Spring Harbor Perspectives in Medicine* **2012**, 2.

(26) Dumas, F; Preira, P; Salome, L. *Biochimie* **2014**, 107.

(27) Kriesel, F; Schelle, L; Baldauf, H. *Microbes and Infection* **2020**, 22,9.

(28) Mislak, A.C; Frey, K.M; Bollini, M; Jorgensen, W.L; Anderson, K,S. *Biochimica et Biophysica Acta* **2014**, 1840, 7.

(29) Pau, A.K; George, J.M. *Infectious Disease Clinics of North America* **2014**, 28, 3

(30) Sebastian, J; Faruki, H. *Medicinal Research Reviews* **2004**, 24,1.

(31) Ratnakar, B.J; Godge, R. K; Shinde, G. S. *World Journal of Pharmaceutical Research* **2019**, 8, 7.

(32) Das, K; Arnold, E. *Current Opinion in Virology*. **2013**, 3.

(33) Reynolds, C; de Koning, C.B; Pelly, S.C; van Otterlo, W.A.L; Bode, M.L *Chemical Society Reviews* **2012**, 41.

(34) Ercana, S; Senyigit, B; Senses, Y. *Journal of Biomolecular Structure And Dynamics* **2020**, 38, 2.

(35) Bode, M.L; Gravestock, D; Moleele, S.S; van der Westhuyzen, C.W; Pelly, S.C; Paul A. Steenkamp, P.A; Hoppe, H.C; Khan, T; Nkabinde, L.A. *Bioorganic & Medicinal Chemistry* **2011**, 19, 14.

(36) Sluis-Cremer, N; Tachedjian, G. Virus Research **2008**, 134, 1-2.

(37) Grobler, J.A; Dornadula, G; Rice, M.R; Simcoe, A.L; Hazuda, D.J; Michael D. Miller, M.D. *Journal of Biological Chemistry*, **2007**, 282, 11.

(38) Zhuang, C; Pannecouque, C; De Clercq, E; Chena, F. *Acta Pharmaceutica Sinica B* **2020**, 10, 6.

(39) Viira, B; Selyutina, A; García-Sosa, A.T; Karonen, M; Sinkkonen, J; Merits, A; Maran, U. *Bioorganic & Medicinal Chemistry* **2016**, 24, 11.

(40) Kohlstaedt, L.A; Wang, J; Friedman, J.M; Rice, P.A; Steitz, T.A. *Science* **1992**; 256, 5065.

(41) Das, K; Bauman, J.D; Clark, A.D Jr; Frenkel, Y.V; Lewi, P.J; Shatkin, A.J; Hughes, S.H; Arnold, E. *Proceedings of the National Academy of Sciences of the United States of America* **2008**, 105, 5.

(42) Chong, P; Sebahar, P; Youngman, M; Garrido, D; Zhang, H; Stewart, E.L; Nolte, R.T; Wang, L; Ferris, R.G; Edelstein M. *Journal of Medicinal Chemistry*. **2012**, 55, 23.

(43) Ganai, A.M; Pathan, T.K; Hampannavar, G.A; Pawar, C; Obakachi, V.A; Kushwaha, B; Narva Deshwar Kushwaha, N.D; Rajshekhar Karpoormath, R. *Chemistry Select* **2021**, 6, 7.

(44) Kumar, R; Kumar, Roy, N. R. K; Singh, A. *Current Medical and Drug Research* **2017**, 1, 1.

(45) Richard N. Butler, Aoife M. Fahy, Anthony Fox, John Stephens, P. McArdle, D. Cunningham, Alan G. Ryder. *Tetrahedron Letters* **2006** , 47.

(46) Sugimura, H; Takeuchi, R; Ichikawa, S; Nagayama, E; Sasaki, I. *Organic Letters* **2018**, 20, 11.

(47) Prokhorov, A. M; Kozhevnikov, D. N. *Chemistry of Heterocyclic Compounds*. **2012**, 48.

(48) Ohsawa, A; Arai, H; Ohnishi, H; Igeta, H. *Journal of the Chemical Society, Chemical. Communications* **1980**, 24.

(49) Boger, D. L; Anderson, E. D; Duerfeldt, A. S; Zhu, K; Glinkerman, C. M. *Organic Letters*. **2014**, 16, 19.

(50) Boger, D.L. *Tetrahedron* **1983**, 39, 18.

(51) Kamber, D. N; Liang, Y; Blizzard, R. J; Liu, F; Mehl, R. A; Houk, K. N; Prescher, J. A. *Journal of the American Chemical Society* **2015,** 137, 26.

(52) Patterson, D. M; Presche, J.A. *Current Opinion in Chemical Biology* **2015**, 28.

(53) Rooshenas, P; Hof, K; Schreiner, P. R; Williams, C. M. *European Journal of Organic Chemistry* **2011**, 5.

(54) Dawane, B. S; Kadam, S. N; Shaikh, B. M. *Der Pharmacia Lettre* **2010**, 2, 4.

(55) David Bartholomew. *Comprehensive Heterocyclic Chemistry II*: Elsevier Ltd **1996**.

(56) Timmerman, P; Prins, L.J. *European Journal of Organic Chemistry* **2001**; 17.

(57) Vora, J.J; Vasava, S. B; Patel, A. D; Parmar, K. C; Chauhan, S. K; Sharma, S. S. *E-Journal of Chemistry*. **2009**, 6, 1.

(58) Hintermann, L; Xiao, L; Labonne, A. *Angewandte Chemie International Edition* **2008**, 47, 43.

(59) Kumar, R; Kumar, N; Roy, R. K; Singh, A. *Current Medical and Drug Research* **2017**, 1,1.

(60) Herrera, A; Riaño, A; Moreno, R; Caso, B; Pardo, Z. D; Fernandez, I; Sáez, E; Molero, D; Sánchez-Vazquez, A; Martinez-Alvarez, R. *The Journal of Organic Chemistry* **2014**, 79, 15.

(61) Lim, J; Simanek, E. E. *Advanced Drug Delivery Reviews* **2012,** 64, 9.

(62) Steffensen, M. B; Hollink, E; Kuschel, F; Bauer, M; Simanek, E. E. *Journal of Polymer Science Part A: Polymer Chemistry* **2006**, 44, 11.

(63) Lim, J; Mintzer, M. A; Perez, L. M; Simanek, E. E. *Organic Letters*. 12. **2010**, 12, 6.

(64). Simanek, E. E; Abdou, H; Lalwani, S; Lim, J; Mintzer, M; Venditto, V. J; Vittur, B. *Proceedings of the Royal Society A* **2010**, 466, 2117.

(65) Cerón, V. D; Illicachi, L. A; Insuasty, B. *Molecules* **2022**, 28, 257.

(66) Vora, J. J; Vasava, S. B; Patel, A. D; Parmar, K. C; Chauhan, S. K; Sharma, S. S. *E-Journal of Chemistry* **2009**, 6, 1**.**

(67) Pal, R. R; Lee, D. S. *Macromolecular Research* **2005**, 13, 5.

(68) Sojitra, P. N, Patel, K. C; Patel, H. S. *High Performance Polymers* **2010**, 22, 8.

(69) Baliani, A; Bueno, G. J; Stewart, M. L; Yardley, V; Brun, R; Barrett, M. P; Gilbert, I. H. *Journal of Medicinal Chemistry* **2005**, 48, 17.

(70) Menicagli, R; Samaritani, S; Signore, G; Vaglini, F; Via, D. L. *Journal of Medicinal Chemistry* **2004**, 47, 19.

(71) Chen, X; Meng, Q; Qiu, L; Zhan, P; Liu, H; De Clercq, E; Pannecouque, C; Liu; X. *Chemical Biology & Drug Design* **2015**, 86, 1.

(72) Henke, B. R; Consler, T. G; Go, N; Hale, R. L; Hohman, D, R; Jones, S, A; Lu, A. T; Moore, L. B; Moore, J. T; Orband-Miller, L. A; Robinett, R. G; Shearin, J; Spearing, P. K; Stewart, E. L; Turnbull, P. S; Weaver, S. L; Williams, S. P; Wisely, G. B; Lambert, M. H. *Journal of Medicinal Chemistry* **2002**, 45, 25.

(73) Asadi, P; Alvani, M; Hajhashemi, V; Rostami, M; Khodarahmi, G. *Journal of Molecular Structure* **2021**, 1243.

(74) Shah, D. R; Modh, R. P; Chikhalia, K. H. *Future Medicinal Chemistry* **2014**, 6, 4.

(75) Patil, V; Noonikara-Poyil, A; Joshi, S. D; Patil, S. A; Patil, S.A; Lewis, A. M; Bugarin, A. *Journal of Molecular structure* **2020**, 1220.

(76) Kothayer, H; Spencer, S. M; Tripathi, K; Westwell, A. D; Palle, K. *Bioorganic & Medicinal Chemistry Letters* **2016**, 26, 8.

(77) Das, K; Bauman, J. D; Clark, A. D. Jr; Frenkel, Y. V; Lewi, P. J; Shatkin, A .J; Hughes, S. H; Arnold, E. *Proceedings of the National Academy of Sciences* **2008**, 105, 5.

(78) Barreiro, G; Guimaraes, C. R. W; Tubert-Brohman, I; Lyons, T.M Tirado-Rives, J; Jorgensen, W. L. *Journal of Chemical Information and Modeling* **2007**, 47, 6.

(79) Ekkati, A. R; Bollini, M; Domaoal, R. A; Spasov, K. A; Anderson, K. S; Jorgensen, W. L. *Bioorganic & Medicinal Chemistry Letters*. **2012**, 22, 4.

(80) Xiong, Y; Chen, F; Balzarini, J; De Clercq, E; Pannecouque, C. *European Journal of Medicinal Chemistry* **2008 ,** 43,6.

(81) Renfrew, H. M; Taylor, J. A; Whitmorea, J. M. J; Williams, A. *Journal of the Chemical Society, Perkin Transactions 2* **1994,** 2, 12.

(82) Viesser, R.V; Ducati, L. C; Tormena, C. F; Autschbach. J. *Physical Chemistry Chemical Physics* **2018**, 20, 16.

(83) Afonso, C. A. M; Lourenço, N. M. T; Rosatella, A. A. *Molecules* **2006**, 11, 1.

(84) Agarwal, A; Srivastava, K; Purib, S. K; Chauhan, P. M. S. *Bioorganic & Medicinal Chemistry Letters* **2005**, 15, 3.

(85) Zacharie, B; Abbott, S. D; Duceppe, J; Gagnon, L; Grouix, B; Geerts, L; Gervais, L; Sarra-Bournet, F; Perron, V; Wilb, N; Penney, C.L; Laurin, P. *Chemistry Open*, **2018**, 7,9.

(86) McKay, G. A; Reddy, R; Arhin, F; Belley, A; Lehoux, D; Moeck, G; Sarmiento, I; Parr, T.R; Gros, P; Pelletier, J; Fara, A. R. *Bioorganic & Medicinal Chemistry Letters* **2006**, 16, 5.

(87) Fontana, P; Peretti, A. *Annali di Chimica 1959, 49.*

(88) Weigert, F. J; Roberts. J. D. *Journal of the American Chemical Society* **1971**, 93, 10.

(89) Treadway, M. D; Joseph, C. J; Richard, C. A; Eric, S. R; Teh, W. T; Anihal, L; Phillips, J. L; Outcalt, R. J. WO8704321.

(90) Giacomelli, G; Porcheddu, A; De Luca, L. *Current Organic Chemistry* **2004**, 8, 15.

(91) Delia, T. J; Nagarajan, A. *Journal of Heterocyclic Chemistry* **1998**, 35, 2.

(92) Bede, L. A; Koffi, A. K; Beke, F. E. D; Semmeq, A; Badawi, M. *Journal of Molecular Modeling* **2021,** 27, 147.

(93) Birkett, H. E; Cherryman, J. C; Chippendale, A. M; Evans, J. S. O; Harris, R. K; James, M; King, I. J; McPherson, G. J. *Magnetic Resonance in Chemistry* **2003**, 41, 5.

(94) Murase, T; Fujita, M. *The Journal of Organic Chemistry* **2005**, 70, 23.

(95) Sharma, G.D; Zervaki, G. E; Angaridis, P.A; Koukaras, E.N; Coutsolelos, A.G. *Inorganic Chemistry Frontiers* **2014**, 1, 3.

(96) SDBSWeb : https://sdbs.db.aist.go.jp (National Institute of Advanced Industrial Science and Technology, Accessed 21 November 2023.

(97) Grate, J. W; Mo, K; Daily, M. D. *Angewandte Chemie International Edition* **2016**, 55, 12.

(98) Bhat, H, R; Singh, U.P; Gahtori, P; Ghosh, S. K; Gogoi, K; Prakash, A; Ramendra K. Singh, R. K. *Chemical Biology and Drug Design* **2015**, 86, 3.

(99) Miguel Vidal Mosquera, Angel Messeguer Peypoch, Jordi Bujons Vilás, Doctoral Thesis, Institute of Advanced Chemistry of Catalonia - CSIC. **2011.**

(100) Díaz-Ortiz, A; Elguero, J; Foces-Foces, C; de la Hoz, A; Moreno, A; Moreno, S; Sánchez-Migallón, A; Valiente, G. *Organic & Biomolecular Chemistry* **2003**, 1, 24.

(101) Antonio, H; Sánchez-Migallón, A. *Targets in Heterocyclic Systems*. **2017**, 20.

(102) Diaz-Ortiz, A; de la Hoz, A; Moreno, A; Sanchez-Migallon, A; Valiente, G. *Green Chemistry* **2002,** 4, 4.

(103)) Zervaki, G. E; Angaridis, P.A; Koukaras, E. N; Sharma, G. D Athanassios G. Coutsolelos, A.G. *Inorganic Chemistry Frontiers* **2014**, 1, 3.

(104) Sunduru, N; Gupta, L; Chaturvedi, V; Dwivedi, R; Sinha, S; Chauhan, P.M.S. *European Journal of Medicinal Chemistry* **2010**, 45, 8.

(105) Mudur, V.V; Prabhakar, C. *Optical Materials* **2020**, 109.

(106)) Feng, D; Zuo, X; Jing, L; Chen, C; Olotu, F. A; Lin, H; Soliman, M; De Clercq, E; Pannecouque, C; Lee, K; Kang, D; Liu, X; Zhan, P. *European Journal of Medicinal Chemistry*, **2021**, 211, 5.

Appendix: 1H & 13C NMR Spectra

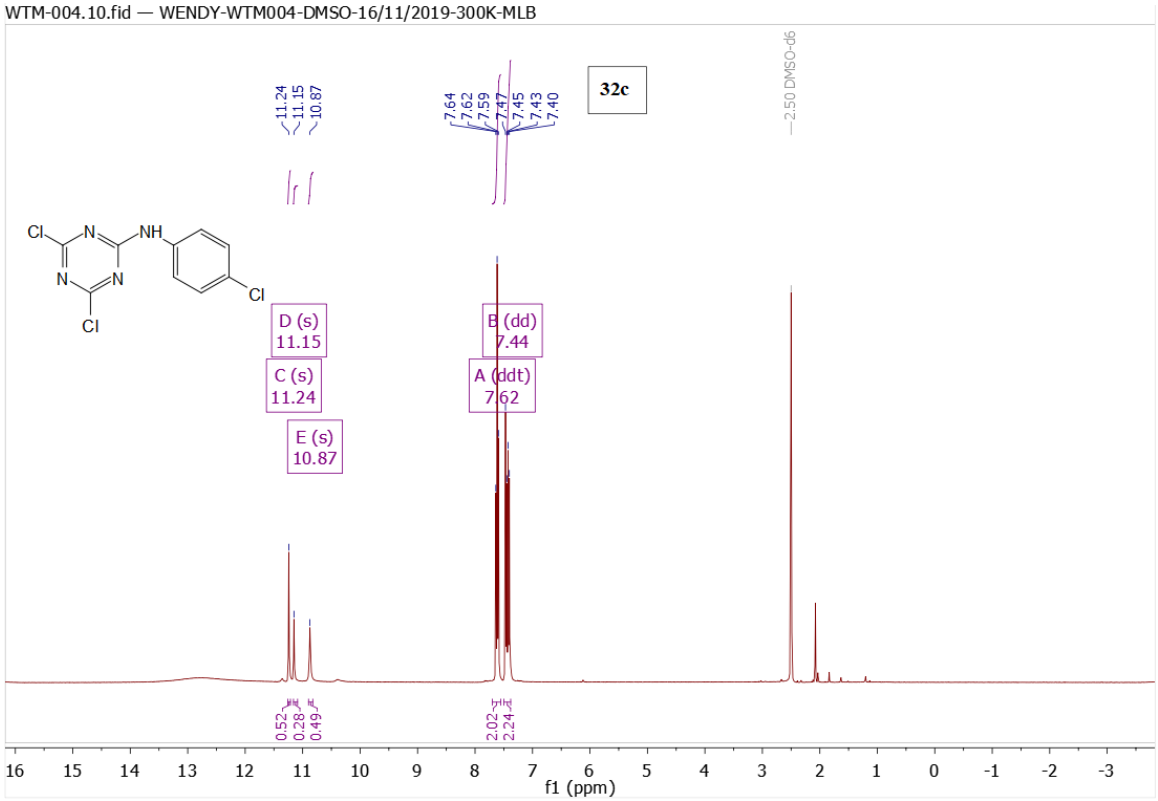

Figure A1

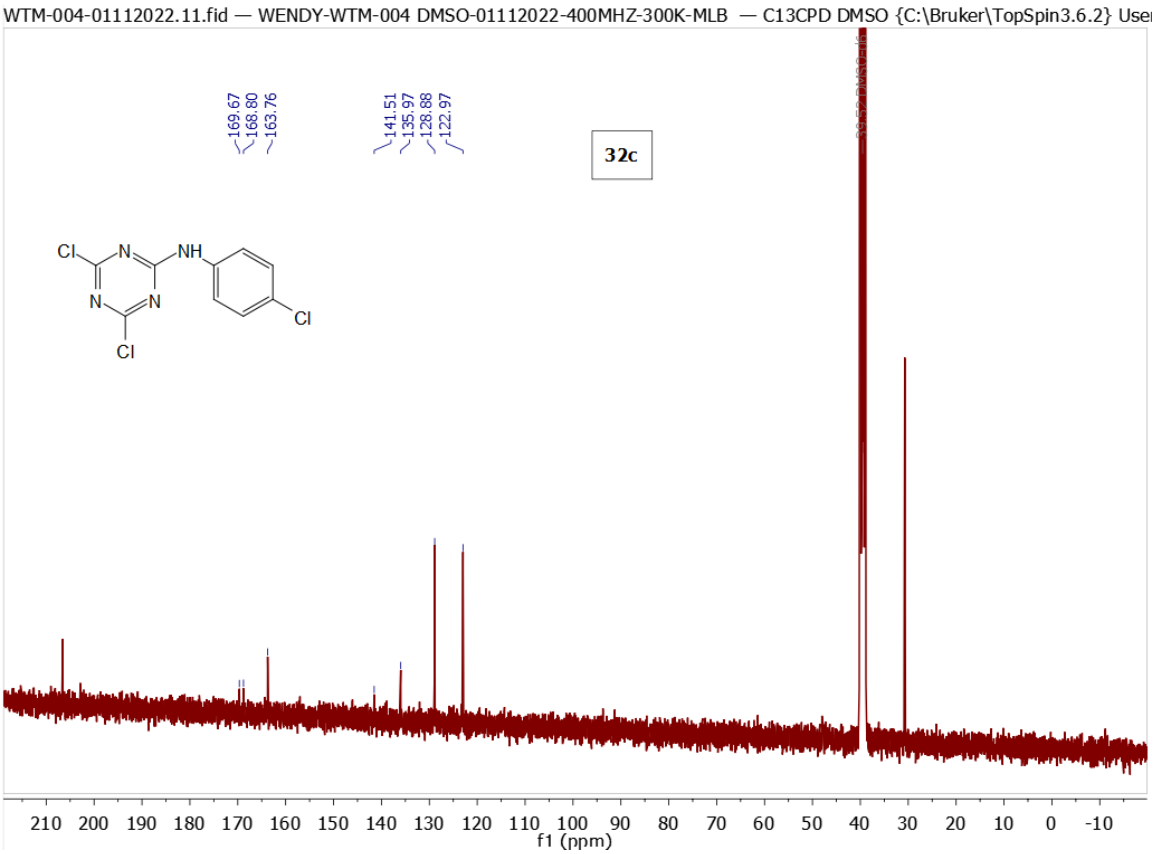
WTM-004-01112022.11.fid — WENDY-WTM-004 DMSO-01112022-400MHZ-300K-MLB — C13CPD DMSO {C:\Bruker\TopSpin3.6.2} Use
169.67
168.80
163.76
141.51
135.97
128.88
122.97
32c
Cl
N
NH
N
N
Cl
Cl
210 200 190 180 170 160 150 140 130 120 110 100 90 80 70 60 50 40 30 20 10 0 -10
f1 (ppm)

Figure A2

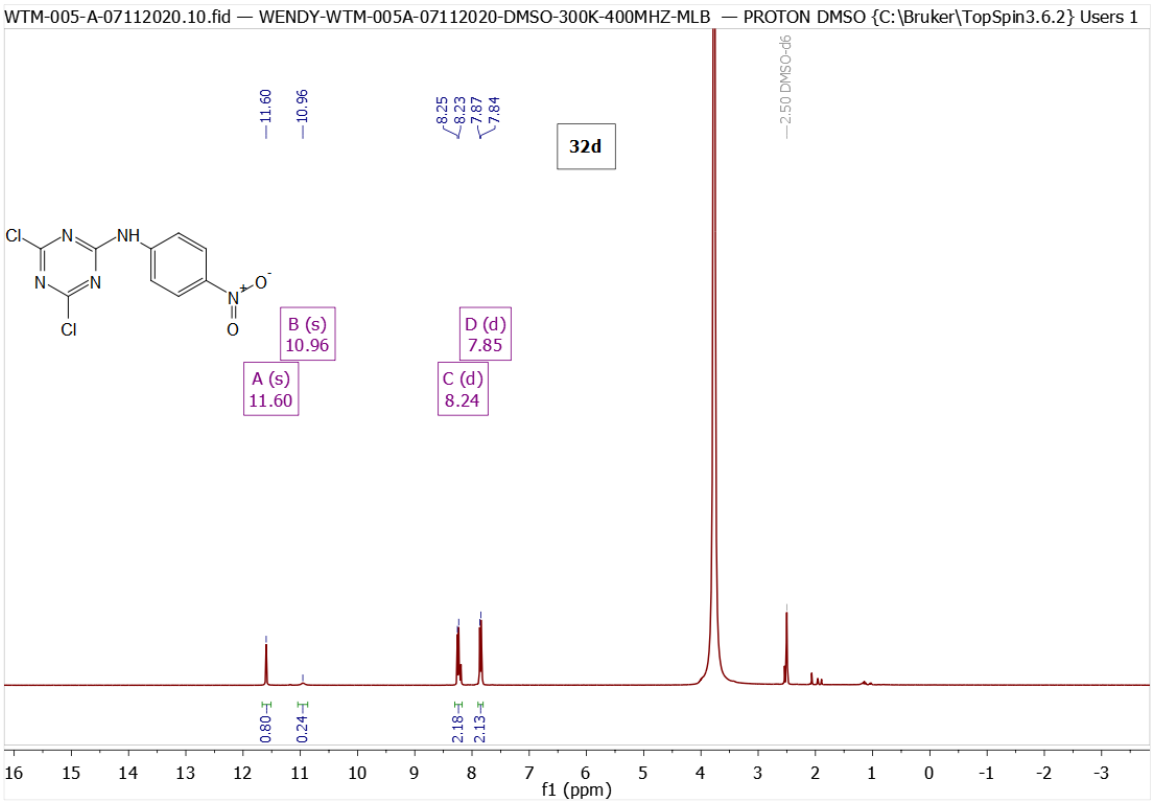
WTM-005-A-07112020.10.fid — WENDY-WTM-005A-07112020-DMSO-300K-400MHZ-MLB — PROTON DMSO {C:\Bruker\TopSpin3.6.2} Users 1
11.60
10.96
8.25
8.23
7.87
7.84
2.50 DMSO-d6
32d
B (s)
10.96
D (d)
7.85
A (s)
11.60
C (d)
8.24
0.80
0.24
2.18
2.13
16 15 14 13 12 11 10 9 8 7 6 5 4 3 2 1 0 -1 -2 -3
f1 (ppm)

Figure A3

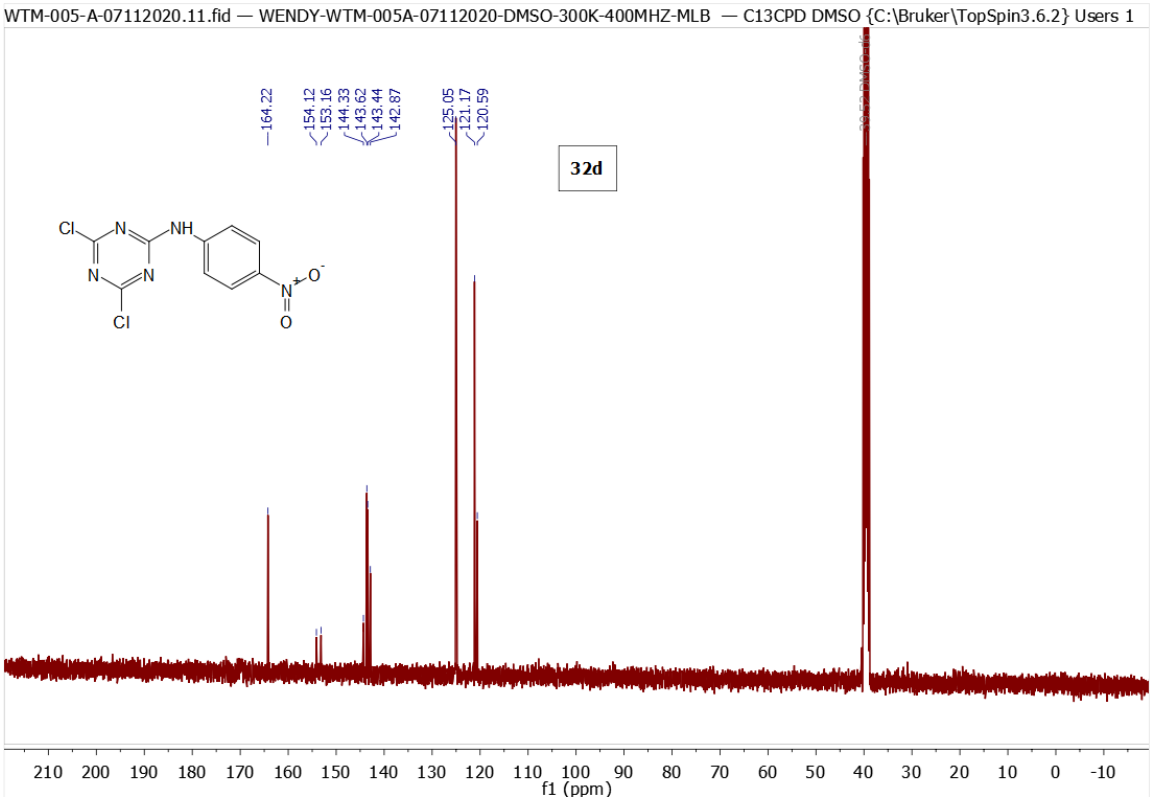
WTM-005-A-07112020.11.fid — WENDY-WTM-005A-07112020-DMSO-300K-400MHZ-MLB — C13CPD DMSO {C:\Bruker\TopSpin3.6.2} Users 1
164.22
154.12
153.16
144.33
143.62
143.44
142.87
125.05
121.17
120.59
32d
Cl
N
NH
N
N
Cl
N+
O-
O
210 200 190 180 170 160 150 140 130 120 110 100 90 80 70 60 50 40 30 20 10 0 -10
f1 (ppm)

Figure A4

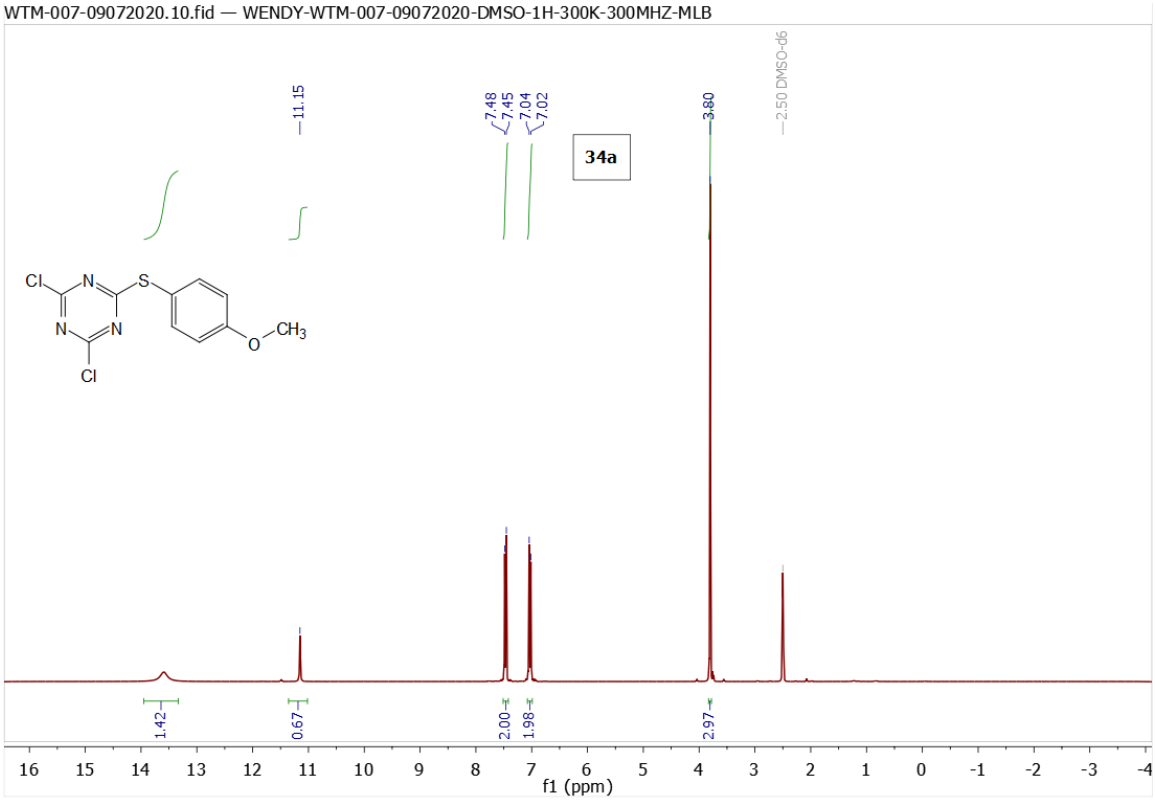
WTM-007-09072020.10.fid — WENDY-WTM-007-09072020-DMSO-1H-300K-300MHZ-MLB
11.15
7.48
7.45
7.04
7.02
3.80
2.50 DMSO-d6
34a
Cl
N
S
N
N
Cl
O
CH3
1.42
0.67
2.00
1.98
2.97
16 15 14 13 12 11 10 9 8 7 6 5 4 3 2 1 0 -1 -2 -3 -4
f1 (ppm)

Figure A5

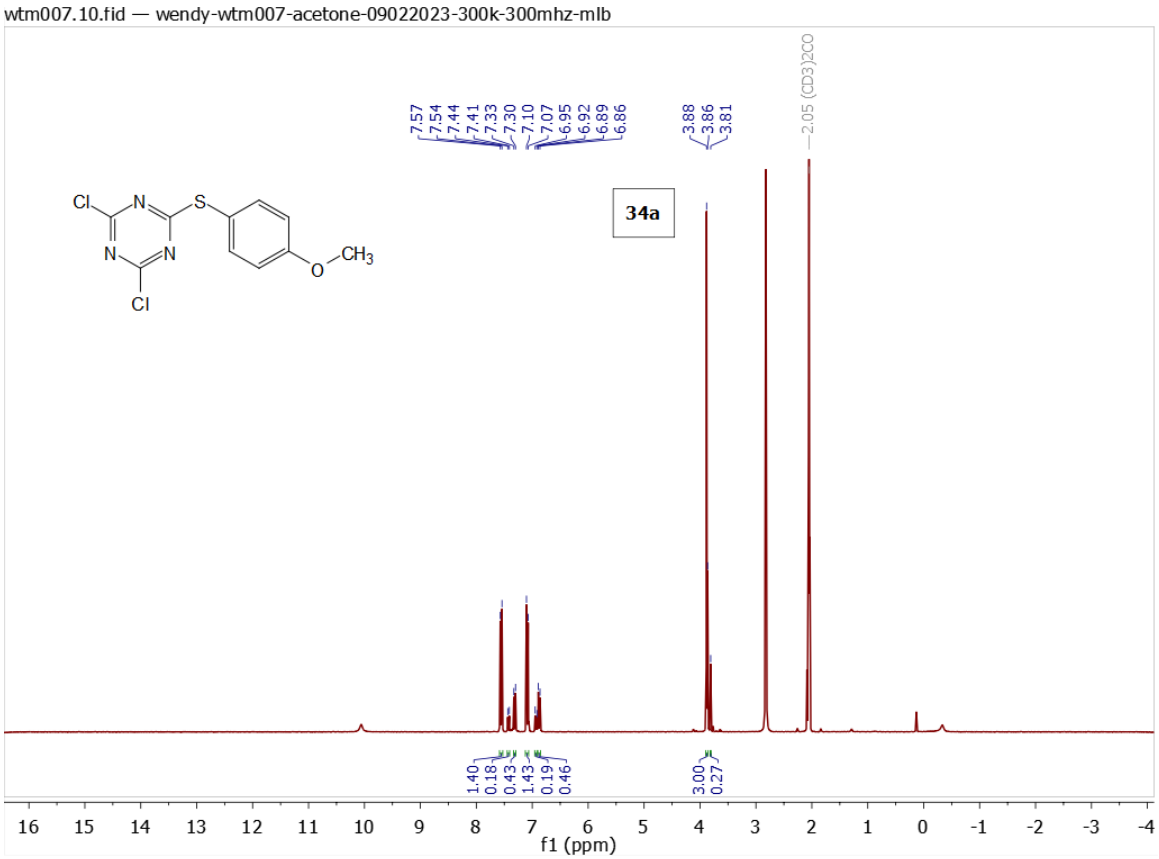
wtm007.10.fid — wendy-wtm007-acetone-09022023-300k-300mhz-mlb
7.57
7.54
7.44
7.41
7.33
7.30
7.10
7.07
6.95
6.92
6.89
6.86
3.88
3.86
3.81
2.05 (CD3)2CO
34a
Cl
N
S
N
N
Cl
O
CH3
1.40
0.18
0.43
1.43
0.19
0.46
3.00
0.27
16 15 14 13 12 11 10 9 8 7 6 5 4 3 2 1 0 -1 -2 -3 -4
f1 (ppm)

Figure A6

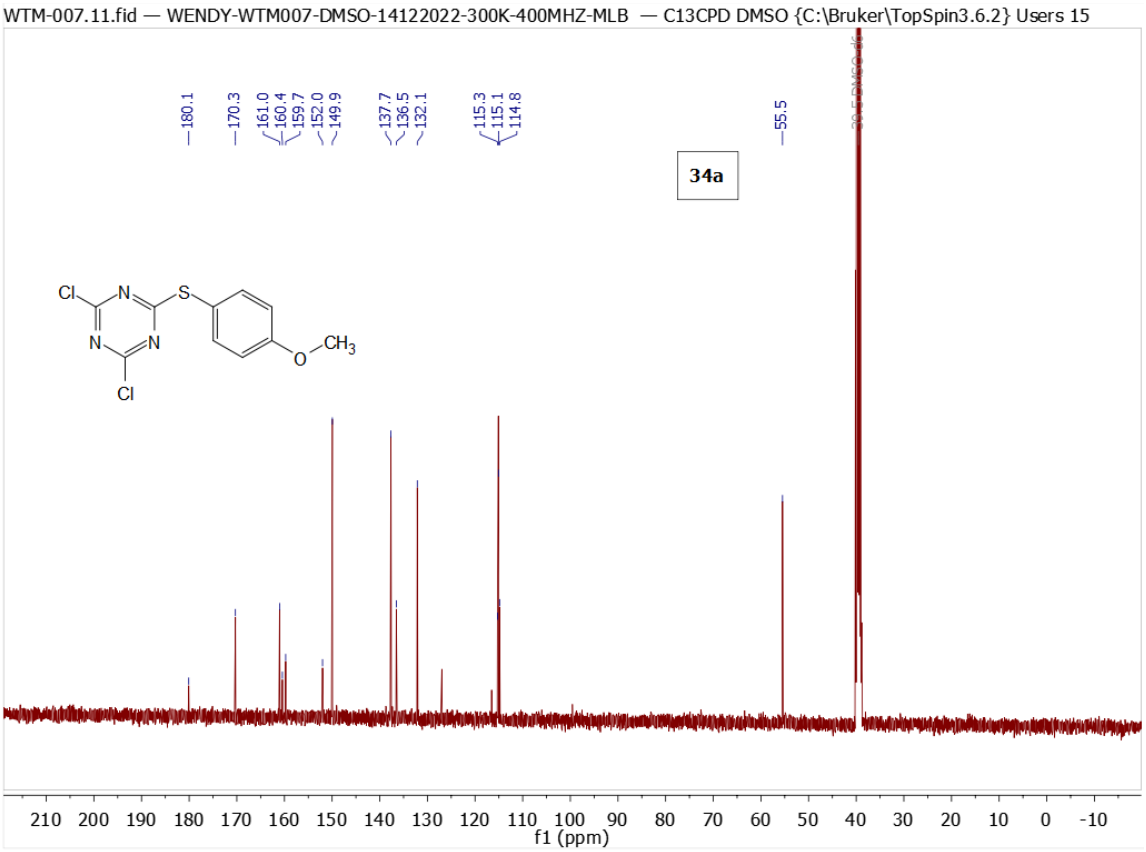
WTM-007.11.fid — WENDY-WTM007-DMSO-14122022-300K-400MHZ-MLB — C13CPD DMSO {C:\Bruker\TopSpin3.6.2} Users 15
180.1
170.3
161.0
160.4
159.7
152.0
149.9
137.7
136.5
132.1
115.3
115.1
114.8
55.5
34a
Cl
N
S
N
N
Cl
O
CH3
210 200 190 180 170 160 150 140 130 120 110 100 90 80 70 60 50 40 30 20 10 0 -10
f1 (ppm)

Figure A7

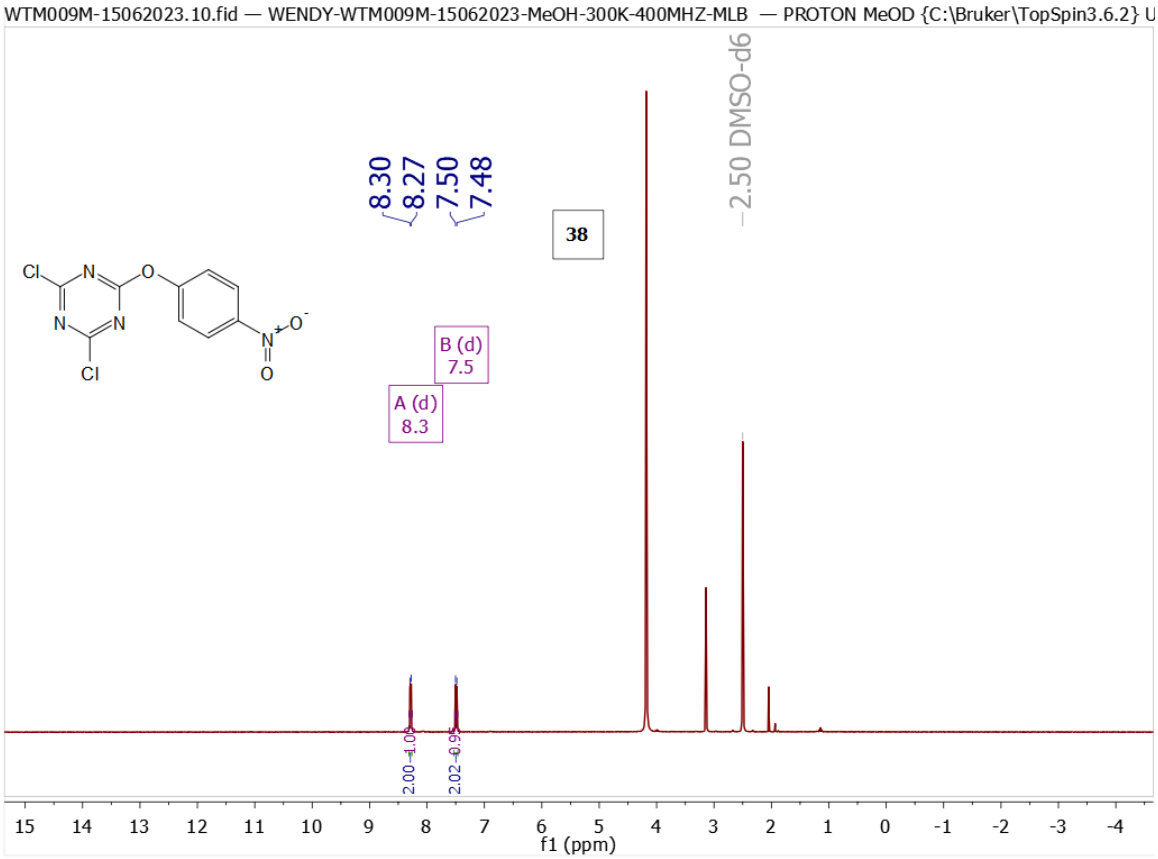
WTM009M-15062023.10.fid — WENDY-WTM009M-15062023-MeOH-300K-400MHZ-MLB — PROTON MeOD {C:\Bruker\TopSpin3.6.2} U
8.30
8.27
7.50
7.48
38
2.50 DMSO-d6
B (d)
7.5
A (d)
8.3
2.00
2.02
f1 (ppm)

Figure A8

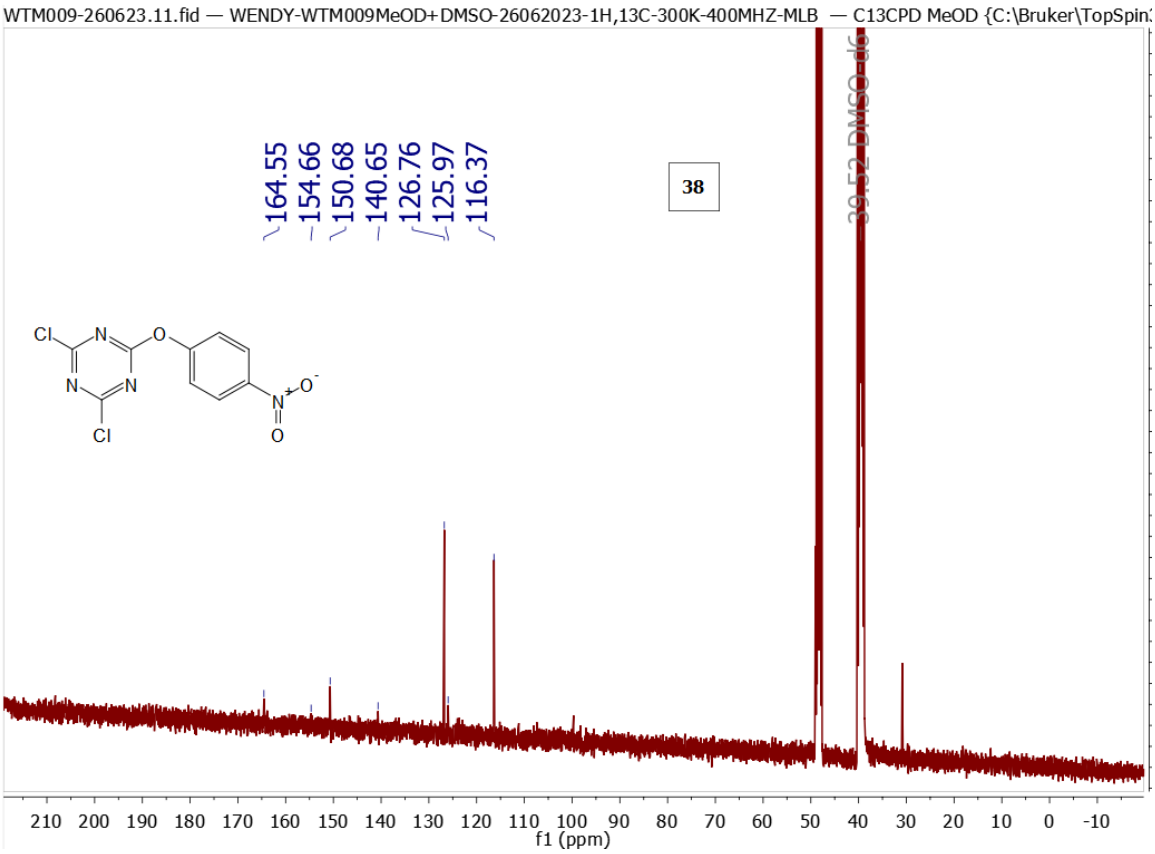
WTM009-260623.11.fid — WENDY-WTM009MeOD+DMSO-26062023-1H,13C-300K-400MHZ-MLB — C13CPD MeOD {C:\Bruker\TopSpin
164.55
154.66
150.68
140.65
126.76
125.97
116.37
38
39.52 DMSO-d6
Cl
N
O
N
N
Cl
N+
O-
O
210 200 190 180 170 160 150 140 130 120 110 100 90 80 70 60 50 40 30 20 10 0 -10
f1 (ppm)

Figure A9

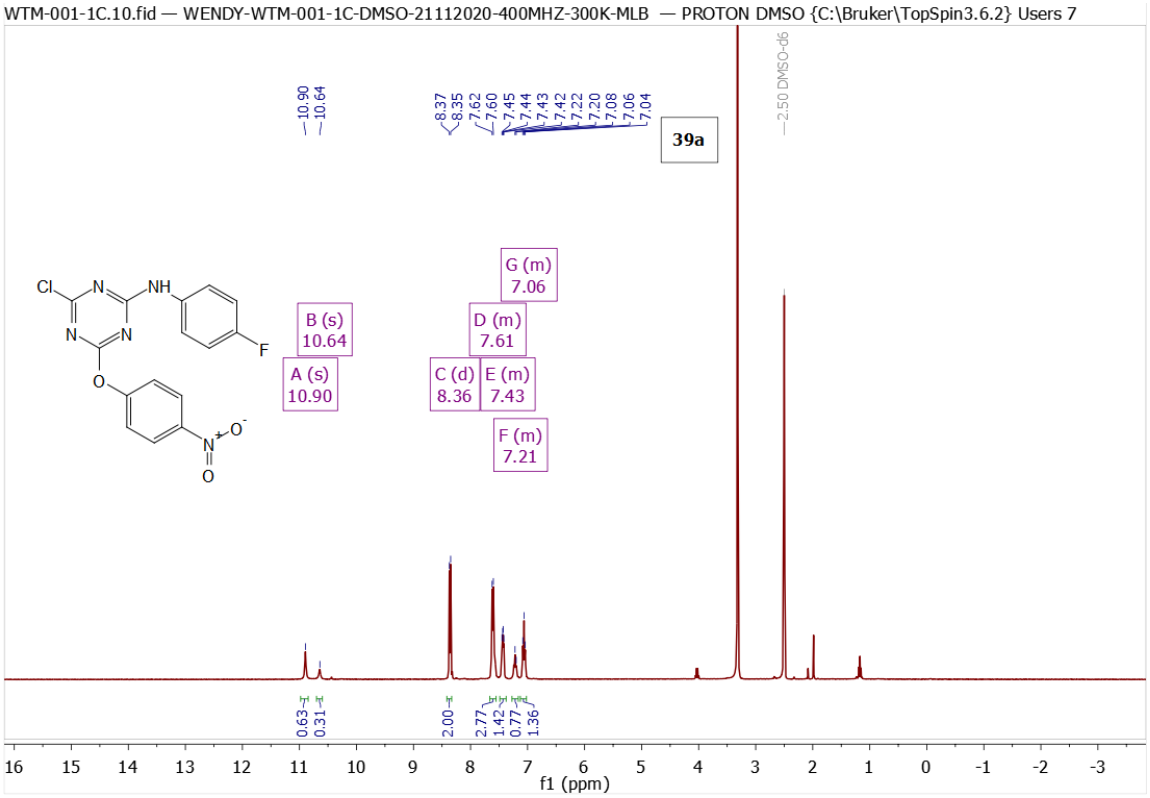
WTM-001-1C.10.fid — WENDY-WTM-001-1C-DMSO-21112020-400MHZ-300K-MLB — PROTON DMSO {C:\Bruker\TopSpin3.6.2} Users 7
39a
B (s) 10.64
A (s) 10.90
G (m) 7.06
D (m) 7.61
C (d) 8.36
E (m) 7.43
F (m) 7.21
f1 (ppm)

Figure A10

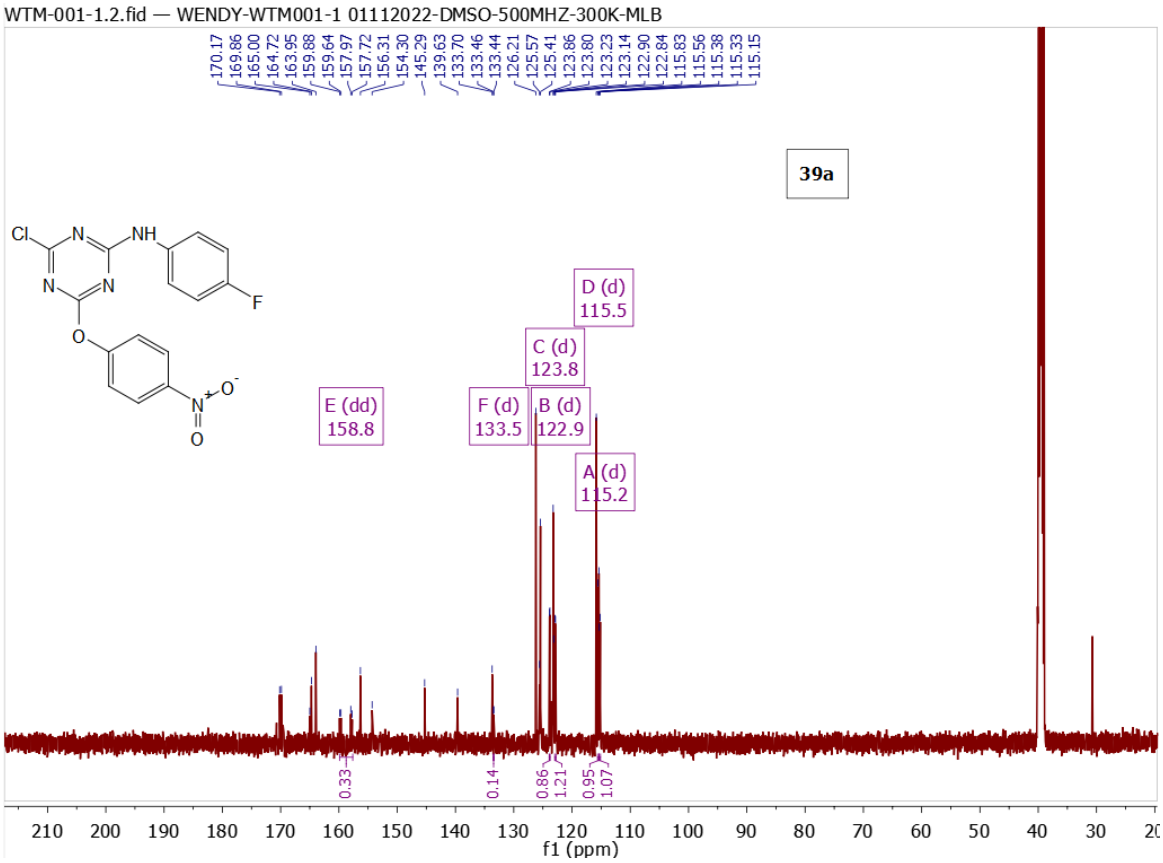
WTM-001-1.2.fid — WENDY-WTM001-1 01112022-DMSO-500MHZ-300K-MLB
170.17
169.86
165.00
164.72
163.95
159.88
159.64
157.97
157.72
156.31
154.30
145.29
139.63
133.70
133.46
133.44
126.21
125.57
125.41
123.86
123.80
123.23
123.14
122.90
122.84
115.83
115.56
115.38
115.33
115.15
39a
Cl
N
NH
N
N
F
O
N+
O-
O
D (d)
115.5
C (d)
123.8
E (dd)
158.8
F (d)
133.5
B (d)
122.9
A (d)
115.2
0.33
0.14
0.86
1.21
0.95
1.07
210
200
190
180
170
160
150
140
130
120
110
100
90
80
70
60
50
40
30
f1 (ppm)

Figure A11

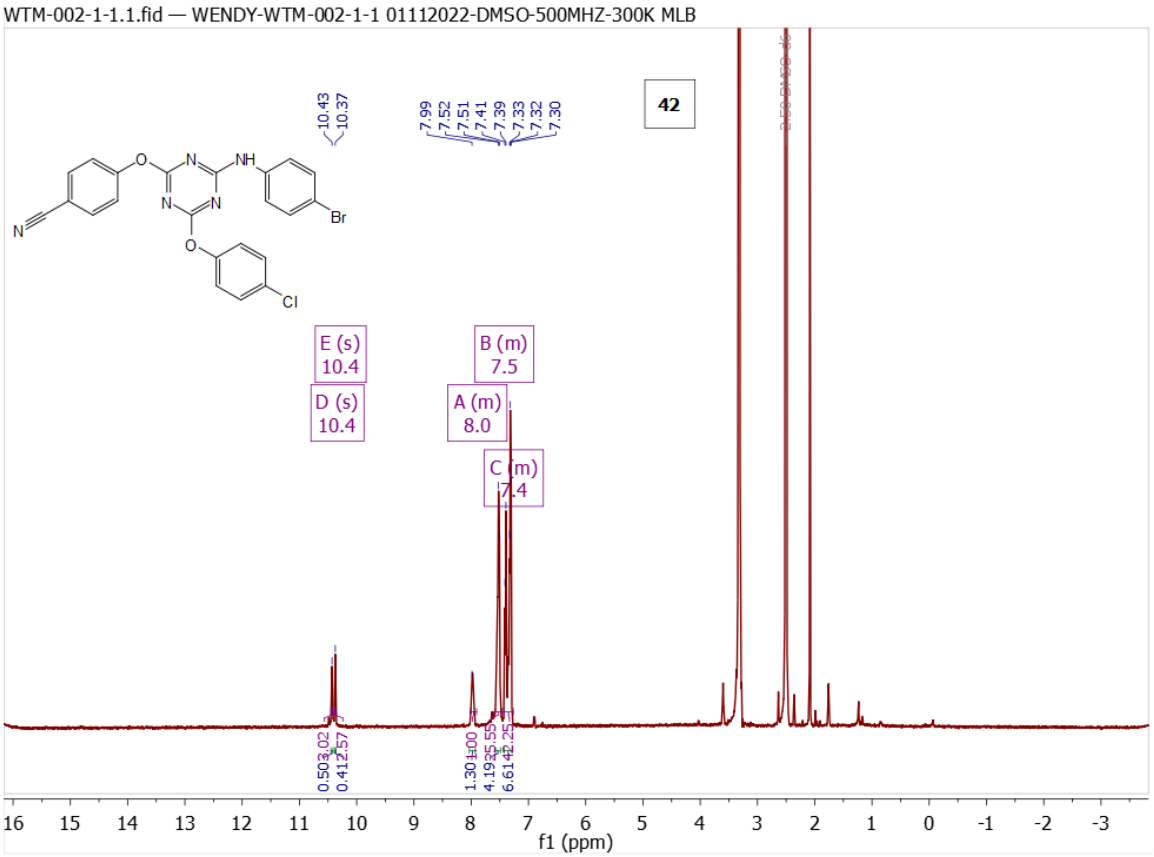
WTM-002-1-1.1.fid — WENDY-WTM-002-1-1 01112022-DMSO-500MHZ-300K MLB
42
10.43
10.37
7.99
7.52
7.51
7.41
7.39
7.33
7.32
7.30
E (s)
10.4
D (s)
10.4
B (m)
7.5
A (m)
8.0
C (m)
7.4
0.503.02
0.412.57
1.3011.00
4.1935.55
6.6142.25
16 15 14 13 12 11 10 9 8 7 6 5 4 3 2 1 0 -1 -2 -3
f1 (ppm)

Figure A12

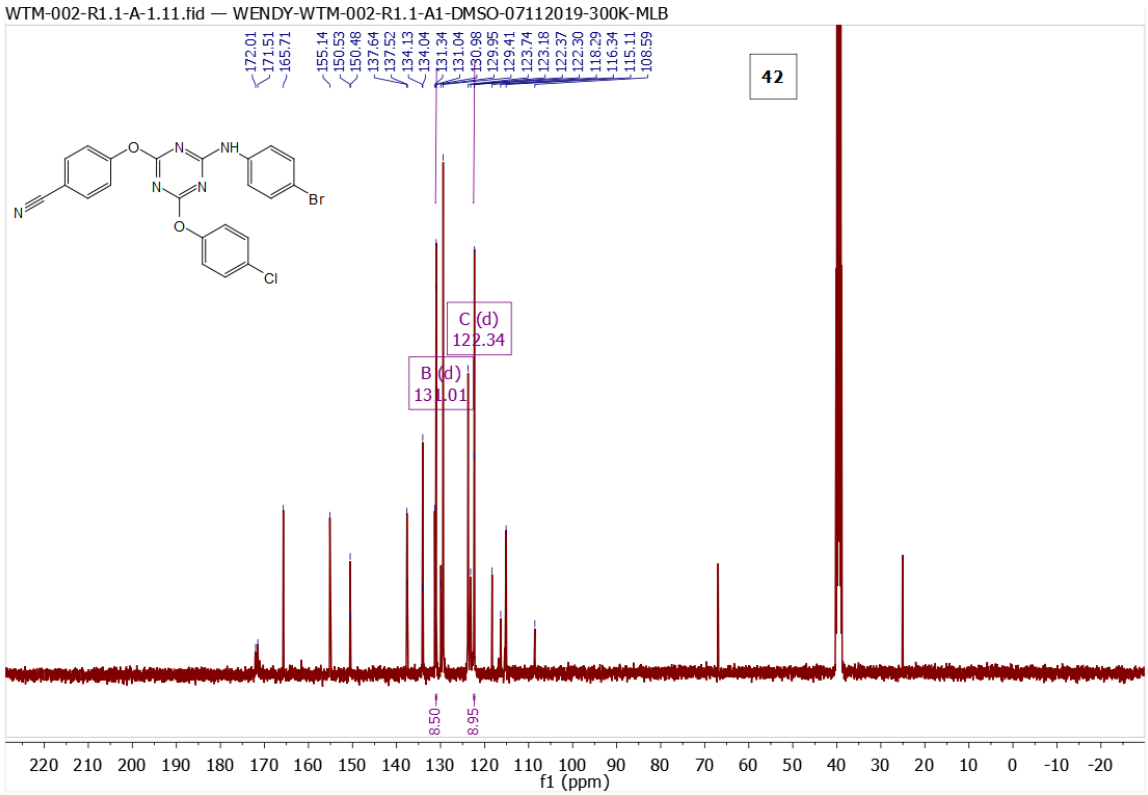
WTM-002-R1.1-A-1.11.fid — WENDY-WTM-002-R1.1-A1-DMSO-07112019-300K-MLB
172.01
171.51
165.71
155.14
150.53
150.48
137.64
137.52
134.13
134.04
131.34
131.04
130.98
129.95
129.41
123.74
123.18
122.37
122.30
118.29
116.34
115.11
108.59
42
C (d)
122.34
B (d)
131.01
8.50
8.95
220 210 200 190 180 170 160 150 140 130 120 110 100 90 80 70 60 50 40 30 20 10 0 -10 -20
f1 (ppm)

Figure A13

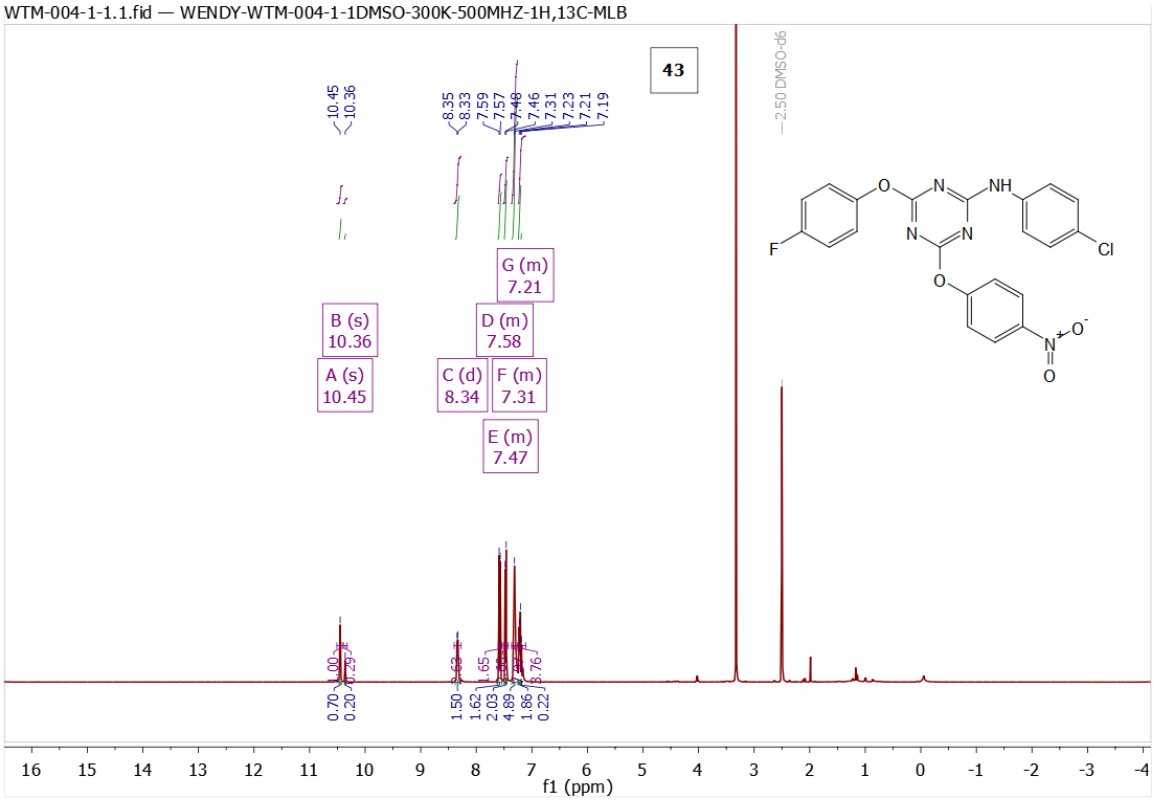
WTM-004-1-1.1.fid — WENDY-WTM-004-1-1DMSO-300K-500MHZ-1H,13C-MLB
43
2.50 DMSO-d6
10.45
10.36
8.35
8.33
7.59
7.57
7.48
7.46
7.31
7.23
7.21
7.19
G (m)
7.21
B (s)
10.36
D (m)
7.58
A (s)
10.45
C (d)
8.34
F (m)
7.31
E (m)
7.47
F
Cl
NH
f1 (ppm)

Figure A14

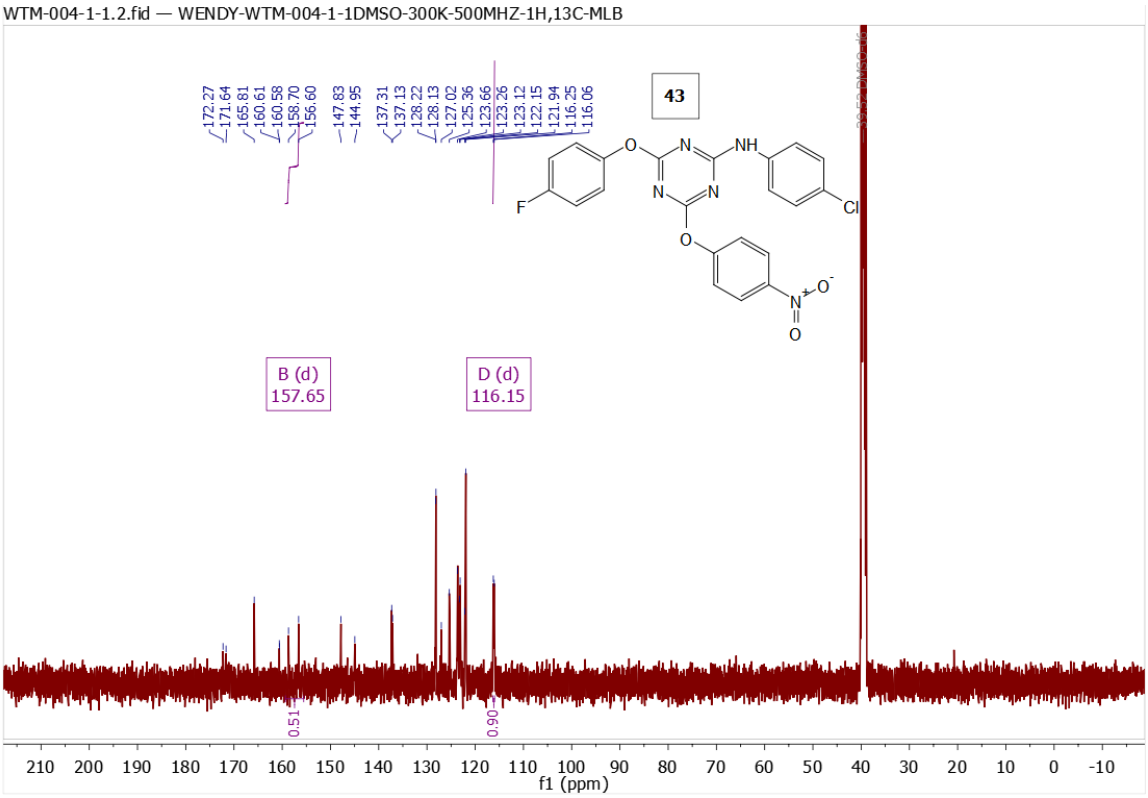
WTM-004-1-1.2.fid — WENDY-WTM-004-1-1DMSO-300K-500MHZ-1H,13C-MLB
172.27
171.64
165.81
160.61
160.58
158.70
156.60
147.83
144.95
137.31
137.13
128.22
128.13
127.02
125.36
123.66
123.26
123.12
122.15
121.94
116.25
116.06
43
B (d)
157.65
D (d)
116.15
0.51
0.90
210 200 190 180 170 160 150 140 130 120 110 100 90 80 70 60 50 40 30 20 10 0 -10
f1 (ppm)

Figure A15

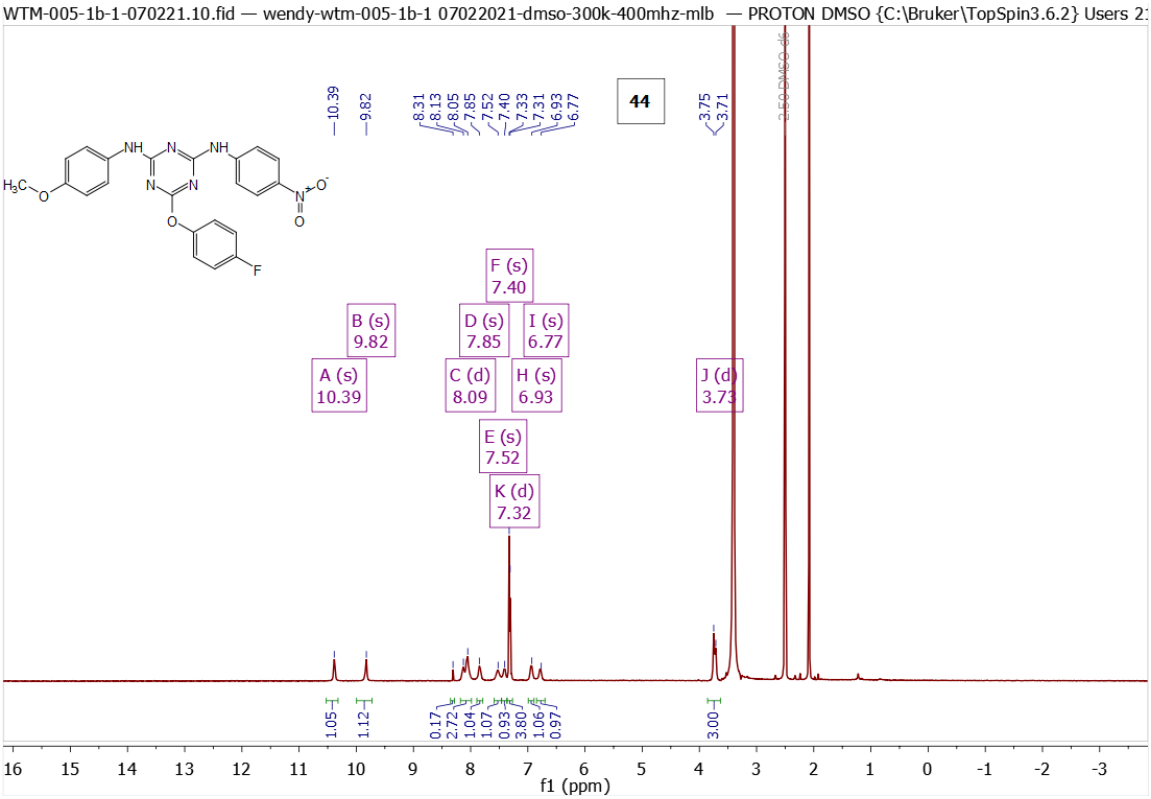
WTM-005-1b-1-070221.10.fid — wendy-wtm-005-1b-1 07022021-dmso-300k-400mhz-mlb — PROTON DMSO {C:\Bruker\TopSpin3.6.2} Users 2
44
A (s) 10.39
B (s) 9.82
C (d) 8.09
D (s) 7.85
E (s) 7.52
F (s) 7.40
H (s) 6.93
I (s) 6.77
J (d) 3.73
K (d) 7.32
f1 (ppm)

Figure A16

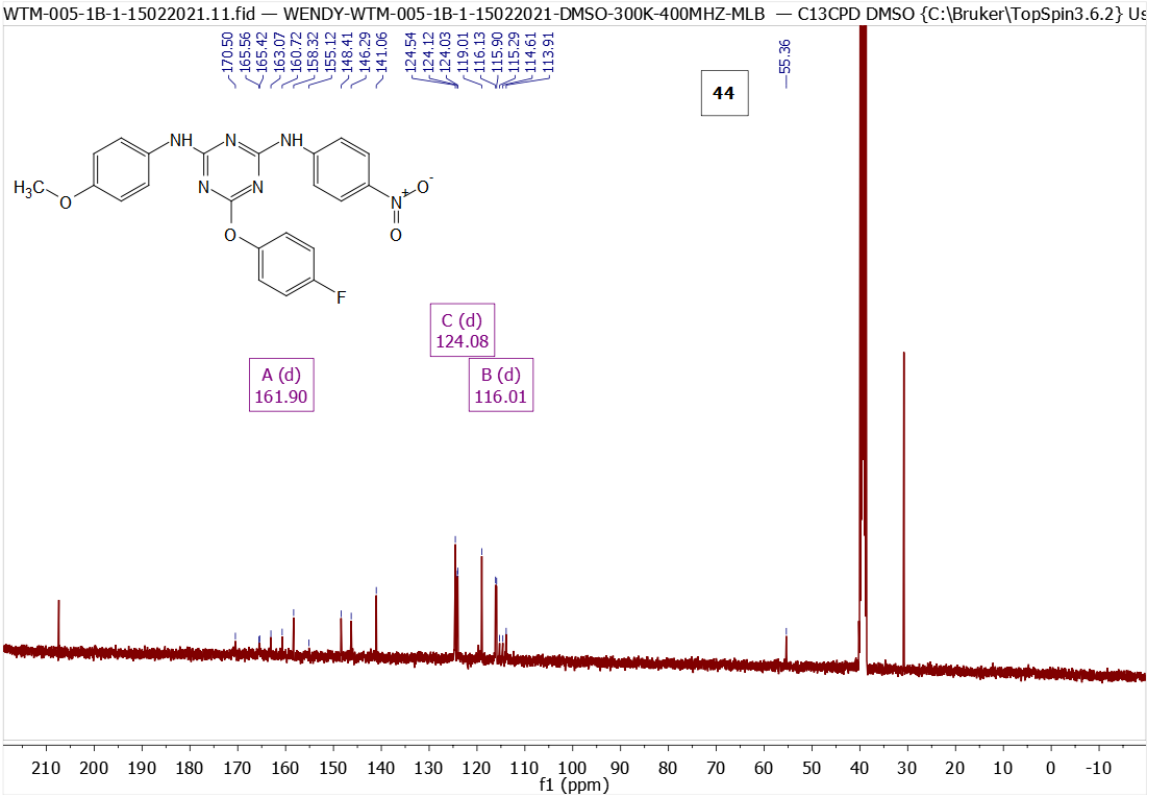
WTM-005-1B-1-15022021.11.fid — WENDY-WTM-005-1B-1-15022021-DMSO-300K-400MHZ-MLB — C13CPD DMSO {C:\Bruker\TopSpin3.6.2} Us
170.50
165.56
165.42
163.07
160.72
158.32
155.12
148.41
146.29
141.06
124.54
124.12
124.03
119.01
116.13
115.90
115.29
114.61
113.91
55.36
44
A (d)
161.90
B (d)
116.01
C (d)
124.08
f1 (ppm)

Figure A17